

# National Technical University of Athens

School of Mechanical Engineering

Section of Mechanical Design and Automatic Control

Control Systems Laboratory



## Grasp Synthesis Algorithms for Multifingered Robot Hands

Christoforos Mavrogiannis

A thesis submitted in partial fulfillment of the requirements for the degree of

**DIPLOMA IN MECHANICAL ENGINEERING**

Advisor: Professor Kostas J. Kyriakopoulos

Athens, February 2013

[This page intentionally left blank.]

# Εθνικό Μετσόβιο Πολυτεχνείο

Σχολή Μηχανολόγων Μηχανικών

Τομέας Μηχανολογικών Κατασκευών και Αυτομάτου Ελέγχου

Εργαστήριο Αυτομάτου Ελέγχου



## Αλγόριθμοι Βελτιστοποίησης Λαβής Αντικειμένων για Επιδέξια Ρομποτικά Χέρια

Χριστόφορος Μαυρογιάννης

Κατατέθηκε για την εκπλήρωση των υποχρεώσεων για την απόκτηση του τίτλου του

ΔΙΠΛΩΜΑΤΟΥΧΟΥ ΜΗΧΑΝΟΛΟΓΟΥ ΜΗΧΑΝΙΚΟΥ

Υπεύθυνος Καθηγητής: Κωνσταντίνος Ι. Κυριακόπουλος

Αθήνα, Φεβρουάριος 2013

# Grasp Synthesis Algorithms for Multifingered Robot Hands

Diploma Thesis

©2012-2013 by Christoforos Mavrogiannis

Contact info:

[ccmavrogiannis@gmail.com](mailto:ccmavrogiannis@gmail.com)

[mavrogiannis@controlsystems-lab.gr](mailto:mavrogiannis@controlsystems-lab.gr)

Submitted in Partial Fulfillment of the Requirements  
for the Degree of Diploma in Mechanical Engineering  
in the School of Mechanical Engineering at the  
National Technical University of Athens, 2013

Athens, Greece

Στη Μνήμη του φίλου μου  
Γιώργου

---

# Acknowledgements

I would like to express my deep gratitude to my advisor Prof. Kostas J. Kyriakopoulos for our collaboration during the past two years. In Prof. Kyriakopoulos' lab, I was given for the first time the opportunity to be involved in the intriguing world of robotics. His experience in the field gave me the chance to face interdisciplinary and demanding projects that helped me develop my background. His guidance and advice, both in a technical and in a personal level were crucial for my success. His inspiring and motivational personality as well as his trust in me strengthened my decision to follow my dream of pursuing a PhD and a career in this field.

Moreover, special thanks should be given to Panagiotis Artemiadis, scientific consultant of the NeuroRobotics Group of NTUA and Professor of Arizona State University, for his advice concerning my diploma thesis and ICRA paper.

Furthermore, I would like to thank the whole team of the Control Systems Lab. First of all, I am really grateful to Charalampos Bechlioulis. His experience, deep analytical knowledge and great character were a great help for me from the beginning of my diploma thesis. I will always remember our interesting *grasping* talks. Besides, I also owe a great debt of gratitude to Minas Liarokapis. His inspirational advice, as well as his true interest during these two years are much appreciated. I consider him as a great friend. In addition, I want to thank Pantelis Katsiaris for being close to me and sharing his great experience of the grasping problem. Last but not least, I want to thank Spyros Maniatopoulos and Ioannis Filippidis for their help and advice during my PhD application process. Besides, I want to thank all the other lab members for creating a great atmosphere in the Control Systems Lab.

I would also like to thank all my close friends for always being a great support. Their company throughout the five years of my studies helped me maintain a personal balance which served as a foundation to achieve a lot.

Finally, I would like to express my gratitude to my parents Ioannis and Aspasia and also to my brother Angelos and grandmother Maria for their priceless moral, emotional and economical support and understanding during the whole period of my studies. I consider myself as really lucky to be a member of such a peaceful and cultivated family.

Christoforos Mavrogiannis,  
Athens, February 2013

# Grasp Synthesis Algorithms for Multifingered Robot Hands

Christoforos Mavrogiannis

School of Mechanical Engineering  
National Technical University of Athens  
Athens, Greece  
2013

## ABSTRACT

The development of complex, human-like, multi-fingered robot hands, aiming at being incorporated in household robotics, prosthetics or even in industrial applications and space has brought the problem of grasping in the spotlight of modern robotics research. Grasping is a multiparametric problem during which the mechanical system (robot hand) interacts with the physical environment in order to perform a manipulation task. Therefore, there arises the need for the development of algorithms that, given sufficient information, produce successful grasps, taking into consideration the constraints imposed by the mechanical structure of the hand and also by the structure of the surrounding environment, aiming at satisfying the grasping task's requirements.

In this diploma thesis, the problem of deriving optimal grasps with respect to different aspects of Grasp Quality is addressed, ensuring that the aforementioned constraints are satisfied. The study conducted involves different approaches of this problem. In particular, optimization schemes are developed for the case of i) a robot hand with 15 actuated DOFs and ii) a hypothetical synergistic underactuated hand. For both, the kinematic model of the DLR/HIT II five-fingered robot hand has been considered. Emphasis is given to the grasping force minimization in order to derive grasps consuming the least possible amount of power and also ensure that the grasped object does not break. Besides, criteria concerning the ability of the hand's mechanism to produce the required forces and the task compatibility of a certain grasp have also been considered. Upon modeling the desired task that needs to be executed by the robot hand, our optimization schemes lead to hand's postures that favor its execution. Finally, an algorithm that aims at improving the Grasp Quality in real-time mode, after assessing information provided by tactile/force/vision sensors, is developed.

The efficiency of all the developed optimization schemes and algorithms is clarified through a simulation study for the model of the DLR/HIT II five-fingered robot hand. 3D plots representing the simulation results of various cases are provided, along with diagrams concerning the convergence of the criteria adopted.

# Αλγόριθμοι Βελτιστοποίησης Λαβής Αντικειμένων για Επιδέξια Ρομποτικά Χέρια

Χριστόφορος Μαυρογιάννης

Σχολή Μηχανολόγων Μηχανικών  
Εθνικό Μετσόβιο Πολυτεχνείο  
Αθήνα, Ελλάδα  
2013

## ΠΕΡΙΛΗΨΗ<sup>1</sup>

Η ανάπτυξη σύνθετων, ανθρωπομορφικών, επιδέξιων ρομποτικών χεριών, με στόχο είτε την ενσωμάτωσή τους σε ρομπότ οικιακής και βιομηχανικής χρήσης, είτε ακόμα την τοποθέτησή τους σε ανθρώπους με αναπηρίες έχει φέρει το πρόβλημα της λαβής αντικειμένων από ρομποτικά χέρια στο προσκήνιο της σύγχρονης ρομποτικής. Πρόκειται για ένα πολυπαραμετρικό πρόβλημα κατά το οποίο το μηχανικό σύστημα (ρομποτικό χέρι) αλληλεπιδρά με το φυσικό περιβάλλον, προκειμένου να εκτελέσει μια επιθυμητή εργασία/χειρισμό. Συνεπώς, προκύπτει η ανάγκη για ανάπτυξη αλγορίθμων που δεδομένων όλων των απαραίτητων πληροφοριών, θα υπολογίζουν όλες τις παραμέτρους μιας επιτυχούς λαβής, λαμβάνοντας υπόψη τους περιορισμούς που επιβάλλονται από την κατασκευή του χεριού αλλά και από τον περιβάλλοντα χώρο, με τελικό στόχο την ικανοποίηση των προδιαγραφών που έχουν τεθεί για τη συγκεκριμένη λαβή.

Σε αυτή την διπλωματική εργασία, ερευνάται το πρόβλημα του υπολογισμού της βέλτιστης λαβής ως προς διάφορες πτυχές, διασφαλίζοντας ότι ικανοποιούνται οι προαναφερθέντες περιορισμοί. Το πρόβλημα αντιμετωπίζεται για δύο διαφορετικούς τύπους ρομποτικού χεριού. Συγκεκριμένα, αλγόριθμοι βελτιστοποίησης έχουν αναπτυχθεί για την περίπτωση i) ενός ρομποτικού χεριού δεκαπέντε βαθμών ελευθερίας και ii) ενός συνεργιστικού υποεπενεργούμενου ρομποτικού χεριού που η κίνησή του διέπεται από τους ίδιους κανόνες με ένα ανθρώπινο χέρι. Και για τις δύο περιπτώσεις, ως κινηματικό μοντέλο έχει ληφθεί αυτό του ρομποτικού χεριού DLR/HIT II. Έμφαση έχει δοθεί στην ελαχιστοποίηση των δυνάμεων επαφής των δακτύλων, προκειμένου να ελαχιστοποιηθεί η ενεργειακή κατανάλωση και επίσης να διασφαλιστεί η ακεραιότητα του αντικειμένου που μας ενδιαφέρει. Επιπλέον, κριτήρια που αφορούν την ικανότητα του μηχανισμού του χεριού να παράγει τις απαιτούμενες δυνάμεις, καθώς επίσης και τη συμβατότητα της λαβής με τον επιθυμητό επακόλουθο χειρισμό/εργασία έχουν επίσης συμπεριληφθεί στην παρούσα ανάλυση. Ειδικότερα, μετά τη μοντελοποίηση της προς εκτέλεση από το ρομποτικό χέρι εργασίας, οι αλγόριθμοι που προτείνονται οδηγούν σε υιοθέτηση από το χέρι συγκεκριμένης κινηματικής κατάστασης που ευνοεί την εκτέλεση της εργασίας. Τέλος, προτείνεται ένας αλγόριθμος που στοχεύει στη βελτίωση της ποιότητας της λαβής ενός αντικειμένου σε πραγματικό χρόνο, μετά από αξιολόγηση πληροφοριών που παρέχονται από αισθητήρες αφής, όρασης και μέτρησης δύναμης.

Η αποτελεσματικότητα όλων των αναπτυχθέντων αλγορίθμων βελτιστοποίησης ελέγχεται και αποτυπώνεται μέσω μιας μελέτης προσομοίωσης. Τρισδιάστατες εικόνες

---

<sup>1</sup> Λόγω του ότι το πρόβλημα που πραγματεύεται η παρούσα εργασία εμπεριέχει μεγάλο πλήθος από εξειδικευμένους όρους, η μετάφρασή των οποίων στα Ελληνικά δεν είναι δόκιμη, κρίθηκε προτιμότερο να γραφτεί εξ' ολοκλήρου στα Αγγλικά.

που αναπαριστούν τα αποτελέσματα των διαφόρων περιπτώσεων που εξετάζονται, παρατίθενται μαζί με διαγράμματα που αφορούν τη σύγκλιση των υιοθετηθέντων κριτηρίων.

---

# Contents

<b>1</b>	<b>Preface</b>	<b>1</b>
1.1	Introduction	1
1.1.1	Robot Hands	1
1.1.2	Grasp Properties	4
1.1.3	Grasp Synthesis	5
1.2	Literature Review	6
1.3	Contributions	8
1.4	Thesis Structure	9
<b>2</b>	<b>Modeling Robotic Grasping</b>	<b>11</b>
2.1	Models and Definitions	11
2.1.1	Hand's Kinematics	12
2.2	Contact Modeling	14
2.3	Force Closure	16
2.4	Grasp Quality Measures	17
2.4.1	Norm of the normal contact force components	17
2.4.2	Volume of the Manipulability Ellipsoid	17
2.4.3	Measure of Distance from Mechanical Joint Limits	18
2.4.4	Task Compatibility	19
2.5	Assumptions	21
2.6	Model adaptation: DLR/HIT II	22
2.7	Summary of adopted notations	24
<b>3</b>	<b>Elements of Nonlinear Programming</b>	<b>25</b>
3.1	Nonlinear Programming Problem Definition	25
3.2	Optimality Conditions for General NLP Problems	26
3.3	Optimization Methods	27
3.4	Optimization Software	27
<b>4</b>	<b>Grasp Quality Optimization for Multifingered Robot Hands</b>	<b>29</b>
4.1	Problem Formulation	30
4.2	Optimization Scheme	31
4.2.1	Parametrized Surface Coordinates as Decision Variables	31
4.2.2	Joint Angular Positions as Decision Variables	32
4.3	Simulation Results	33
4.3.1	Parametrized Surface Coordinates as Decision Variables	33
4.3.2	Joint Angular Positions as Decision Variables	35
4.4	Discussion	38

<b>5</b>	<b>Grasp Quality Optimization for Synergistic Underactuated Hands</b>	<b>39</b>
5.1	From Human to Robot Hands: Kinematics . . . . .	40
5.1.1	Modeling the Human Hand's Kinematics . . . . .	40
5.1.2	Experimental Procedure . . . . .	42
5.1.3	Post Processing . . . . .	42
5.2	Problem Formulation . . . . .	44
5.2.1	Hand Model . . . . .	44
5.2.2	Object's Equilibrium: Contact Force Distribution . . . . .	44
5.2.3	Optimization Scheme . . . . .	44
5.3	Simulation Results . . . . .	45
5.4	Discussion . . . . .	48
<b>6</b>	<b>Grasp Compatibility Optimization</b> . . . . .	<b>49</b>
6.1	Task Definition . . . . .	49
6.2	Problem Formulation . . . . .	49
6.2.1	Optimization Scheme . . . . .	50
6.3	Simulation Results . . . . .	52
6.4	Discussion . . . . .	55
<b>7</b>	<b>Sequential Improvement of Grasp based on Sensitivity Analysis</b>	<b>57</b>
7.1	Problem Formulation . . . . .	57
7.1.1	The Sequential Grasp Improvement Algorithm . . . . .	60
7.2	Simulation Results . . . . .	62
7.3	Discussion . . . . .	64
<b>8</b>	<b>Conclusions and Future Directions</b> . . . . .	<b>65</b>
8.1	Discussion . . . . .	65
8.2	Future Research Directions . . . . .	66
	<b>Bibliography</b> . . . . .	<b>67</b>
	<b>Appendix A Kinematics of the DLR/HIT II</b> . . . . .	<b>72</b>
A.1	Forward Kinematics . . . . .	72
A.2	Inverse Kinematics . . . . .	76
	<b>Appendix B Apparatus</b> . . . . .	<b>79</b>
B.1	Cyberglove Systems Cyberglove II . . . . .	79

---

# List of Figures

1.1	Barrett Hand, Barrett Technology Inc. [1]. . . . .	2
1.2	DLR/HIT Hand I (left) and II (right) [2]. . . . .	2
1.3	Shadow Hand, Shadow Robot Company [3]. . . . .	3
1.4	Robonaut 2, NASA [4]. . . . .	3
1.5	General Structure of the Strategy adopted in the existing Grasp Synthesis Algorithms, as visualized by P. Bidaud et al. in [5]. Given the hand and object model, as well as the constraints imposed by the environment and the specifications of a certain task (criteria to be optimized and constraints to be respected), the Grasp Synthesis Algorithm provides a set of feasible solutions from which the best one is finally selected. . . . .	6
1.6	The effect of different contact points and configurations to the grasp quality. . . . .	7
2.1	Model of a five-fingered hand grasping a cylindric object: The global reference frame $\{\mathbf{N}\}$ as well as the frame at the object's center of mass $\{\mathbf{B}\}$ are attached. The positions of the contact frames $\{\mathbf{C}_i\}$ and of the wrist's frame $\{\mathbf{W}\}$ are noted. . . . .	11
2.2	DLR/HIT II: DOFs of its fingers-Figure extracted from the documentation of the hand, courtesy of DLR German Aerospace Center [2]. . . . .	22
2.3	DLR/HIT II: The model of our lab. As it can be seen, its size is comparable to the size of an adult's hand. In particular it is about 20% bigger. . . . .	23
4.1	A diagram of the proposed optimization scheme. . . . .	29
4.2	Definition of surface coordinates for a cylindric object. . . . .	31
4.3	Surface coordinates as decision variables: Initial (green color) and final (blue color) posture of the robot hand. The object's weight is drawn with a red vector at the object's center of mass (it is coincident with $y$ axis). The algorithm converged to this solution after about 70 iterations and terminated due to insufficient decrease of the objective function. . . . .	33
4.4	Surface coordinates as decision variables: Rear view of the initial (blue hand) and the final (green hand) hand's postures. . . . .	34
4.5	Surface coordinates as decision variables: Objective function convergence for the simulation depicted in Figs. 4.3 and 4.4. . . . .	35
4.6	Surface coordinates as decision variables: Convergence of the Objective Function Components. . . . .	35
4.7	Joint angular displacements as decision variables: Initial (blue hand) and final (green hand) posture of the robot hand. . . . .	36
4.8	Joint angular displacements as decision variables: Initial (green color) and final (blue color) posture of the robot hand. . . . .	37

4.9	Joint angular displacements as decision variables: Objective function convergence for the simulation depicted in Figs. 4.8 and 4.7. . . . .	37
4.10	Joint angular displacements as decision variables: Convergence of the Objective Function Components . . . . .	38
5.1	CyberGlove II, CyberGlove Systems [6]. . . . .	40
5.2	25 DOF kinematic model of the human hand [7]. The nomenclature of the DOFs's type is noted, along with the fingers' names. . . . .	41
5.3	Synergies based Grasping Optimization: Initial (green color) and final (blue color) postures of the robot hand. The final posture is more <i>anthropomorphic</i> . . . . .	46
5.4	Synergies based Grasp Quality Optimization: Top View of the initial (blue hand) and final (green hand) posture. . . . .	46
5.5	Synergies based Grasp Quality Optimization: Side view. . . . .	47
5.6	Synergies based Grasp Quality Optimization: Covergence of the combined objective function $z$ . . . . .	47
5.7	Synergies based Grasp Quality Optimization: Comparative figure with the convergence of the components of the objective function. The low force distribution can be interpreted as a result of the <i>successful initial guess</i> of the configuration and contact points of the robot hand. . . . .	48
6.1	Illustration of the scheme that takes into consideration the task to be executed by the robot hand. . . . .	50
6.2	Comparative Illustration: DLR/HIT II on the left and synergistic underactuated hand (5 principal components) with the same model on the right. The cyan vector illustrates the direction of the desired task execution, the transmission of angular velocity and torque along the positive side of axis $y$ . . . . .	53
6.3	Grasp Compatibility Optimization: Second view of the same simulation. . . . .	53
6.4	Grasp Compatibility Optimization: Third view. . . . .	54
6.5	Convergence of the proposed algorithm <i>with</i> and <i>without</i> synergies. . . . .	54
6.6	Convergence of the Objective Function Components for the case of the DLR/HIT II (without synergies) and for the case of a synergistic underactuated hand with the model of the DLR/HIT II (with synergies label). . . . .	55
7.1	The optimal states $s^*$ wrt the function $z(\mathbf{f}, \mathbf{p})$ are affected by small perturbations of the parameters $\mathbf{p}$ . . . . .	58
7.2	Cylindrical object: The initial (green color) and the final (blue color) hand configuration as well as the transitions (red color) between the contact points. . . . .	62
7.3	Cylindrical object: Comparative illustration of the cost function components. . . . .	63
7.4	Spherical object: The initial (green color) and the final (blue color) hand configuration as well as the transitions (red color) between the determined contact points. . . . .	63

7.5	Spherical object: Comparative illustration of the cost function components. . . . .	63
A.1	DLR/HIT II: The 3D model of the palm as depicted in the documentation of the hand. Frames are attached at its wrist and fingers' bases. . . . .	72
A.2	DLR/HIT II: The fingers' model with the joint frames attached. The Denavit-Hartenberg notation was adopted for the attachment of the frames. . . . .	74
B.1	CyberGlove, a glove which captures human hand's kinematics in real-time mode [6]. . . . .	79

---

# List of Tables

2.1	DLR/HIT II: Alternative views of the model of the NeuroRobotics Group. . . . .	23
2.2	Adopted notations, their definitions and assumed values . . . . .	24
5.1	Grasping experiments . . . . .	42
5.2	Variance of the Principal Components representing the Human Grasp as extracted by PCA . . . . .	43
A.1	DH parameters of the fingers. . . . .	74
A.2	Fingers' Joint Limits. . . . .	75

[This page intentionally left blank.]

---

# CHAPTER 1

## Preface

### 1.1 Introduction

Nowadays, robot hands are getting more and more complex and sophisticated. Simple grippers have been largely replaced by state-of-the-art, multi-fingered, human-like robot hands with many degrees of freedom and high levels of dexterity. Consequently, there arises the need for the design of corresponding, equivalently complex and general algorithms that can efficiently control robot hands and exploit the capabilities of their hardware.

In this direction, specific emphasis has been devoted to the fundamental problem of robot grasping. Grasping, an essential requirement for almost every manipulation task is a complex problem of mechanics which can be approached by many different points of view. Besides, human experience has proven that an object can be grasped in many different ways depending on the task that we need to execute. However, as humans grow older and get more and more aware of their environment as well as of their body, they adopt intuitive optimization schemes, so that they grasp objects consuming the least possible amount of energy and facilitating the desired task execution.

Inspired by this simple idea, this thesis addresses the problem of the grasp optimization, taking into consideration the geometrical and mechanical constraints imposed by the hand's design and the grasped object's surface properties.

#### 1.1.1 Robot Hands

The evolution of the design of robot hands has led to the creation of state-of-the-art multi-fingered robot hands which can play a significant role especially in the area of service robots for domestic use but also in the area of rehabilitation robotics or even in the high precision space exploration industry. The trend of imitating the complex nature of the human hand has led many companies to build different types of hands, incorporating different types of technologies. One of the first and most widely known multifingered robot hands was the three-fingered Barrett Hand, developed by Barrett Technology Inc (see Fig. 1.1).

Some of today's most representative robot hands have been developed by NASA [8], Shadow [9], DLR [10] and DLR/HIT [11,12]. In general, the modern human-like robot hands can be separated in two main categories depending on their type of actuation:

- External Actuation Hands, in which all the actuators are mounted in the forearm (NASA Fig. 1.4 and Shadow Fig. 1.3).

- Internal Actuation Hands, in which all the actuators and electronics are integrated in the finger body and the palm (DLR, HIT Fig. 1.2)

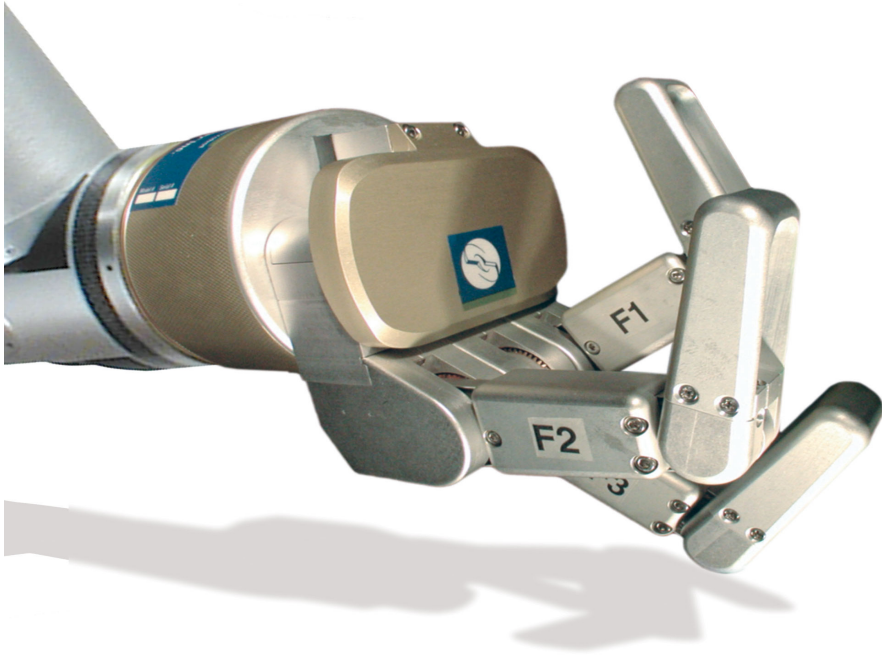


**Figure 1.1** – Barrett Hand, Barrett Technology Inc. [1].



**Figure 1.2** – DLR/HIT Hand I (left) and II (right) [2].



**Figure 1.3** – Shadow Hand, Shadow Robot Company [3].



**Figure 1.4** – Robonaut 2, NASA [4].

Due to their fundamental differences in actuation, in the first category the hand body is usually bigger than in the latter. Hence, in order for the Internal Actuation Hands to be more competitive, it is important that they are built in smaller dimensions. The reduction of the motor's and circuits' size is crucial in this direction.

### 1.1.2 Grasp Properties

There are numerous ways that a robot hand can grasp an object. From a mathematical point of view, this is because there is a large number of parameters that are involved in the grasping problem. From a physical and mechanical perspective, we can note that a complex mechanical artifact such as a multifingered robot hand can be associated in many ways with an object. This can also be verified by the human experience. In every-day life environments, humans grasp and manipulate numerous functional objects in order to execute different kinds of tasks. Depending on the object and the task, grasps can differ in many ways. Consequently, in order for robots to grasp objects in a way appropriate and compatible with the task we need them to execute subsequently, it is important that their grasp is characterized by several basic properties. Subsequently, we provide the most important properties that can describe the robot grasping problem, using the definitions of N'Guyen in [13] and Pollard in [14] :

- **Feasibility**

A grasp is kinematically feasible if there exist joint configurations for the individual fingers, such that the fingertips contact the grasped object at the desired contact points.

- **Reachability**

A grasp is reachable if there exist collision-free paths for the fingers from their current configurations to their respective grasp configurations.

- **Force-Closure**

The most important and common property when grasping an object is Force Closure. In particular, a grasp is said to be force closure if it can be maintained in the face of any object wrench [15]. For example, in order to lift an object, we must be able to compensate its weight by applying appropriate forces at the contact points. In the real world, this is more complicated because of the surface properties of objects. In order to lift the object, our contact forces must be such that they can prevent sliding at the contact points. In the next chapter, Force Closure is going to be mathematically defined as it is crucial in the development of the problem formulation of this thesis.

- **Equilibrium**

A grasp is in equilibrium if and only if the sum of forces and moments acting on the object is zero. There is a balance between the weight of the object and the contact forces exerted by the fingers.

- **Stability**

A grasp is stable if and only if the grasped object is always pulled back to its equilibrium configuration, whenever it is displaced from its configuration.

- **Compliance**

A grasp is compliant if the grasped object behaves as a generalized spring, damper or impedance, in complying with external constraints such as a hard surface or in reacting to errors between controlled and actual state variables, such as position, velocity or force.

### 1.1.3 Grasp Synthesis

During the 80's and early 90's, roboticists were devoted to the study of the Grasp Analysis, paying more attention to the complex mechanics of the problem and the formulation of grasp optimization problems. Since grasping constituted a new research direction, this was necessary and very important. However, due to the computational difficulties of that time, it was difficult to solve such a problem in order to generate a grasp with the desired properties.

Since the mid-90's and up until nowadays though, Grasping research, based on the important theoretical analysis and explorations of the past and making use of state-of-the-art computational, simulational but also mechanical tools and innovations, has become more applied and has approached more efficiently the real world and the physical environment. In particular, a lot of research studies have been devoted to the development of intelligent algorithms and their applications to real, mechanical and complex robot hands. Nowadays, a high level, human-like grasp decision can lead to the appropriate grasp selection and its successful implementation. Therefore, there are almost unlimited opportunities in Grasp Synthesis research, i.e., the research devoted in the successful generation of a grasp.

Indeed, there exists a great amount of research devoted to the development of Grasp Synthesis algorithms. Based on the work of P. Bidaud et al. in [5], we could classify the Grasp Synthesis algorithms in two main categories of approaches: the analytical ones and the empirical ones. By the term *analytical approaches*, we mean those based on geometric, kinematic and/or dynamic formulations of grasp synthesis problems. On the contrary, by the term *empirical approaches*, we denote those which avoid the computation of the mathematical and physical models by miming or imitating human strategies.

In the context of this thesis, we have adopted an analytical approach of the Grasping problem. Such an approach requires good knowledge of the system parameters, including both the hand's architecture and the surrounding environment, which is not always easy to be acquired. Besides, the number of the physical, geometrical and mechanical conditions that must be satisfied in order to ensure a successful grasp and task execution are also indicative of the complexity of the computation of such a problem. However, the advantage of this approach is that is closer to the physical environment. Making use of the laws of nature, an *analytical* algorithm makes use of the laws of nature, taking also into consideration the hardware limitations of the system. This is exactly the philosophy behind the algorithms developed and presented in this document. Fig. 1.5 provides a complete, visualized presentation of the analytical grasp synthesis approach.

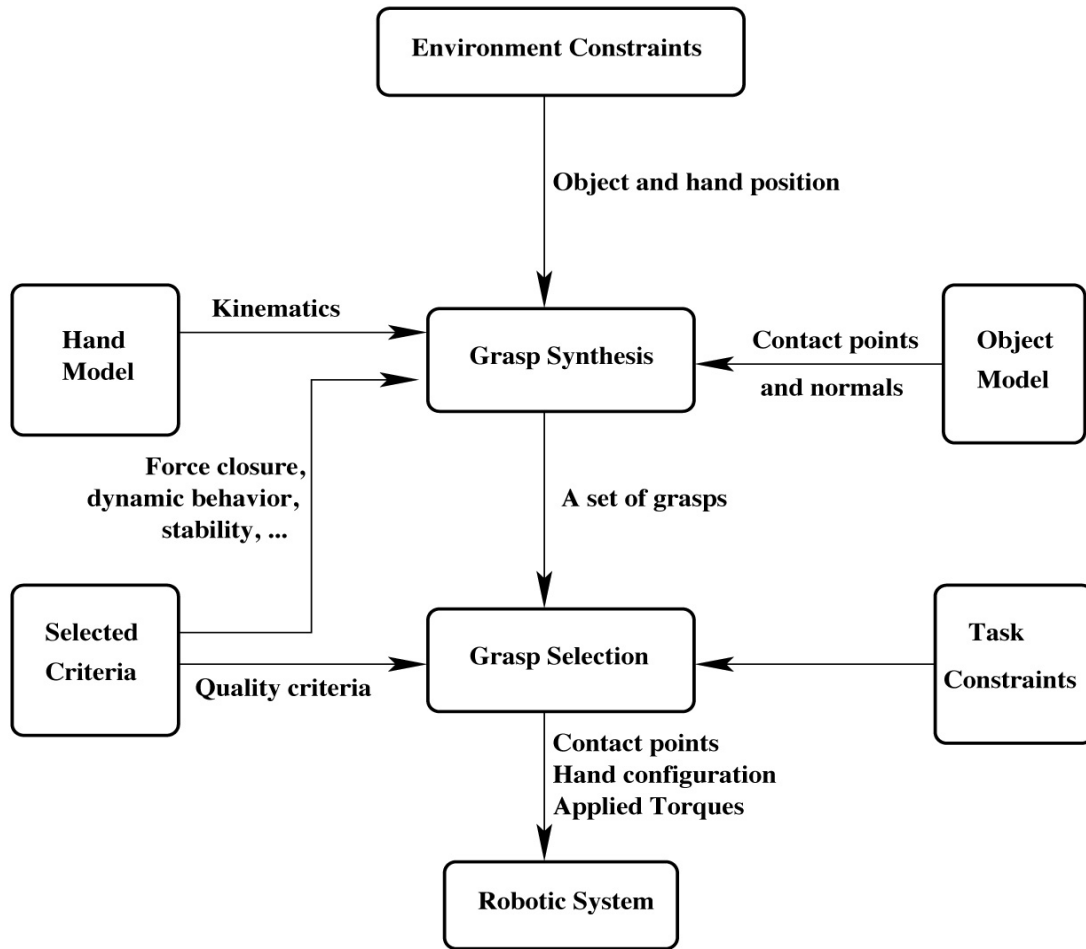


**Figure 1.5** – General Structure of the Strategy adopted in the existing Grasp Synthesis Algorithms, as visualized by P. Bidaud et al. in [5]. Given the hand and object model, as well as the constraints imposed by the environment and the specifications of a certain task (criteria to be optimized and constraints to be respected), the Grasp Synthesis Algorithm provides a set of feasible solutions from which the best one is finally selected.

## 1.2 Literature Review

Over the last decades, there has been a tremendous progress in the field of robot hands [16]. Simple grippers have been replaced by complex human-like hands, built to grasp and manipulate a wide range of every-day-life objects. However, to perform successfully, efficient algorithms, that guarantee certain quality criteria concerning the desired grasp properties for the task to be executed, have to be employed. As a result, a lot of research has been conducted in the field of grasp quality, which is defined by metrics that quantify the performance of a grasp. A fundamental and widely accepted quality criterion for a grasp is force closure [17]. It ensures both that the grasped object’s weight is compensated as well as that the contact friction constraints are not violated. However, force closure is quite a wide criterion. Therefore and owing to the increasing needs for precise and human-like grasps, several other quality measures have been presented. Ferrari and Canny in [18] addressed the problem of minimizing contact forces and proposed two different optimality criteria.

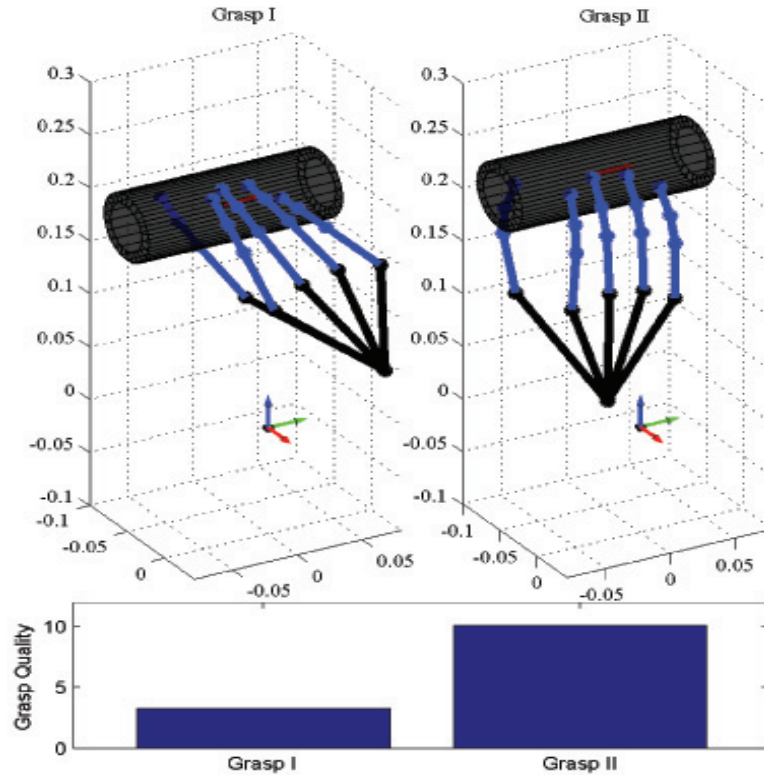


**Figure 1.6** – The effect of different contact points and configurations to the grasp quality.

Based on [18], Miller and Allen in [19], implemented 3D grasp quality computations for the Barrett and the DLR hands. Moreover, Mishra, in [20] compared various metrics and presented a corresponding mathematical analysis. A useful review on various grasp quality measures can be found in [21].

A lot of grasp synthesis algorithms have been proposed combining different quality measures. Various approaches have been presented both empirical and analytical. The empirical approaches use mainly learning techniques in order to mimic human grasping (see for example [22]). On the other hand, the analytical techniques use mathematical formulations considering the kinematics and the dynamics in order to determine optimal grasps regarding certain criteria [5]. In [23], a grasp optimization algorithm wrt (with respect to) an uncertainty grasp index as well as a task compatibility index is proposed. Particular emphasis has also been devoted to the grasping force optimization (GFO) problem (i.e., the problem of finding the minimal forces that satisfy the force closure sufficient conditions); many algorithms have been proposed in this direction (a complete and thorough overview of grasp synthesis algorithms concerning force optimization but also other metrics and approaches can be found in [5]). The problem of optimizing the maximum external wrench that a multifingered robot hand can withstand is studied in [24]. Finally the force limitations due to hardware and the increasing needs for real time computations have also been taken into consideration in the ongoing research [25].

Another important issue regarding grasp quality is the selection of contact points, which affects severely the force distribution yielded by the aforementioned grasping force optimization algorithms as well as other aspects of grasp quality. Fig. 1.6 depicts how different contact points and configurations affect the grasp quality. Op-

tinality criteria for the selection of contact points were proposed in [26] and [27]. A study on how infinitesimal perturbations of contact points would affect a class of grasp quality functions was presented in [28]. In [29], it is shown how different contact locations can affect the optimal force distribution wrt various quality measures.

The main goal of all these studies is to be incorporated as part of an algorithm for planning optimal grasps. In [30] a multi-criteria optimization algorithm regarding the fingers ability for force and velocity exertion was presented and was applied specifically for the case of the NASA-JSC robonaut hand. In [31], a strategy of moving fingers to neighboured joint positions to produce optimal force distribution is proposed, whereas in [32], a complete grasp improvement strategy is presented for objects of known geometry. It takes into consideration not only the force minimization requirement, but also the ability of the hand mechanism to exert forces while satisfying the mechanical limits of the finger joints. However, the grasp optimization is implemented through an evolutionary algorithm, which searches for contact points all over the object geometry, thus requiring global knowledge of the object geometry and consequently large number of operations and high computational time. Such an issue is the main drawback of the analytical approaches; they require global knowledge of the object's geometry, which in general is difficult to be acquired accurately in everyday life grasp problems [33].

### 1.3 Contributions

The main contributions of this thesis can be summarized as follows:

- Formulation and development of a Grasp Quality optimization algorithm for a multifingered robot hand with fifteen actuated DOFs, such as the DLR/HIT II five-fingered robot hand, which is part of the NeuroRobotics Lab equipment. In particular, the problem of grasping a known object with minimal amounts of power, while the mechanical and geometrical constraints are respected, is addressed. Emphasis is given to the contact points selection of the grasp, which can severely affect not only the contact force distribution but also other aspects of grasp quality.
- Adaptation of the aforementioned algorithm for the case of a hypothetical synergistic underactuated robot hand with the same number of DOFs. Grasping experiments were conducted by human subjects and through the measurements, a model was extracted to describe the relationship between the human hand's kinematics and the robot hand's kinematics. Based on this model, a Grasp Quality Optimization Scheme for Synergistic Underactuated Hands was developed, that leads to a *force closure* grasp, which respects the geometric and mechanical constraints of the robot hand.
- Formulation and development of a Grasp Synthesis algorithm that takes into consideration a task's requirements in wrench and velocity transmission to the grasped object and converges to a configuration and corresponding contact points and force distribution that favor the task execution, guaranteeing a stable grasp's sufficient conditions. Again, the scheme is tested both for a

hand with fifteen actuated DOFs and for a synergistic underactuated hand of the same model (DLR/HIT II).

- Development of a Grasp Improvement Algorithm which, requiring *only local knowledge* of the surface of a generally unknown object, can improve the grasp wrt predefined Grasp Quality measures, respecting the mechanical and geometrical limitations of the robot hand. The local knowledge of the object's surface properties can be acquired by an appropriate tactile sensors suite. This work was accepted for publication in the proceedings of the *IEEE International Conference on Robotics and Automation (ICRA)*, Karlsruhe, Germany, 2013 [34].

## 1.4 Thesis Structure

This thesis is organised as follows:

- In chapter 2 we introduce the reader to the grasping problem. The relevant theoretical background, including the adopted models, the terminology and the parameters used to describe the problems examined, are defined and described. Significant adopted transformations are also provided along with a number of assumptions that have been made for the sake of simplification reasons. A summary of all the notations is presented in the end of the chapter.
- Subsequently, chapters 4,5, 6 and 7 contain the developed formulations and optimization schemes. For each chapter, simulation results are provided and a corresponding discussion is made.
- Chapter 8 summarizes the main conclusions of the thesis and mentions possible future research directions concerning the problem of Grasp Synthesis.
- Finally, two appendices are provided. Appendix A contains significant transformations such as the Forward and Inverse Kinematics of the Robot Hand, while Appendix B provides information concerning the Cyberglove Hand which was used for the experiments performed in the context of chapter 5.

---

[This page intentionally left blank.]

---

# CHAPTER 2

## Modeling Robotic Grasping

In this chapter, the grasping problem is being modeled. The basic parameters and quantities needed for its complete description and analysis are defined and proper notations are adopted. Emphasis is also devoted to the concept of *Grasp Quality* which is defined and considered by different aspects.

### 2.1 Models and Definitions

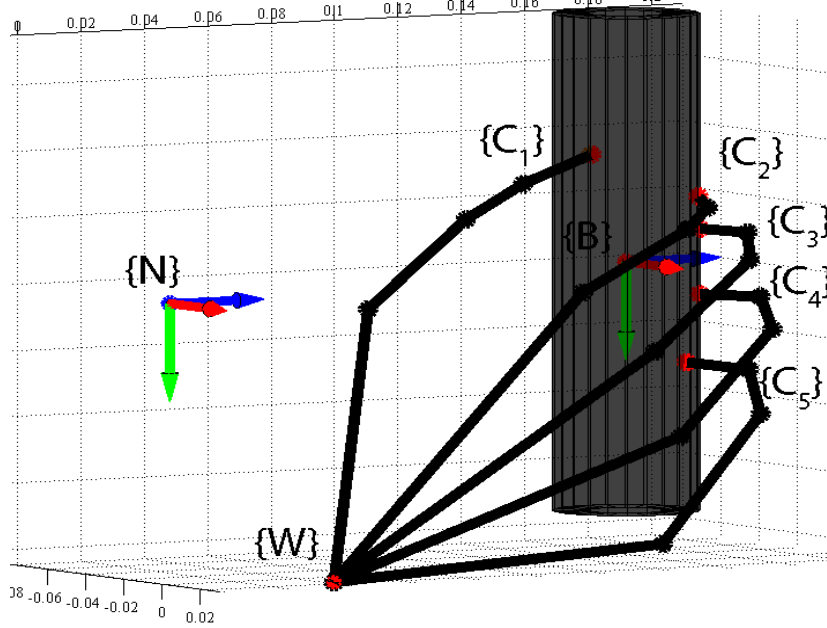


**Figure 2.1** – Model of a five-fingered hand grasping a cylindric object: The global reference frame  $\{\mathbf{N}\}$  as well as the frame at the object's center of mass  $\{\mathbf{B}\}$  are attached. The positions of the contact frames  $\{\mathbf{C}_i\}$  and of the wrist's frame  $\{\mathbf{W}\}$  are noted.

Consider the case of an  $n_c$ -fingered robot hand, grasping an object with  $n_c$  fingertip contacts. Let  $\{\mathbf{N}\}$  represent a conveniently chosen fixed global reference frame and  $\{\mathbf{B}\}$  a frame fixed to the object's center of mass.  $\{\mathbf{B}\}$ 's origin is defined relative to  $\{\mathbf{N}\}$  by the vector  $\mathbf{c}_m \in \mathbb{R}^3$  (for simplification reasons, we define frame  $\{\mathbf{B}\}$  parallel to frame  $\{\mathbf{N}\}$ ). The position of each contact point  $i$  wrt  $\{\mathbf{N}\}$  is defined by the vector  $\mathbf{c}_i \in \mathbb{R}^3$ . At each contact point, we assume that there is a unique, well defined tangent plane, on which we define a frame  $\{\mathbf{C}_i\}$ , with axes  $\{\hat{\mathbf{n}}_i, \hat{\mathbf{t}}_i, \hat{\mathbf{o}}_i\}$ . Each unit vector  $\hat{\mathbf{n}}_i$  is normal to the contact tangent plane and directed toward the object,

while the other two are orthogonal and lie in the tangent plane of the contact. A 3D plot with the aforementioned frames attached is depicted in Fig 2.1.

Let also  $\mathbf{f} \in \mathfrak{R}^3$  be the force applied to the object at the point  $\mathbf{c}_m$  and  $\mathbf{m} \in \mathfrak{R}^3$  be the applied moment. If we combine them into a single vector, we derive the object wrench  $\mathbf{g} = [\mathbf{f}^T \ \mathbf{m}^T]^T \in \mathfrak{R}^6$ , where  $\mathbf{f}$  and  $\mathbf{m}$  are expressed in  $\{\mathbf{N}\}$ . The wrench applied to the object can be partitioned into two main parts: contact and non-contact wrench. Throughout this thesis, by  $\mathbf{w}$  we will refer to non-contact wrench and particularly to the object's weight.

## 2.1.1 Hand's Kinematics

### Forward Kinematics

We assume that the hand is composed of a palm that serves as a common basis for its  $n_c$  fingers. Throughout this thesis, the base of the palm will be referred to as wrist. At the hand's wrist, we attach a frame  $\{\mathbf{W}\}$ , whose position is defined relative to  $\{\mathbf{N}\}$  by the vector  $\mathbf{p}_w = [x \ y \ z]^T \in \mathfrak{R}^3$ , each element of which accounts for a respective displacement along each of  $\{\mathbf{N}\}$ 's axes. Wrist's orientation is defined relative to  $\{\mathbf{N}\}$ , using the X-Y-Z fixed angles convention [62, 63], by the vector  $\mathbf{r}_w = [\alpha \ \beta \ \gamma]^T \in \mathfrak{R}^3$ . If we combine  $\mathbf{p}_w$  and  $\mathbf{r}_w$ , we derive the vector  $\mathbf{w} = [\mathbf{p}_w^T \ \mathbf{r}_w^T]^T \in \mathfrak{R}^6$  which contains wrist's position and orientation.

The hand's fingers consist of  $n_q$  rotational degrees of freedom in total. Their angular displacements are contained in the vector  $\mathbf{q} = [q_1 \ \dots \ q_{n_c}]^T \in \mathfrak{R}^{n_c}$ . Given each finger's joints positions, we can derive its end effector's position and orientation. In particular, let us denote by  $\{\mathbf{E}_i\}$  the frame attached on the end effector of each finger. We can now derive wrt  $\{\mathbf{E}_i\}$ 's position and orientation wrt wrt  $\{\mathbf{N}\}$  through the following transformation:

$${}^{\mathbf{N}}\mathbf{T}_{\mathbf{E}_i} = {}^{\mathbf{N}}\mathbf{T}_{\mathbf{W}} \cdot {}^{\mathbf{W}}\mathbf{T}_{\mathbf{E}_i} \quad (2.1)$$

where,  $\mathbf{T}$  is the symbol of the homogeneous transformation. In general, the structure of a homogeneous transformation describing the position and orientation of a frame  $\{\mathbf{2}\}$  wrt frame  $\{\mathbf{1}\}$  is the following:

$${}^1\mathbf{T}_2 = \begin{bmatrix} {}^1\mathbf{R}_2 & {}^1\mathbf{d}_2 \\ 0 & 1 \end{bmatrix} \quad (2.2)$$

where  $\mathbf{T}$ 's left upper superscript denotes the transformation's reference frame, while its right lower subscript denotes its referred frame.  ${}^1\mathbf{R}_2 \in \mathfrak{R}^{3 \times 3}$  is the transformation's rotation matrix and  ${}^1\mathbf{d}_2 \in \mathfrak{R}^3$  is the corresponding position vector.

### Significant Transformations

The complex nature of the Grasping Problem, which involves a significant number of variables, has led to the development of useful tools which implement a mapping between them. In particular, there are two main important transformation matrices that are widely accepted and used: the Grasp Matrix and the Hand Jacobian, which are subsequently defined and described. In order to proceed with their derivation, let us point out that each contact of a grasp should be considered as two coincident points: one on the hand's fingertip and one on the object.

## Grasp Matrix

The Grasp Matrix is a transformation matrix which relates the fingertips velocities to the object's center of mass velocity. In order to derive it, let us denote by  $\boldsymbol{\nu} = [\mathbf{v}^T \ \boldsymbol{\omega}^T]^T \in \mathfrak{R}^6$  the grasped object's twist wrt to  $\{\mathbf{N}\}$ , where  $\mathbf{v} \in \mathfrak{R}^3$  is the object's translational velocity and  $\boldsymbol{\omega} \in \mathfrak{R}^3$  is its angular velocity. Furthermore, let us represent by  $\boldsymbol{\nu}_{i,obj} = [\mathbf{v}_{i,obj}^{\mathbf{N}} \ \boldsymbol{\omega}_{i,obj}^{\mathbf{N}}]^T \in \mathfrak{R}^6$  the velocity transmitted at the  $i$  contact by the finger to the object wrt  $\{\mathbf{N}\}$ . Then the object's twist can be expressed relative to each contact's velocity contribution as follows:

$$\boldsymbol{\nu} = \mathbf{P}_i \cdot \boldsymbol{\nu}_{i,obj}^{\mathbf{N}} \quad (2.3)$$

where

$$\mathbf{P}_i = \begin{bmatrix} \mathbf{I}_{3 \times 3} & \mathbf{0}_{3 \times 3} \\ \mathbf{S}(\mathbf{c}_i - \mathbf{c}_m) & \mathbf{I}_{3 \times 3} \end{bmatrix} \quad (2.4)$$

$\mathbf{I}_{3 \times 3} \in \mathfrak{R}^{3 \times 3}$  is the identity matrix and  $\mathbf{S}(\mathbf{c}_i - \mathbf{c}_m)$  is the cross product matrix which, given a vector  $\mathbf{r} = [r_x \ r_y \ r_z]^T \in \mathfrak{R}^3$  is defined as follows:

$$\mathbf{S}(\mathbf{r}) = \begin{bmatrix} 0 & -r_z & r_y \\ r_x & 0 & -r_x \\ -r_y & r_x & 0 \end{bmatrix} \quad (2.5)$$

It is now important to introduce in our analysis the object twist at contact  $i$ , relative to frame  $\{\mathbf{C}_i\}$ . Let  $\mathbf{R}_i = [\hat{\mathbf{n}}_i \ \hat{\mathbf{t}}_i \ \hat{\mathbf{o}}_i] \in \mathfrak{R}^{3 \times 3}$  represent the orientation of the  $i$  contact frame wrt the inertial frame  $\{\mathbf{N}\}$ . Then the object twist referred to frame  $\{\mathbf{C}_i\}$ , can be derived from equation:

$$\boldsymbol{\nu}_{i,obj}^{\mathbf{N}} = \bar{\mathbf{R}}_i \cdot \boldsymbol{\nu}_{i,obj} \quad (2.6)$$

where

$$\bar{\mathbf{R}}_i = \begin{bmatrix} \mathbf{R}_i & \mathbf{0} \\ \mathbf{0} & \mathbf{R}_i \end{bmatrix} \in \mathfrak{R}^{6 \times 6} \quad (2.7)$$

is the blockdiagonal rotation matrix implementing the map from frame  $\{\mathbf{C}_i\}$  to frame  $\{\mathbf{N}\}$ . Substituting equation 2.6 into equation 2.3, we derive:

$$\boldsymbol{\nu} = \mathbf{P}_i \cdot \bar{\mathbf{R}}_i \cdot \boldsymbol{\nu}_{i,obj} \quad (2.8)$$

which maps the object's twist at contact  $i$  from  $\{\mathbf{C}_i\}$  to  $\{\mathbf{N}\}$ . Equation 2.8 yields the partial grasp matrix  $\widetilde{\mathbf{G}}_i \in \mathfrak{R}^{6 \times 6}$ :

$$\widetilde{\mathbf{G}}_i = \mathbf{P}_i \cdot \bar{\mathbf{R}}_i \quad (2.9)$$

If we now consider the twist contributions of all the hand's fingertip contacts to the object's twist at its center of mass, we derive the complete Grasp Matrix  $\widetilde{\mathbf{G}} \in \mathfrak{R}^{6 \times 6n_c}$ :

$$\widetilde{\mathbf{G}} = \left[ \widetilde{\mathbf{G}}_1 \quad \dots \quad \widetilde{\mathbf{G}}_{n_c} \right] \quad (2.10)$$

It is important to point out that from the definition of the Grasp Matrix, it is profound that it can also be used in order to express the contribution of contact wrenches to the wrench applied at the object's center of mass.

## Hand Jacobian

The hand Jacobian is a matrix transformation which maps the hand's joint velocities to their end effector twists. There are two main methods to derive it. The first one is based on the differentiation of the Hand's Forward Kinematics, while the second one, which will be subsequently presented, involves a geometrical approach.

Let us denote by  $\boldsymbol{\nu}_{i,hnd}^N = \begin{bmatrix} \mathbf{v}_{i,obj}^N \mathbf{T} & \boldsymbol{\omega}_{i,hnd}^N \mathbf{T} \end{bmatrix}^T \in \mathfrak{R}^6$  the twist of each fingertip, expressed relative to the global reference frame  $\{\mathbf{N}\}$ . The fingertip's twist is related to the joint velocities of its corresponding finger as follows:

$$\boldsymbol{\nu}_{i,hnd}^N = \mathbf{Z}_i \cdot \dot{\mathbf{q}} \quad (2.11)$$

where  $\dot{\mathbf{q}} \in \mathfrak{R}^{n_q}$  is the vector containing the angular velocities of the hand's joints and  $\mathbf{Z}_i \in \mathfrak{R}^{6 \times n_q}$  is defined as follows:

$$\mathbf{Z}_i = \begin{bmatrix} \mathbf{S}(\mathbf{c}_i - \boldsymbol{\zeta}_1)^T \hat{\mathbf{z}}_1 & \dots & \mathbf{S}(\mathbf{c}_i - \boldsymbol{\zeta}_{n_q})^T \hat{\mathbf{z}}_{n_q} \\ \hat{\mathbf{z}}_1 & \dots & \hat{\mathbf{z}}_{n_q} \end{bmatrix} \quad (2.12)$$

where  $\boldsymbol{\zeta}_j$  is the origin of the coordinate frame<sup>2</sup> associated with the  $j$ th joint<sup>3</sup> and  $\hat{\mathbf{z}}_j$  is the unit vector in the direction of the  $\mathbf{z}$ -axis in the same frame. Both axes are expressed relative to  $\{\mathbf{N}\}$ . Now, if we map  $\boldsymbol{\nu}_{i,hnd}$  from  $\{\mathbf{N}\}$  to  $\{\mathbf{C}_i\}$ , we derive:

$$\boldsymbol{\nu}_{i,hnd} = \overline{\mathbf{R}}_i^T \cdot \boldsymbol{\nu}_{i,hnd}^N \quad (2.13)$$

By the substitution of eq. 2.11 into eq. 2.13, we derive the following expression:

$$\boldsymbol{\nu}_{i,hnd} = \overline{\mathbf{R}}_i^T \cdot \mathbf{Z}_i \cdot \dot{\mathbf{q}} \quad (2.14)$$

which yields the partial Hand Jacobian  $\tilde{\mathbf{J}}_i \in \mathfrak{R}^{6 \times n_q}$ :

$$\tilde{\mathbf{J}}_i = \overline{\mathbf{R}}_i^T \cdot \mathbf{Z}_i \quad (2.15)$$

As we did for the case of the Grasp Matrix, if we consider all the hand's fingers, we derive the complete Hand Jacobian  $\tilde{\mathbf{J}} \in \mathfrak{R}^{6n_c \times n_q}$ :

$$\tilde{\mathbf{J}} = \begin{bmatrix} \tilde{\mathbf{J}}_1 \\ \vdots \\ \tilde{\mathbf{J}}_{n_c} \end{bmatrix} \quad (2.16)$$

## 2.2 Contact Modeling

Grasping is a complex and multivariable robotics problem. In order to simplify it, it is important to introduce several conventions. A significant one is the modeling of the contacts between the hand and the object. It has already been said that throughout this thesis we will only consider the case of fingertip-contact grasps. These contacts have to be modeled in a way compatible with the problem's requirements.

<sup>2</sup>At each joint a coordinate frame has been attached using the Denavit-Hartenberg notation.

<sup>3</sup>We assume that all hand's joints are rotational.

In the Grasping Literature there have been proposed several different models in this direction, making the rigid body assumption for the fingers and the object. They mainly differ in the number of velocity/force components transmitted through the contacts between the hand and the grasped object. The most commonly used models are the following three: *Point-Contact-Without-Friction*, *Hard Finger* and *Soft Finger*.

The *Point-Contact-Without-Friction* or (*PCWF*) model is mostly used when the contact patch is very small and the object and hand surfaces are slippery, that is, when there is no significant friction between them. In this case only the normal translational velocity component is considered to be transmitted between the hand and the object. Likewise, this model only considers the normal contact force component and ignores frictional forces and moments.

The *Hard Finger* model or (*HF*) is applied when the frictional forces between the hand and the object can not be ignored but the contact patch is so small that no significant friction moment appears. In this case, only the three translational velocity components and the three contact force components are considered to be transmitted through the contacts.

The *Soft Finger* model or (*SF*) can be used when the frictional force and the moment component about the contact normal are appreciable due to the significant size of the contact patch. In this case, the three translational velocity components as well as the angular velocity component about the contact normal are considered to be transmitted through the contact. Likewise, the three force components as well as the moment component about the contact normal are transmitted.

Since the main purpose of this thesis is to provide an analysis to be applied to the DLR/HIT II Five-Fingered Robot Hand, we had to choose the appropriate contact model to describe our problem. The Hand's fingertips are covered with a hard plastic material but we can not totally ignore the friction between their surface and the object's. For this reason, the *Hard Finger* Model was adopted in our analysis.

In order to incorporate the *Hard Finger* contact model in our analysis, we have to mathematically define it and update the Grasp Matrix and the Hand Jacobian. Adopting the notation proposed in the Grasping Chapter of the Handbook of Robotics [15], our contact model can be defined through a matrix  $\mathbf{H}_i \in \mathbb{R}^{3 \times 6}$  for each contact  $i$  between the hand and the object:

$$\mathbf{H}_i = [\mathbf{I}_{3 \times 3} \quad \mathbf{0}_{3 \times 3}] \quad (2.17)$$

We can combine these matrices to form the complete Contact Model matrix  $\mathbf{H}$ :

$$\mathbf{H} = \text{Blockdiag}(\mathbf{H}_1, \dots, \mathbf{H}_{n_c}) \in \mathbb{R}^{3n_c \times 6n_c} \quad (2.18)$$

The Contact Model Matrix can now update the Grasp Matrix and the Hand Jacobian by keeping only the components that are compatible with the adopted model:

$$\mathbf{G} = \tilde{\mathbf{G}}\mathbf{H}^T \in \mathbb{R}^{6 \times 3n_c} \quad (2.19)$$

$$\mathbf{J} = \tilde{\mathbf{H}}\mathbf{J} \in \mathbb{R}^{3n_c \times n_q} \quad (2.20)$$

In accordance to the contact model we adopted and for simplification reasons, if we stack in  $\dot{\mathbf{x}} \in \mathbb{R}^{3n_c}$  all the translational fingertip contact velocities expressed in the

contact frames, we derive the following maps:

$$\dot{\mathbf{x}} = \mathbf{J}\dot{\mathbf{q}} \quad (2.21)$$

$$\dot{\mathbf{x}} = \mathbf{G}^T \boldsymbol{\nu} \quad (2.22)$$

In addition, if we stack in  $\mathbf{f} \in \mathbb{R}^{3n_c}$  all the contact forces  $\mathbf{f}_i = [f_{n_i} \ f_{t_i} \ f_{o_i}]^T$  expressed in  $\{\mathbf{N}\}$ , we derive their contribution to the object's wrench:

$$\mathbf{g} = \mathbf{G}\mathbf{f} \quad (2.23)$$

Furthermore, if the vector  $\boldsymbol{\tau} \in \mathbb{R}^{n_q}$  contains the torques on the hand's joints, then:

$$\boldsymbol{\tau} = \mathbf{J}^T \mathbf{f} \quad (2.24)$$

is the equation which relates the contact forces to the torques exerted on the hand's joints.

## 2.3 Force Closure

Force Closure is a significant requirement for the successful execution of almost every grasp and manipulation task. It relies on the ability of the hand to squeeze arbitrarily tightly in order to produce frictional forces that can compensate the external wrenches applied on the object [15]. This implies that friction is an essential property in the definition of Force Closure. For this reason it is important that we first select and define an appropriate Friction Model.

### Friction Model

In general, the Friction Law imposes constraints in the magnitude and direction of the contact forces and moments. Since we have chosen the Hard Finger Model for the contact modeling, there are only contact force components at the fingertip contacts. These forces are constrained to lie inside certain surfaces so that no sliding phenomena arise. Throughout this thesis, the Coulomb Friction Model is adopted. According to the Coulomb Friction Model, for each pair of surfaces that are in contact there is a coefficient which constrains the relationship between normal and tangential forces in the static state. This coefficient is referred to as the "static friction coefficient" and here we denote it by the greek letter  $\mu$ .

According to Coulomb's Model, for the Hard Finger case in the 3D space, at each contact the following condition must hold in order to avoid slippage:

$$\sqrt{f_{t_i}^2 + f_{o_i}^2} \leq \mu f_{n_i}, \quad i = 1 \dots n_c \quad (2.25)$$

From a geometric point of view, these relationships define the following 3D surfaces:

$$\mathcal{F}_i = \{(f_{n_i}, f_{t_i}, f_{o_i}) \mid \sqrt{f_{t_i}^2 + f_{o_i}^2} \leq \mu f_{n_i}\}, \quad i = 1 \dots n_c \quad (2.26)$$

commonly referred to as "friction cones".

### Force Closure Definition

Now that we described the adopted friction model, we can mathematically define Force Closure. Force Closure requires that the contact forces not only must be able to compensate for the external wrench applied to the grasped object but they should also respect the constraints imposed by the friction cones. Consequently, if for example the only external wrench  $\mathbf{w} \in \mathbb{R}^6$  exerted on a grasped object's center of mass is its weight, then the Force Closure conditions for this system are the following:

$$\mathbf{G}\mathbf{f} = -\mathbf{w} \quad (2.27)$$

$$\mathbf{f}_i \in \mathcal{F}_i \quad (2.28)$$

## 2.4 Grasp Quality Measures

Force Closure is quite an important and essential criterion in robotic grasping but it is also a generic one. For this reason, it should be combined with other criteria, depending on the task and the environment. In this respect, a lot of research has been done and many different criteria have been proposed in order to quantify the grasp performance. In this section, based on the models, the notations and the variables that we defined in the previous section, we define a number of useful and functional fundamental grasp quality metrics that will be subsequently adopted in the formulations of the grasping optimization problems that we address and solve in the context of this thesis. A complete, thorough and up to date overview and presentation of the most significant grasp quality measures proposed in the Grasping Literature can be found in [35].

### 2.4.1 Norm of the normal contact force components

Robot hands are mechanical artifacts requiring power to execute the task they have been programmed for. Hence, a fundamental requirement for a grasp concerns its implementation using the lowest possible amount of energy. This implies that the required contact forces exerted by the hand's fingers will be produced by low joint torques, demanding low amounts of energy. Towards this goal, many metrics associated with the contact forces have been proposed. In our analysis we adopted the following function :

$$F(\mathbf{f}) = \sqrt{\sum_{i=1}^{n_c} f_{ni}^2} \quad (2.29)$$

The minimization of this criterion, through the satisfaction of the friction cone constraints leads to the minimization of the contact force distribution.

### 2.4.2 Volume of the Manipulability Ellipsoid

Multifingered robot hands consist of separate robot manipulators that play the role of fingers. As such, their kinematics is constrained both by the architecture of the hand's mechanism and by the mechanical limits of the hand's joints. This affects

and constrains the fingertips' ability for force and velocity exertion. In particular, the velocity and force transmission characteristics of a manipulator at any posture can be represented geometrically as ellipsoids [36]. Consider a unit sphere in the joint velocity space:

$$\dot{\mathbf{q}}^T \dot{\mathbf{q}} = \mathbf{1} \quad (2.30)$$

and also the minimum-norm solution of eq. 2.21:

$$\dot{\mathbf{q}} = \mathbf{J}^\dagger(\mathbf{q})\dot{\mathbf{x}} \quad (2.31)$$

where

$$\mathbf{J}^\dagger = \mathbf{J}^T(\mathbf{J}\mathbf{J}^T)^{-1} \quad (2.32)$$

is the right pseudo-inverse of  $\mathbf{J}$ . If we substitute eq. 2.31 into eq. 2.30, we derive:

$$\dot{\mathbf{x}}^T(\mathbf{J}^{\dagger T}(\mathbf{q})\mathbf{J}^\dagger(\mathbf{q}))\dot{\mathbf{x}} = \mathbf{1} \quad (2.33)$$

which, through eq. 2.32 yields:

$$\dot{\mathbf{x}}(\mathbf{J}(\mathbf{q})\mathbf{J}^T(\mathbf{q}))^{-1}\dot{\mathbf{x}} = \mathbf{1} \quad (2.34)$$

the equation which maps the unit ball in the joint space to the points on the surface of an ellipsoid in the end-effector velocity space, each component of which is expressed in the corresponding contact frame  $\{\mathbf{C}_i\}$ . This ellipsoid is referred to as the "Velocity Manipulability Ellipsoid". The volume of the ellipsoid is proportional to the quantity:

$$\mathbf{M}(\mathbf{q}) = \sqrt{\det(\mathbf{J}(\mathbf{q})\mathbf{J}^T(\mathbf{q}))} \quad (2.35)$$

which is called the "Manipulability Measure". This measure expresses the ability of the end effector to exert velocities. Therefore, maximizing it, we also maximize the ability of the end effector to locally move to a random direction. Thus, the redundancy of the hand's degrees of freedom is exploited to move away from singularities [37]. The latter represents the way this measure is going to be incorporated in this thesis.

### 2.4.3 Measure of Distance from Mechanical Joint Limits

The motors in the robot joints usually have mechanical limits. This implies that the hand's configurations are constrained by the kinematic abilities of the finger joint motors. In order to ensure that a grasp is implemented in a feasible way wrt the robot hand's kinematic abilities we can use the following metric, defined in [35]:

$$Q(\mathbf{q}) = \sum_{i=1}^{n_q} \left( \frac{q_i - q_{0i}}{q_{max_i} - q_{min_i}} \right)^2 \quad (2.36)$$

where  $q_i$  is the  $i$ -th joint angle,  $q_{0i}$  is the middle range position of the  $i$ -th joint and  $q_{max_i}$ ,  $q_{min_i}$  are the corresponding upper and lower bounds respectively. By minimizing  $Q$ , the joint angles tend to be positioned in the middle of their mechanical limits. Hence, this quality metric forces the configuration inside the feasible region.

## 2.4.4 Task Compatibility

### Hand-Object Jacobian

Depending on the task, the requirements for force and velocity transmission to the grasped object may differ. Therefore, there arises the need of a transformation that describes the transmission of joint velocities and torques to the object's twist and wrench respectively. According to [35], the relationship between the hand space and the object space is given by the hand-object Jacobian, which is subsequently derived.

From eqs. (2.21) and (2.22), we derive the following equation:

$$\mathbf{G}^T \boldsymbol{\nu} = \mathbf{J} \dot{\mathbf{q}} \quad (2.37)$$

Then

$$\boldsymbol{\nu} = (\mathbf{G}^\dagger)^T \mathbf{J} \dot{\mathbf{q}} \quad (2.38)$$

where

$$\mathbf{G}^\dagger = \mathbf{G}^T (\mathbf{G} \mathbf{G}^T)^{-1} \quad (2.39)$$

is the right inverse of the Grasp Matrix  $\mathbf{G}$ .

Now we can define the *Hand-Object Jacobian* [35, 38] as the matrix:

$$\mathbf{H} = (\mathbf{G}^\dagger)^T \mathbf{J} \quad (2.40)$$

and rewrite eq. (2.38) as:

$$\boldsymbol{\nu} = \mathbf{H} \dot{\mathbf{q}} \quad (2.41)$$

This equation maps the joint angular velocities to the grasped object's twist. Besides, from eq. (2.23), we can derive:

$$\mathbf{f} = \mathbf{G}^\dagger \mathbf{g} \quad (2.42)$$

which when substituted to eq. (2.24), yields:

$$\boldsymbol{\tau} = \mathbf{J}^T \mathbf{G}^\dagger \mathbf{g} \quad (2.43)$$

This is equal to:

$$\boldsymbol{\tau} = \mathbf{H}^T \mathbf{g} \quad (2.44)$$

which maps the wrench exerted to the grasped object to the required torques that produce it.

### Force/Velocity Ellipsoids

Consider a unit ball in the space of the joint angular velocities:

$$\dot{\mathbf{q}}^T \dot{\mathbf{q}} = \mathbf{1} \quad (2.45)$$

Then through eq. (2.41), we can easily derive:

$$\boldsymbol{\nu}^T (\mathbf{H} \mathbf{H}^T)^{-1} \boldsymbol{\nu} = \mathbf{1} \quad (2.46)$$

Furthermore, if we consider a unit ball in the domain of the joint torques:

$$\boldsymbol{\tau}^T \boldsymbol{\tau} = 1 \quad (2.47)$$

then through eq. (2.44), we derive:

$$\mathbf{g}^T (\mathbf{H}\mathbf{H}^T) \mathbf{g} = 1 \quad (2.48)$$

The aforementioned equations can be geometrically represented as ellipsoids in the domains of the joint angular velocities and joint torques respectively. The matrices  $(\mathbf{H}\mathbf{H}^T)^{-1}$  and  $(\mathbf{H}\mathbf{H}^T)$  are the inverse of each other and consequently they have the same eugenvalues and eigenvectors and also the same volume. Hence, their principal axes coincide, but their respective lengths are in inverse proportion. This means that the direction with the maximum force transmission ratio is coincident with the direction with the minimum velocity transmission ratio. From this observation, we should point out the following:

- The optimal direction for velocity transmission is the direction of the major axis of the velocity ellipsoid, because along this, the velocity transmission ratio is maximum. Similarly, The optimal direction for force transmission is the direction of the major axis of the force ellipsoid, because along this, the force transmission ratio is maximum.
- The optimal direction for achieving accurate control of velocity is along the direction of the minor axis of the velocity ellipsoid, while the optimal direction for achieving accurate force control is along the direction of the minor axis of the force ellipsoid.

More on ellipsoids can be found in [37] and in [36].

### **Wrench/Twist Transmission Ratios**

The distance between the center of an ellipsoid and its surface along a particular direction is commonly referred to as the *transmission ratio* along this direction [36]. Hence, consider a direction defined by the unit vector  $\boldsymbol{\eta} \in \mathbb{R}^6$ . Let  $\alpha$  be a scalar that represents the distance from the center to the surface of the force ellipsoid along the vector  $\boldsymbol{\eta}$  and  $\beta$  be a scalar that represents the distance from the center to the surface of the velocity ellipsoid. Then the vectors  $\alpha\boldsymbol{\eta}$  and  $\beta\boldsymbol{\eta}$  must satisfy the following equations:

$$(\alpha\boldsymbol{\eta})^T (\mathbf{H}\mathbf{H}^T) (\alpha\boldsymbol{\eta}) = 1 \quad (2.49)$$

and

$$(\beta\boldsymbol{\eta})^T (\mathbf{H}\mathbf{H}^T)^{-1} (\beta\boldsymbol{\eta}) = 1 \quad (2.50)$$

Then we can derive the expressions of the force and velocity transmission ratios:

$$\alpha = [\boldsymbol{\eta}^T (\mathbf{H}\mathbf{H}^T) \boldsymbol{\eta}]^{-1/2} \quad (2.51)$$

and

$$\beta = [\boldsymbol{\eta}^T (\mathbf{H}\mathbf{H}^T)^{-1} \boldsymbol{\eta}]^{-1/2} \quad (2.52)$$

Physically, the transmission ratios express how much a unitary change of the joint angular velocities and of the joint torques can affect the wrench and twist on the object's center of mass. Therefore, given a task's requirements in wrench/twist transmission to the object (mainly the desired direction  $\boldsymbol{\eta}$ ), in order to ensure that our mechanism will be mechanically able to transmit wrench and twist to the grasped object along the required directions, we have to maximize the corresponding transmission ratios. The maximization of each of the transmission ratios, geometrically can be thought as an alignment with the principal axis of the corresponding ellipsoid.

### Grasp Compatibility Index

From the previous observations and definitions, it is obvious that by varying the hand's configuration and the points at which the hand makes contact with the object, we can control its ability of contributing to the grasped object's wrench and twist. In particular, the variation of the hand's kinematics can lead to different postures which are characterized by ellipsoids of different shapes and orientations. Hence, by adopting postures that align the optimal directions for force and velocity transmission or control for the hand's mechanism with the corresponding requirements in the object's wrench and twist space, we can maximize the grasp's compatibility with the task. In this direction, Chiu has proposed a task compatibility index for postures of general manipulators [36]. If we generalize his work for the case of a multi-fingered robot hand, we can derive the following index:

$$C = \sum_{i=1}^l w_i \alpha_i^{\pm 2} + \sum_{j=l+1}^m w_j \beta_j^{\pm 2} \quad (2.53)$$

where  $\alpha_i, i = 1, 2, \dots, l$  and  $\beta_j, j = l + 1, l + 2, \dots, m$  are the force and velocity transmission ratios respectively along the directions of interest. The + sign is used for the directions along which the magnitude is of interest, while, the - sign is used for the directions along which the control accuracy is of interest.  $w_i$  and  $w_j$  are weighting factors that indicate the relative magnitude or accuracy requirements in the respective task directions. Thus, by finding the hand's posture that maximizes this index, we can achieve optimal performance wrt a grasp's requirements in force and velocity transmission and control.

## 2.5 Assumptions

The grasping optimization problems that are presented in this thesis are based on the following assumptions:

- The grasped object's geometry is analytically available (results are presented for the case of a sphere and a cylinder). In experimental applications, a tactile and vision system can provide the required information for the developed schemes and algorithms.
- The hand's fingers can transmit through their fingertips contact forces to arbitrary directions.

- The object’s weight is the only external wrench that we consider to be exerted at the object’s center of mass.
- The value of the friction coefficient is set to 0.8, since between the surfaces of the DLR hand’s fingertips and a typical everyday life object such as a cup, high frictional forces can be produced.
- The robot hand is capable of exerting the required magnitudes of force and velocity that are produced from the execution of the algorithms presented.
- The formulations only consider the robot hand’s kinematics. It is assumed that the hand will be attached on the end effector of a dexterous manipulator which will be able to provide the wrist’s position/orientation that is extracted by the execution of the developed algorithms.
- The grasps that are studied are *static*, i.e. , no motion of the grasped object is considered. Hence the inertia terms are negligible.

## 2.6 Model adaptation: DLR/HIT II

Throughout this thesis, we have adopted the kinematic model of the DLR/HIT II five-fingered robot hand in order to conduct our simulation study and verify the developed optimization algorithms and schemes.

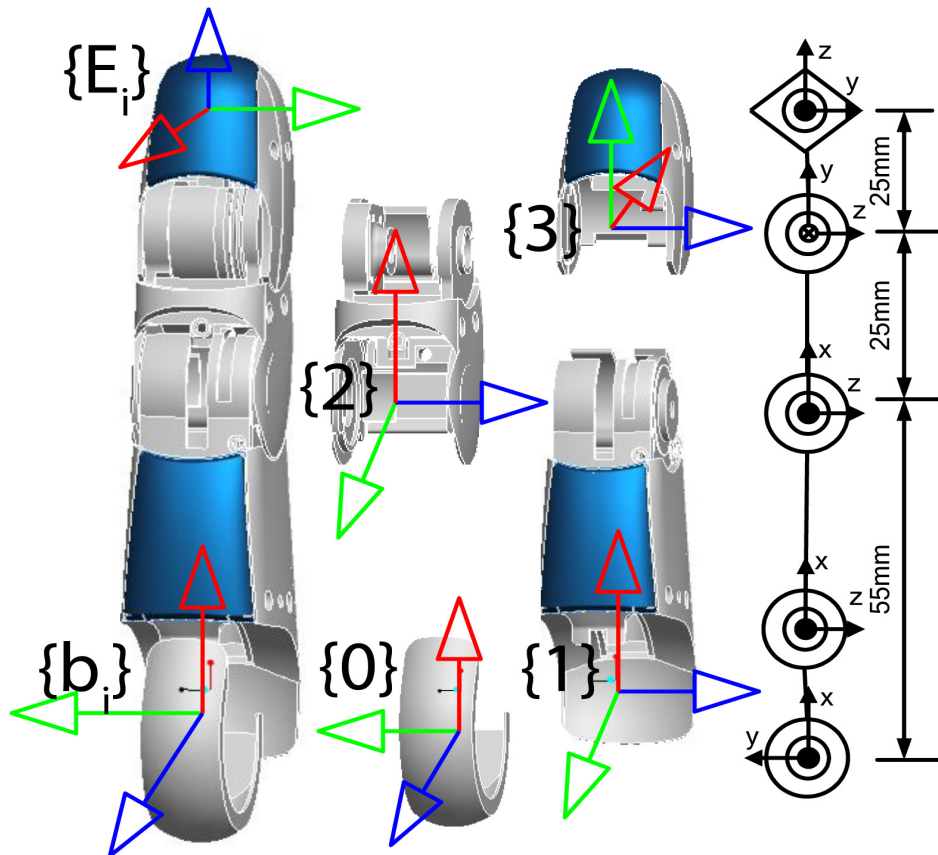


**Figure 2.2** – DLR/HIT II: DOFs of its fingers-Figure extracted from the documentation of the hand, courtesy of DLR German Aerospace Center [2].

The DLR/HIT Hand II (table 2.1) is a robot hand jointly developed by DLR (German Aerospace Center) and HIT (Harbin Institute of Technology). It is a multisensory five-fingered hand with in total fifteen DOFs. The hand consists of an independent palm and five identical modular fingers, each of which consists of four joints and has three DOFs. Fig. 2.2 illustrates the DOFs of each finger of the robot hand. In particular, each finger's kinematics is defined by the movement of the rotational joints 0, 1, 2 and 3, around the  $z$  axes (blue color). Motors are placed at joints 0, 1 and 2, while the 3rd joint is mechanically coupled with the 2nd in a 1:1 ratio.

**Table 2.1** – DLR/HIT II: Alternative views of the model of the NeuroRobotics Group.

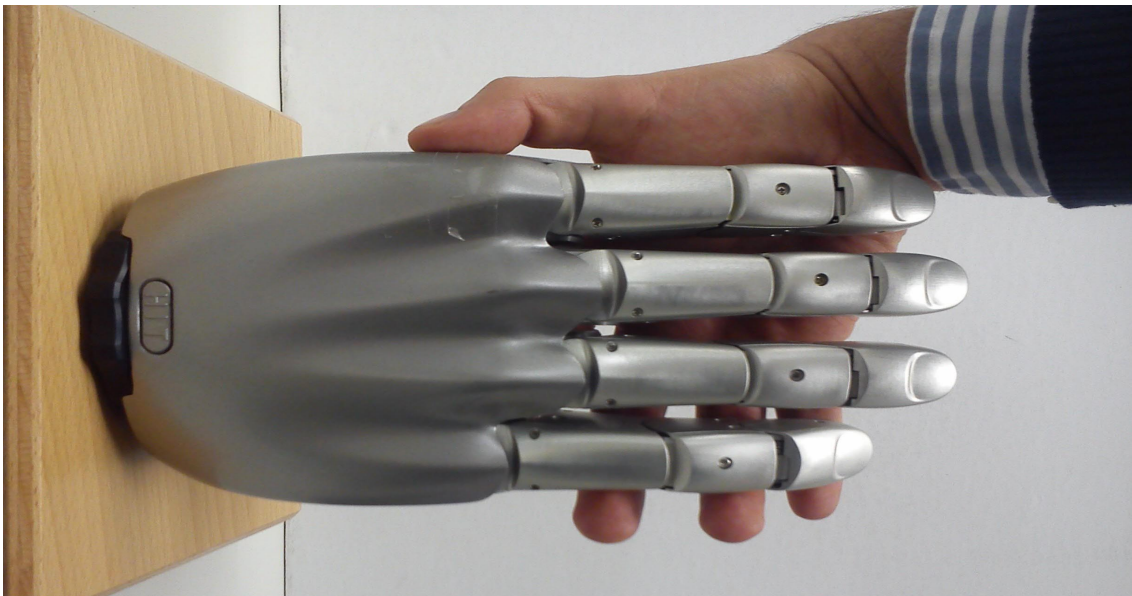


**Figure 2.3** – DLR/HIT II: The model of our lab. As it can be seen, its size is comparable to the size of an adult's hand. In particular it is about 20% bigger.

All actuators, gears, electronics and communication controllers for each finger are fully integrated in the finger's base or the finger's body directly. The DLR/HIT Hand II is close to the size of an adult human hand (Fig. 2.3). The weight of the hand is about 1.5 kg. More information about the DLR/HIT Hand II can be found in [12].

## 2.7 Summary of adopted notations

In this section we summarize the most significant notations adopted in this chapter and we update them wrt DLR/HIT II five-fingered Robot Hand's kinematics and the assumptions that have been made regarding the grasping problem (see table 2.2). In the following chapters the developed methodologies will be presented in a general form, with the symbols and notations of this chapter.

**Table 2.2** – Adopted notations, their definitions and assumed values

Notation	Definition
$n_c = 5$	Number of contacts
$n_q = 15$	Number of joints of the hand
$\boldsymbol{\nu} \in \mathcal{R}^6$	Twist at the Object's center of mass
$\mathbf{g} \in \mathcal{R}^6$	Wrench at the object's center of mass
$\mathbf{w} \in \mathcal{R}^6$	The Object's weight
$\mu = 0.8$	Friction Coefficient at the contacts
$\mathbf{w} \in \mathcal{R}^6$	Wrist's Position/Orientation
$\mathbf{f} \in \mathcal{R}^{15}$	Contact forces
$\mathbf{q} \in \mathcal{R}^{15}$	Joint displacements of independent DOFs
$\boldsymbol{\tau} \in \mathcal{R}^{15}$	Joint torques
$\{\mathbf{N}\}$	Fixed global reference frame
$\{\mathbf{C}_i\}$	Frame at contact $i$
$\{\mathbf{B}\}$	Frame fixed at the object's center of mass
$\{\mathbf{W}\}$	Frame fixed at the hand's wrist
$\mathbf{G} \in \mathcal{R}^{6 \times 15}$	Grasp Matrix
$\mathbf{J} \in \mathcal{R}^{15 \times 15}$	Hand Jacobian
$\mathbf{H} \in \mathcal{R}^{6 \times 15}$	Hand-Object Jacobian
$F$	Norm of the Normal Contact Force Components
$M$	Volume of the Manipulability Measure
$Q$	Measure of Distance from Mechanical Joint Limits
$C$	Grasp Compatibility Index

---

# CHAPTER 3

## Elements of Nonlinear Programming

The grasping problem, i.e., the problem of finding a set of contact forces in order to satisfy the force closure sufficient conditions, is a problem with an infinite number of solutions. Therefore, it can be formulated as an optimization problem. In particular, it can be characterised as a nonlinearly constrained optimization problem due to the nonlinear nature of the friction cone constraints that need to be satisfied. Furthermore, upon the introduction of constraints imposed by the physical environment as well as of the mechanical nature of the robot hand, the problem can become strongly constrained, more complicated and computationally intense. Besides, even the selection of the objective function and the decision variables can play a role on such issues. In a problem such as grasping, such issues need to be studied in order for the developed algorithms to work efficiently in real-time mode. Nevertheless, the objective of this thesis is more fundamental; to propose complete schemes for the selection and computation of grasps. Therefore, optimization is treated as a useful tool and not as the main element of interest. However, a complete presentation of the work conducted in the context of this thesis, has to include basic elements of Nonlinear Programming.

### 3.1 Nonlinear Programming Problem Definition

Consider a vector  $\mathbf{x} = [x_1 \ x_2 \ \dots \ x_n]^T \in \mathfrak{R}^n$ . A general optimization problem is the problem of selecting the  $n$  values  $x_1, x_2, \dots, x_{n_x}$  in such a way as to optimize (minimize or maximize) a given function  $f(x_1, x_2, \dots, x_{n_x})$ . The elements of  $\mathbf{x}$  and the function  $f$  are commonly referred to as "decision variables" and "objective function" respectively. The solution  $\mathbf{x}$  to the problem can be subject to constraints (constrained problem) or not (unconstrained problem). In the first case, the solution vector  $\mathbf{x}$  can be everywhere in  $\mathfrak{R}^{n_x}$ , while in the second case it has to lie inside a specified subset of  $\mathfrak{R}^{n_x}$ . The space  $\mathbf{X}$  where the vector  $\mathbf{x}$  has to belong is the "feasible region" of the problem.

The problem is called a *nonlinear programming problem* (NLP) if the objective function is nonlinear and/or the feasible region is determined by nonlinear constraints. Thus, in minimization form, the general nonlinear program can be described as:

$$\mathbf{x}^* = \underset{\mathbf{x}}{\operatorname{argmin}} f(\mathbf{x}) \quad (3.1)$$

subject to:

$$\mathbf{g}(\mathbf{x}) \leq \mathbf{0} \quad (3.2)$$

$$\mathbf{h}(\mathbf{x}) = \mathbf{0} \quad (3.3)$$

$$\mathbf{x} \in \mathbf{X} \quad (3.4)$$

where 3.3 and 3.4 contain respectively the inequality and equality constraints of the problem. The constraint functions  $\mathbf{g}$  and  $\mathbf{h}$  are defined as follows:  $\mathbf{h} : \mathbf{X} \rightarrow \mathfrak{R}^{n_h}$  and  $\mathbf{g} : \mathbf{X} \rightarrow \mathfrak{R}^{n_g}$ . By  $\mathbf{x}^*$  we denote a local optimal solution (i.e., local minimum) of the NLP which minimizes the objective function. Throughout this thesis the formulation of the optimization problems presented is done in minimization form.

## 3.2 Optimality Conditions for General NLP Problems

Based on the definition of the NLP problem of the previous section, we define the necessary and sufficient conditions for optimality.

### Theorem 1 (First and Second-Order Necessary Conditions).

Let  $f : \mathfrak{R}^{n_x} \rightarrow \mathfrak{R}$ ,  $g_i : \mathfrak{R}^{n_x} \rightarrow \mathfrak{R}, i = 1, \dots, n_g$  and  $h_j : \mathfrak{R}^{n_x} \rightarrow \mathfrak{R}, j = 1, \dots, n_h$  be twice continuously differentiable functions on  $\mathfrak{R}^{n_x}$ . Consider the problem (P) to minimize  $f(\mathbf{x})$  subject to the constraints  $\mathbf{g}(\mathbf{x}^*) = \mathbf{0}$  and  $\mathbf{h}(\mathbf{x}^*) = \mathbf{0}$ . If  $\mathbf{x}^*$  is a local minimum of the (P) problem and is a regular point of the constraints, then there exist unique vectors (Lagrange Multipliers)  $\boldsymbol{\mu}^* \in \mathfrak{R}^{n_g}$  and  $\boldsymbol{\lambda}^* \in \mathfrak{R}^{n_h}$  such that

$$\nabla f(\mathbf{x}^*) + \nabla \mathbf{g}(\mathbf{x}^*)^T \boldsymbol{\mu}^* + \nabla \mathbf{h}(\mathbf{x}^*)^T \boldsymbol{\lambda}^* = \mathbf{0} \quad (3.5)$$

$$\boldsymbol{\mu}^* \geq \mathbf{0} \quad (3.6)$$

$$\mathbf{g}(\mathbf{x}^*) \leq \mathbf{0} \quad (3.7)$$

$$\mathbf{h}(\mathbf{x}^*) = \mathbf{0} \quad (3.8)$$

$$\boldsymbol{\mu}^{*\top} \mathbf{g}(\mathbf{x}^*) = 0 \quad (3.9)$$

and

$$\mathbf{y}^T (\nabla^2 f(\mathbf{x}^*) + \nabla^2 \mathbf{g}(\mathbf{x}^*)^T \boldsymbol{\mu}^* + \nabla^2 \mathbf{h}(\mathbf{x}^*)^T \boldsymbol{\lambda}^*) \mathbf{y} \geq 0 \quad (3.10)$$

for all  $\mathbf{y}$  such that  $\nabla g_i(\mathbf{x}^*)^T \mathbf{y} = 0, i \in \mathcal{A}(\mathbf{x}^*)$  and  $\nabla \mathbf{h}(\mathbf{x}^*)^T \mathbf{y} = \mathbf{0}$ , where  $\mathcal{A}(\mathbf{x}^*)$  is the set containing the active constraints. ■

By the term "active" we denote the constraints that are on the feasible boundaries. Equations (3.5-3.9) are commonly referred to as the Karush-Kuhn-Tucker Conditions (KKT).

### Theorem 2 (Second-Order Sufficient Conditions).

Let  $f : \mathfrak{R}^{n_x} \rightarrow \mathfrak{R}$ ,  $g_i : \mathfrak{R}^{n_x} \rightarrow \mathfrak{R}, i = 1, \dots, n_g$  and  $h_j : \mathfrak{R}^{n_x} \rightarrow \mathfrak{R}, j = 1, \dots, n_h$  be twice continuously differentiable functions on  $\mathfrak{R}^{n_x}$ . Consider the problem (P) to minimize  $f(\mathbf{x})$  subject to the constraints  $\mathbf{g}(\mathbf{x}^*) = \mathbf{0}$  and  $\mathbf{h}(\mathbf{x}^*) = \mathbf{0}$ . If there exist  $\mathbf{x}^*, \boldsymbol{\mu}^*$  and  $\boldsymbol{\lambda}^*$  satisfying the KKT conditions and

$$\mathbf{y}^T \nabla_{xx}^2 \mathcal{L}(\mathbf{x}^*, \boldsymbol{\mu}^*, \boldsymbol{\lambda}^*) \mathbf{y} > 0$$

for all  $\mathbf{y} \neq \mathbf{0}$  such that

$$\begin{aligned}\nabla g_i(\mathbf{x}^*)^\top \mathbf{y} &= 0, \quad i \in \mathcal{A}(\mathbf{x}^*) \text{ with } \mu_i^* > 0 \\ \nabla g_i(\mathbf{x}^*)^\top \mathbf{y} &\leq \mathbf{0}, \quad i \in \mathcal{A}(\mathbf{x}^*) \text{ with } \mu_i^* = 0 \\ \nabla \mathbf{h}(\mathbf{x}^*)^\top \mathbf{y} &= 0\end{aligned}$$

where  $\mathcal{L}^4 = f(\mathbf{x}) + \boldsymbol{\mu}^\top \mathbf{g}(\mathbf{x}) + \boldsymbol{\lambda}^\top \mathbf{h}(\mathbf{x})$ , then  $\mathbf{x}^*$  is a strict local minimum of (P). ■

### 3.3 Optimization Methods

Optimization problems can be categorized to many different categories, depending on whether the search space is continuous or discrete, whether a local or a global minimum is being searched and even whether the principles that govern the examined system are deterministic or stochastic. In order to confront the various different difficult nonlinear optimization problems, numerous different approaches have been employed. A complete, thorough and up to date overview of the most significant works and algorithms can be found in [39].

In general, the optimization approaches can largely be divided in two main categories: the deterministic and the stochastic. With the term *deterministic* we refer to the approaches that use the generalized the derivative of the objective function, whose values can either be straightway calculated or approximated. On the contrary, the main characteristic of stochastic approaches is that they use elements of random search of the optimal solution. Modern approaches also include the development of hybrid optimization algorithms which simultaneously combine elements from both approaches [40]. The main advantage of the deterministic approaches is that they can converge more easily. However, when a global minimum is demanded there exists the danger that they are trapped in a local minimum. On the other hand, the stochastic approaches are more general and can be more easily modified to solve different types of problems. They can trace the global minimum independently to their initial conditions setting. However their main disadvantage is that they are comparatively slow. In the world of robotics, the computational time is a significant factor that has to be taken into consideration for the real-time implementation of all studies. Therefore, in this thesis, the development of all grasp synthesis algorithms has been made by adopting deterministic approaches.

### 3.4 Optimization Software

The problems that are described and formulated in the following chapters, are solved using *fmincon* (with the exception of chapter 7, in the context of which a custom algorithm was developed), a powerful routine for Constrained Nonlinear Optimization problems, developed by Mathworks [41] for the MATLAB Optimization Toolbox [42]. *Fmincon* includes a series of optimization algorithms, each of which can be more or less suitable depending on the type of the optimization problem that one has to solve.

---

<sup>4</sup>The "Lagrangian" of (P)

Throughout this thesis, due to the nonlinear complicated nature of the grasping problems that we are studying, the "Active-Set" algorithm was chosen. Its solution procedure consists of two phases. The first phase involves the calculation of a feasible point. The second phase involves the generation of an iterative sequence of feasible points that converge to the solution. In this method an *active set*  $\bar{\mathbf{A}}_{\mathbf{k}}$  is maintained that is an estimate of the active constraints at the solution point.  $\bar{\mathbf{A}}_{\mathbf{k}}$  is updated at each iteration  $\mathbf{k}$ , and this is used to form a basis for a search direction  $\mathbf{d}_{\mathbf{k}}$ . Equality constraints always remain in the active set. The search direction  $\mathbf{d}_{\mathbf{k}}$  is calculated and minimizes the objective function while remaining on any active constraint boundaries. The feasible subspace for  $\mathbf{d}_{\mathbf{k}}$  is formed from a basis  $\mathbf{Z}_{\mathbf{k}}$  whose columns are orthogonal to the estimate of the active set  $\bar{\mathbf{A}}_{\mathbf{k}}$  (i.e.,  $\bar{\mathbf{A}}_{\mathbf{k}}\mathbf{Z}_{\mathbf{k}} = \mathbf{0}$ ). Thus a search direction, which is formed from a linear summation of any combination of the columns of  $\mathbf{Z}_{\mathbf{k}}$ , is guaranteed to remain on the boundaries of the active constraints (more on *fmincon*, the *active-set* algorithm and the rest of them that it supports can be found in [42]).

---

## CHAPTER 4

# Grasp Quality Optimization for Multifingered Robot Hands

In this chapter, a general Grasping Force Optimization Scheme is presented. We aim at satisfying the force closure sufficient conditions, grasping an object of known geometry at contact points which guarantee the use of low contact force distribution and also favor the ability of the fingers for local force exertion. The general idea for the development of this optimization scheme is illustrated in Fig. 4.1. In particular, the Optimization Algorithm takes as input the grasped object's properties (i.e., its surface geometry, the friction coefficient and weight) and an initial grasp (i.e., random contact points produced by a feasible configuration) and generates a force closure grasp with a feasible configuration. The final grasp is optimal wrt a function, the minimization of which guarantees a low force distribution and good ability of the hand's mechanism for force/velocity exertion at the contact points.

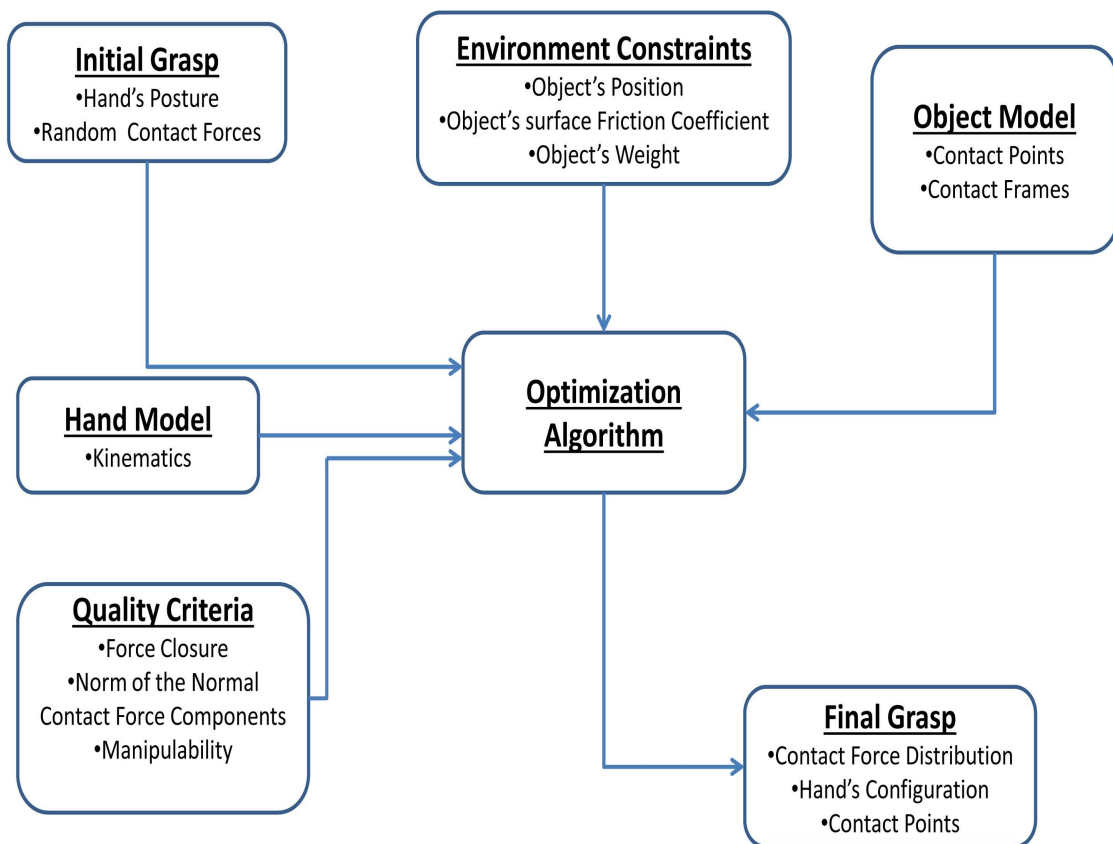


Figure 4.1 – A diagram of the proposed optimization scheme.

Subsequently, we formulate the optimization problem for a hand actuated by fifteen DOFs and present results from a simulation study for the DLR/HIT II. Finally we discuss the results and the whole approach.

## 4.1 Problem Formulation

For the case of a five-fingered robot hand grasping an object with five "Hard Finger" fingertip contacts, there can be numerous different contact force distributions that lead to Force Closure of an object. This is because the total number of the contact force components (15) is greater than the dimension of the object's external wrench (6) which means that the problem of finding contact forces that compensate the object's wrench is a typical statically indeterminate problem [43], although the friction cone constraints limits the feasible solutions set.

A solution to the problem of finding the contact forces that lead to the object's state of equilibrium, can be found from eq. (2.27) if we inverse the Grasp Matrix [44]:

$$\mathbf{f} = \mathbf{G}^\dagger(-\mathbf{w}) + \mathbf{V}\boldsymbol{\lambda} \in \mathfrak{R}^{3n_c} \quad (4.1)$$

where  $\mathbf{V} = (\mathbf{I} - \mathbf{G}^\dagger\mathbf{G})$ . The first component represents the contact forces that compensate for the object's wrench, while the second component represents the internal forces produced during the grasp. The columns of  $\mathbf{V}$  form the basis of the null space of  $\mathbf{G}$  and the vector of free variables  $\boldsymbol{\lambda}$  has the same dimension with the null space of  $\mathbf{G}$ . In the case of a five-fingered robot hand, which grasps objects in the 3D space with the assumption of the "Hard Finger" Contact Model,  $\mathbf{G} \in \mathfrak{R}^{6 \times 3n_c}$  and consequently  $\boldsymbol{\lambda} \in \mathfrak{R}^{3n_c}$ .

By adopting the aforementioned force expression, the Force Closure requirement can be satisfied if we find a force distribution  $\mathbf{f} \in \mathfrak{R}^{3n_c}$  which also satisfies the friction cone constraints at the fingertip contacts. However, for a real mechanism such as a multifingered robot hand, there are also additional constraints associated with the mechanical and geometric limitations of the hardware. In particular, a complete algorithm has to lead to configurations and contact points that are compatible with the kinematic capabilities of the hand, respecting the angular limitations of the fingers' joint motors. Besides, collisions between fingers have to be prevented.

In order to find a solution to the problem described above, we have to select an appropriate objective function to minimize. Our approach aims at the minimization of an objective function which contains a component that minimizes contact forces (*Norm of the Normal Contact Force components*) and also a component that ensures the kinematic compatibility of the contact points with the mechanism of the hand (*Volume of the Manipulability Measure*). At the same time, inequality constraints ensure that the joint limits are not violated and that the fingers normal succession is guaranteed, leading to configurations that avoid collisions between the fingers. Besides, the requirement that the fingertips are in contact with the grasped object can be included in the formulation either implicitly (by considering the object's surface coordinates as decision variables representing the contact points) or explicitly (by considering the joints angular positions and requiring that the fingertips locations expressions wrt them are in contact with the object).

## 4.2 Optimization Scheme

Both aforementioned approaches are developed and discussed below.

### 4.2.1 Parametrized Surface Coordinates as Decision Variables

Given that the analytical description of an object's surface is available, we can represent each point on it by using two numbers, the parametrized surface coordinates. In this chapter we consider a cylindric object and therefore, each contact point can be defined by cylindrical coordinates. The definition of these coordinates is considered as shown in Fig. 4.2.

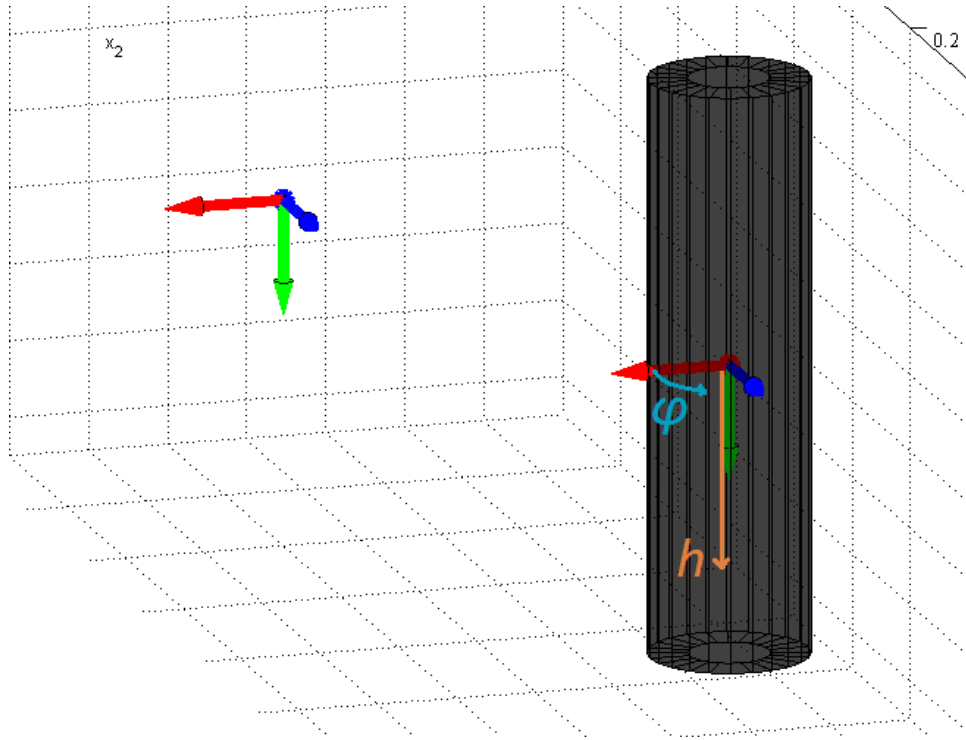


**Figure 4.2** – Definition of surface coordinates for a cylindric object.

In particular, a vector  $\mathbf{h} \in \mathbb{R}^{n_c}$  contains the height of each contact point along axis  $y$ , while a vector  $\boldsymbol{\phi} \in \mathbb{R}^{n_c}$  contains the angular displacement of each contact point around axis  $y$ . If we stack in a vector

$$\mathbf{p} = [\boldsymbol{\lambda}^T \quad \mathbf{h}^T \quad \boldsymbol{\phi}^T \quad \mathbf{w}^T]^T \in \mathbb{R}^{5n_c+6} \quad (4.2)$$

all the decision variables and denote by

$$z = w_F F(\mathbf{f}(\mathbf{p})) + w_M \frac{1}{M(\mathbf{q}(\mathbf{p}))} \quad (4.3)$$

the objective function that we want to minimize, the optimization problem can be formulated as follows:

$$\mathbf{p}^* = \underset{\mathbf{p}}{\operatorname{argmin}} z(\mathbf{p}) \quad (4.4)$$

s.t.

$$\sqrt{f_{t_i}(\mathbf{p})^2 + f_{o_i}(\mathbf{p})^2} \leq \mu f_{n_i}(\mathbf{p}), \quad i = 1 \dots n_c \quad (4.5)$$

$$\mathbf{q}_{\min} \leq \mathbf{q}(\mathbf{h}, \boldsymbol{\phi}, \mathbf{w}) \leq \mathbf{q}_{\max} \quad (4.6)$$

$$(\mathbf{h}, \boldsymbol{\phi}) \in \mathbf{S} \quad (4.7)$$

where  $w_F$  and  $w_M$  represent weighting factors of the two objective function components. The force distribution  $\mathbf{f}$  is calculated via eq. (6.1) and the joint angular positions are derived through the computation of the inverse kinematics of the fingers<sup>5</sup> at each iteration. The vectors  $\mathbf{q}_{\min} \in \mathbb{R}^{n_q}$  and  $\mathbf{q}_{\max} \in \mathbb{R}^{n_q}$  contain the lower and upper joint limits of the DLR hand respectively. The constraint 4.7 expresses the fingers succession requirement which forces the fingers to avoid collisions by keeping their natural succession imposed by the design of the hand. The set  $\mathbf{S}$  consists of all the feasible contact points wrt the collision avoidance.

## 4.2.2 Joint Angular Positions as Decision Variables

Likewise, our objective is to minimize the objective function

$$z = w_F F(\mathbf{f}(\mathbf{p})) + w_M \frac{1}{M(\mathbf{q})} \quad (4.8)$$

where the vector

$$\mathbf{p} = [\boldsymbol{\lambda}^T \quad \mathbf{q}^T \quad \mathbf{w}^T]^T \in \mathbb{R}^{3n_c + n_q + 6} \quad (4.9)$$

contains the decision variables of the problem. Therefore, the Optimization Problem is formulated as follows:

$$\mathbf{p}^* = \underset{\mathbf{p}}{\operatorname{argmin}} z(\mathbf{p}) \quad (4.10)$$

s.t.

$$\sqrt{f_{t_i}(\mathbf{p})^2 + f_{o_i}(\mathbf{p})^2} \leq \mu f_{n_i}(\mathbf{p}), \quad i = 1 \dots n_c \quad (4.11)$$

$$\mathbf{q}_{\min} \leq \mathbf{q} \leq \mathbf{q}_{\max} \quad (4.12)$$

$$\mathbf{s}(\mathbf{q}) \in \partial \mathbf{O} \quad (4.13)$$

$$\mathbf{s}(\mathbf{q}) \in \mathbf{S} \quad (4.14)$$

The basic difference from the previous formulation is the necessary introduction of the equality constraint (4.13) which forces the fingertips locations (derived through the forward kinematics) to lie on the boundary of the object,  $\partial \mathbf{O}$ . Although an equality constraint makes the problem more computationally intense and difficult to solve, the advantage of this formulation is that it is more general than the previous one and it can easily handle information for the object's surface geometry, acquired through the use of proper vision or tactile sensors. The force distribution  $\mathbf{f}$  is again calculated via eq. (4.1).

---

<sup>5</sup>The derivation of the Forward and Inverse Kinematics of the DLR/HIT Hand II five-fingered robot hand is presented in the Appendix Chapter.

### 4.3 Simulation Results

Simulation results are presented for the grasp of a cylindric object. The diameter of the object is 4 cm, its height is 15 cm and its weight is 2 N (supposed mass 200 gr). The weighting factors of the objective function components were chosen so as to bring both of them in the same scale in order to guarantee sufficient minimization of both. The robot hand initializes from a random posture and contact points and finally converges to a local minimum, respecting the friction cone constraints as well as the joint limits, avoiding simultaneously any singularities. Both approaches mentioned above were tested and comparative figures are provided.

#### 4.3.1 Parametrized Surface Coordinates as Decision Variables

For the description of the object only two variables were used: Figs. 4.3 and 4.4 depict different views of the initial (green color) and final (blue color) posture of the hand. Fig. 4.5 depicts the convergence of the combined objective function  $z$ , while fig. 4.6 illustrates the convergence of the components of the objective function. As it can be observed from the diagrams presented in Figs. 4.5 and 4.6, the algorithm initializes from an infeasible region wrt the constraints of the problem. This is why at the beginning the transitions from step to step are not smooth and in accordance with the required minimization of the objective function.

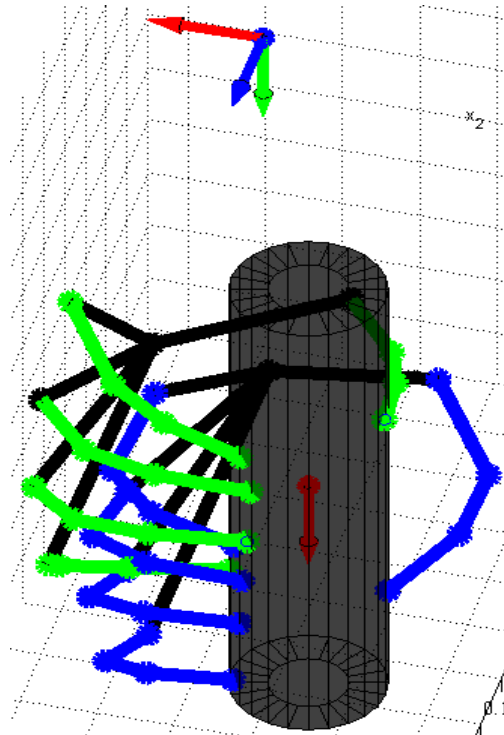


**Figure 4.3** – Surface coordinates as decision variables: Initial (green color) and final (blue color) posture of the robot hand. The object’s weight is drawn with a red vector at the object’s center of mass (it is coincident with  $y$  axis). The algorithm converged to this solution after about 70 iterations and terminated due to insufficient decrease of the objective function.

However, once an initial feasible point is found, the algorithm continues by implementing sequential minimization steps and finally, after about 70 iterations, converges, providing a force distribution whose norm of normal contact force components is equal to about 1.65 N. At the same time, the scaled manipulability inverse is kept in a low value, guaranteeing kinematic compatibility of the adopted postures with the hand's mechanism but also improvement of the ability of the mechanism for force exertion at the contact points. The algorithm terminated due to insufficient relative decrease of the objective function. In particular, after only 30 iterations the algorithm has approached in a satisfying level the final point of convergence. However, depending on the requirements set by the task to be executed and the hardware that we use, even small amounts of improvement of the objective function can be really significant. This is why the tolerance of the change in the value of the objective function is set to a very low value.

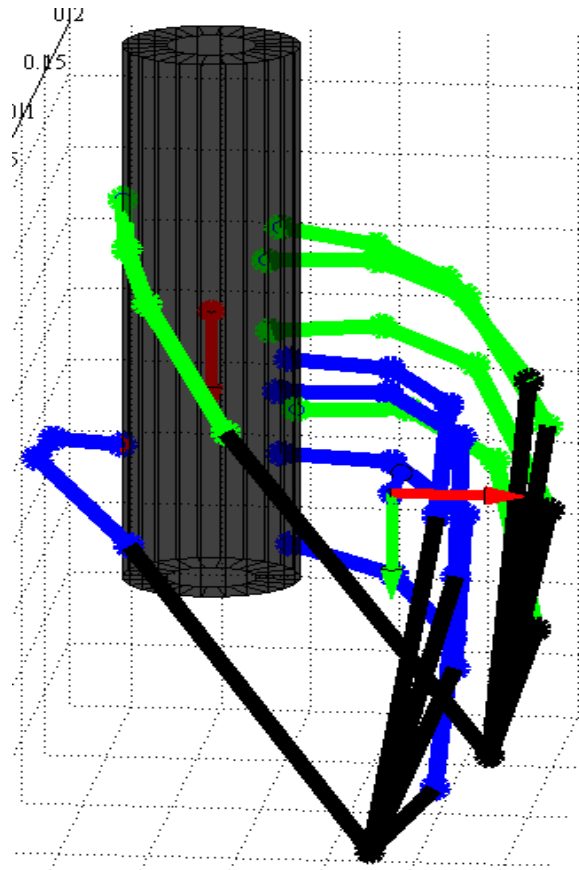


**Figure 4.4** – Surface coordinates as decision variables: Rear view of the initial (blue hand) and the final (green hand) hand's postures.

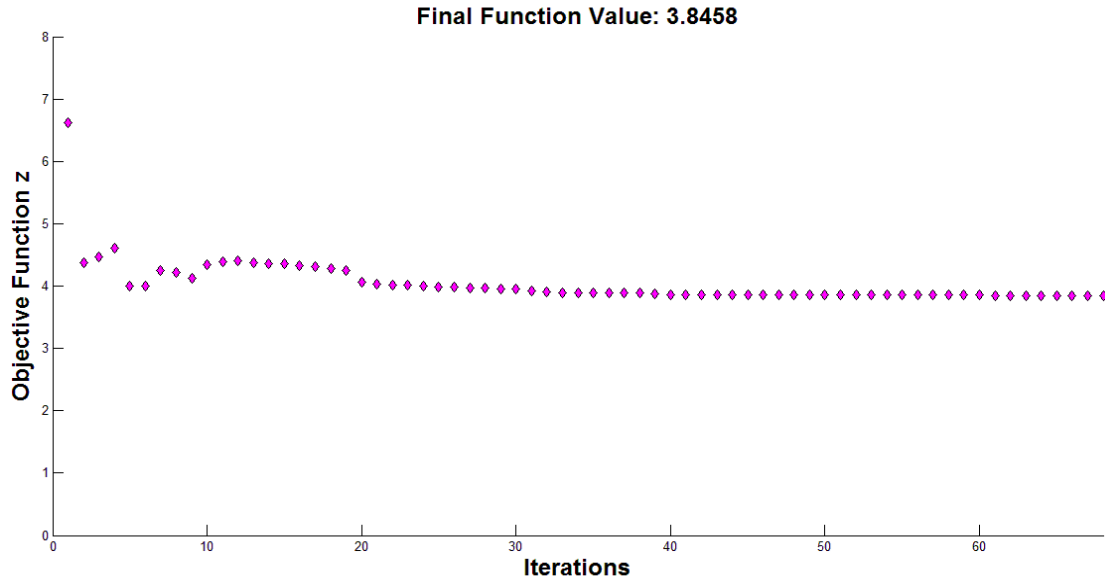


**Figure 4.5** – Surface coordinates as decision variables: Objective function convergence for the simulation depicted in Figs. 4.3 and 4.4.

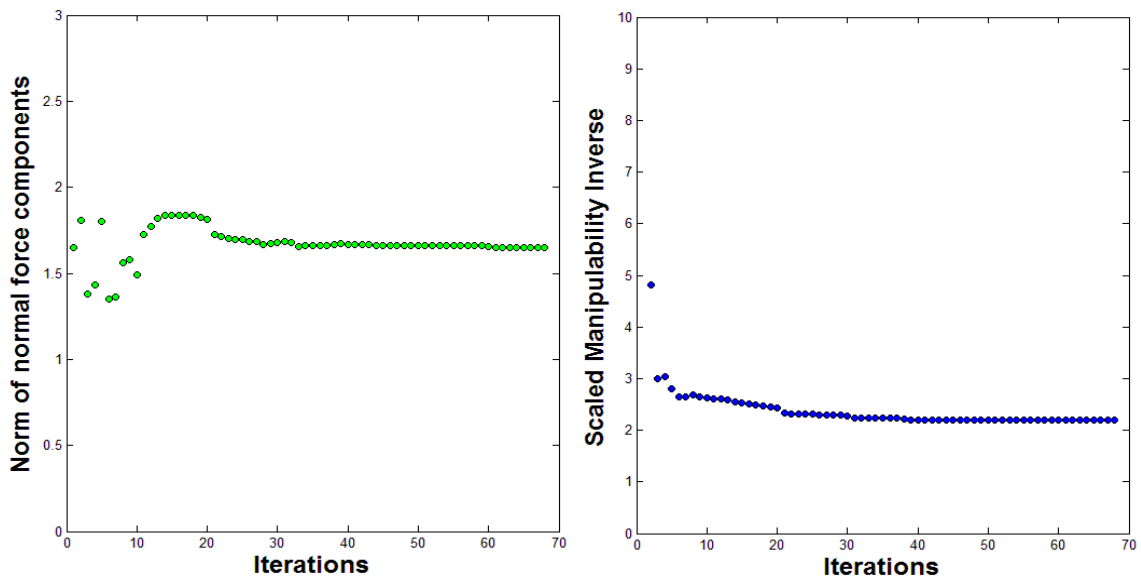


**Figure 4.6** – Surface coordinates as decision variables: Convergence of the Objective Function Components.

### 4.3.2 Joint Angular Positions as Decision Variables

The same types of figures are selected to present the results of the formulation described in section 4.2.2. Figs. 4.8 and 4.7 depict different views of the initial (green

color) and final hand's postures. Fig. 4.9 presents the convergence of the combined objective function, while fig. 4.10 presents the convergence of the components of the objective function. The hand initializes from the same posture as in the previous simulation. Its behavior during the sequential transitions is similar to the one presented in the previous section. However, the final posture and value of the objective function, as well as of its components is different. In particular, after about 70 iterations, after which no significant change of the value of the objective function were observed, the algorithm terminated, providing a final force distribution whose norm of the normal contact force components was about 2.2 N. The scaled manipulability inverse has the same behavior as in the previous formulation.



**Figure 4.7** – Joint angular displacements as decision variables: Initial (blue hand) and final (green hand) posture of the robot hand.

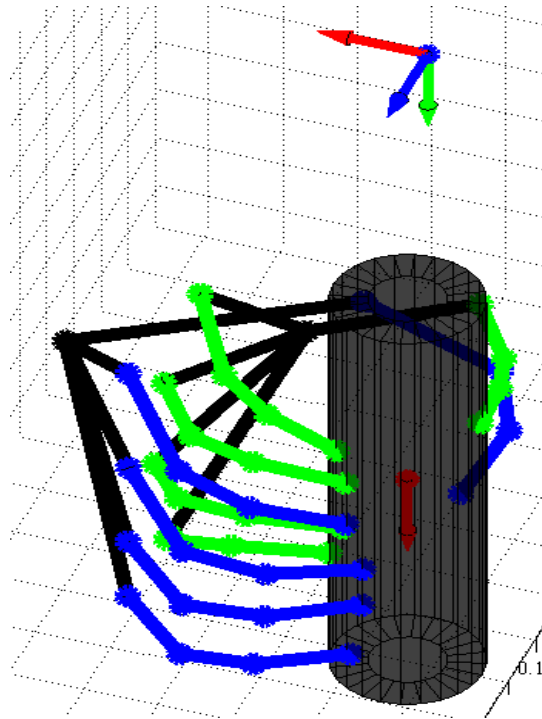


**Figure 4.8** – Joint angular displacements as decision variables: Initial (green color) and final (blue color) posture of the robot hand.

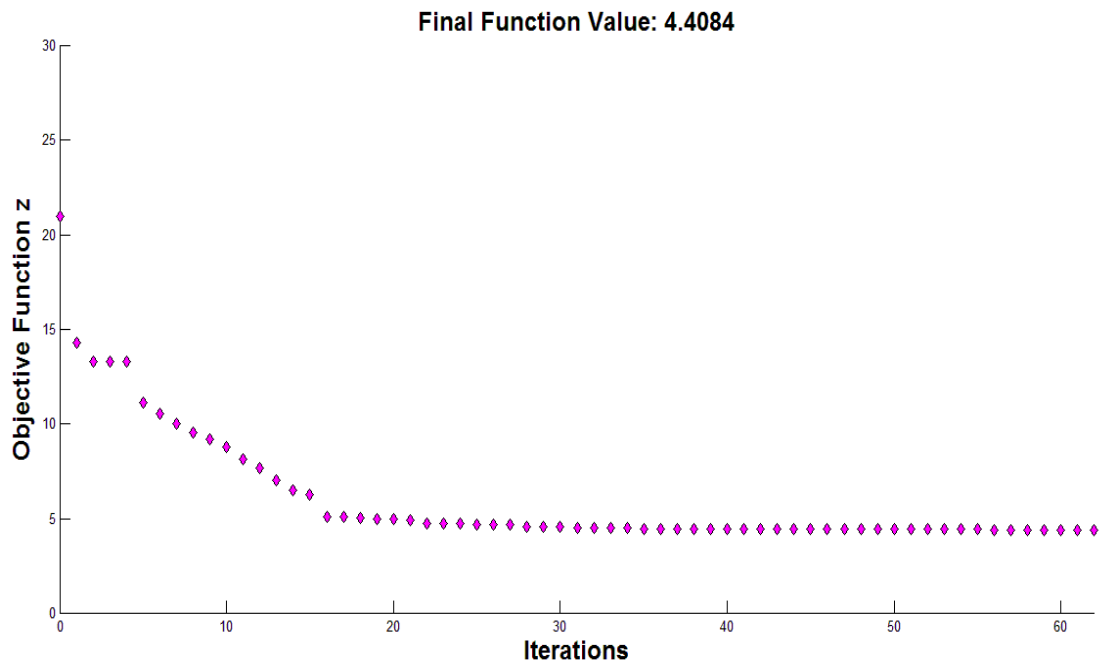


**Figure 4.9** – Joint angular displacements as decision variables: Objective function convergence for the simulation depicted in Figs. 4.8 and 4.7.

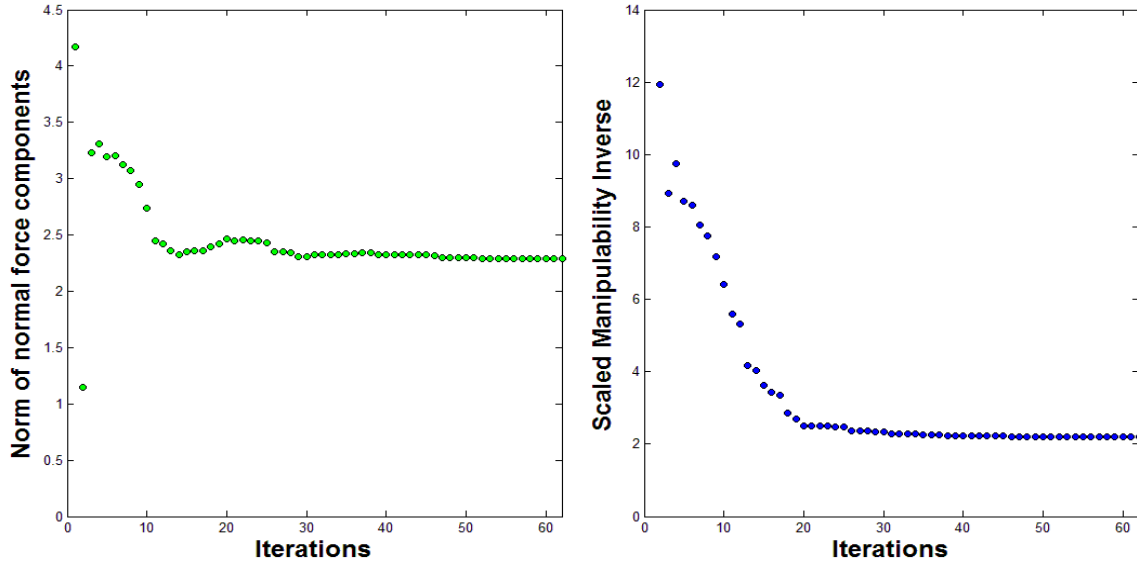


**Figure 4.10** – Joint angular displacements as decision variables: Convergence of the Objective Function Components

## 4.4 Discussion

The difference between the convergence of the two different formulations is mainly due to the different types of constraints of the two problems. The first one only has to only satisfy inequality constraints, while the second one, apart from the same inequalities has to also respect an equality constraint (the fingertips are explicitly constrained to lie on the surface of the grasped object). In general, equality constraints are difficult to be satisfied in nonlinear programs and also can lead to a different convergence of the same problem, as it happens here. The satisfaction of the geometry constraints leads the hand to a different posture, in which, in order to satisfy the rest of the constraints, different contact forces are needed. However, as it was mentioned above, this formulation can prove to be significant in the experimental validation of the algorithm, when partial information of the object's surface will only be available through the use of tactile/vision/force sensors.

All in all, both approaches lead to relatively fast convergence, provided that an object of known geometry, weight and friction properties are known. The parametrization of the cylinder's surface leads to even faster and easier convergence, since it implicitly incorporates the requirement for the fingertips to lie on the surface of the grasped object without using an equality constraint.

---

## CHAPTER 5

# Grasp Quality Optimization for Synergistic Underactuated Hands

Nowadays, one of the most active research directions in the context of the general area of robot grasping is the study of synergistic underactuated hands. As *underactuated* we characterize a mechanism which has fewer actuators than degrees of freedom (in that sense, the DLR/HIT II is also an underactuated hand, since its kinematics is mechanically constrained by the couple between its fingers' last two joints). As for the word *synergistic*, it is associated with the kinematics of such hands, which is defined by the same laws as the human hands.

Inspired by the way that human hands move, grasp and manipulate objects, roboticists model and design mechanical hands, actuated in a human-like way. The motivation for this trend is dual. First, in the context of bringing robotics close to the modern society, it is important that they function in an anthropomorphic way, close to what humans are familiar with, in order to serve them properly and in a natural way. However, the most significant reason for conducting research on underactuated mechanisms and in particular on synergistic underactuated mechanical hands is of mechanical nature. Constructing robot hands that resemble human hands and function in an equivalently dexterous manner is an extremely difficult project given the existing technology. In particular, it is almost impossible nowadays to build robot hands with human-like size and the same number and kind of DOFs. The limitations arise from the size of existing actuators and controllers but also by the incredibly complex design of the human hand. Besides, the use of less actuators means less consumption of energy, which is also a key-feature of modern robot design. All in all, synergistic underactuated hands may not have the dexterity of fully actuated hands but for every-day life applications, it has been verified that even humans do not make total use of their hands' kinematic capabilities. In particular, several studies (see for example [45, 46]) have shown that when humans grasp simple objects, the kinematics of their hand can be described in a very satisfactory way by much less components than the number of its dofs. This means that during a grasp, there exist correlations between the hand's dofs. These correlations are commonly referred to as "synergies" by neurophysiologists.

In the context of this thesis' study of the grasping optimization problem, the methodology described in chapter 4 is also applied for the case of a multifingered synergistic underactuated robot hand with the design, kinematic model and mechanical constraints of the DLR/HIT II hand. In order to do that, it was important to develop a model to describe the kinematics of a human hand. For this reason, human grasping experiments were first conducted by several subjects and objects and kinematic data was collected. After the data processing, the principal components

of the human hands' kinematics were extracted via a dimensionality reduction technique. Subsequently, by including the space of these principal components in the vector of the decision variables, the Grasp Quality Optimization scheme presented in 4 is adapted for the case of a synergistic underactuated hand. In this chapter, the experimental procedure is described, accompanied by data processing results, as well as by simulation results of the optimization scheme.

## 5.1 From Human to Robot Hands: Kinematics

Our main objective is to adapt the already proposed and described algorithm concerning general multifingered robot hands to synergistic underactuated hands which reflect the human hand's grasping behavior. In order to do that, we need to develop a mapping from human to robot hands.

This can be done through the use of an appropriate *interface*. In our case, the CyberGlove II (see Appendix B.1) was used. Via CyberGlove (Fig. 5.1), the human hand's kinematics can be recorded in real time and stored for further post processing. In particular, the relative angles between the fingers are measured. Based on data provided by the CyberGlove, our aim is to derive a model that describes the human grasp.



**Figure 5.1** – CyberGlove II, CyberGlove Systems [6].

### 5.1.1 Modeling the Human Hand's Kinematics

In order to successfully record the human grasp's kinematics and properly adapt them to a hypothetical synergistic underactuated hand with the DOFs and design of the DLR/HIT II, we need to use a suitable kinematic model of the human hand. In this direction, several studies have been conducted to model the complex nature of the human hand's kinematics. Among them, one of the most representative and widely accepted, is the model proposed by Esteban Pitarch in [7]. In this model, illustrated in Fig. 5.2, 25 DOFs are considered to generate the hand's kinematics.

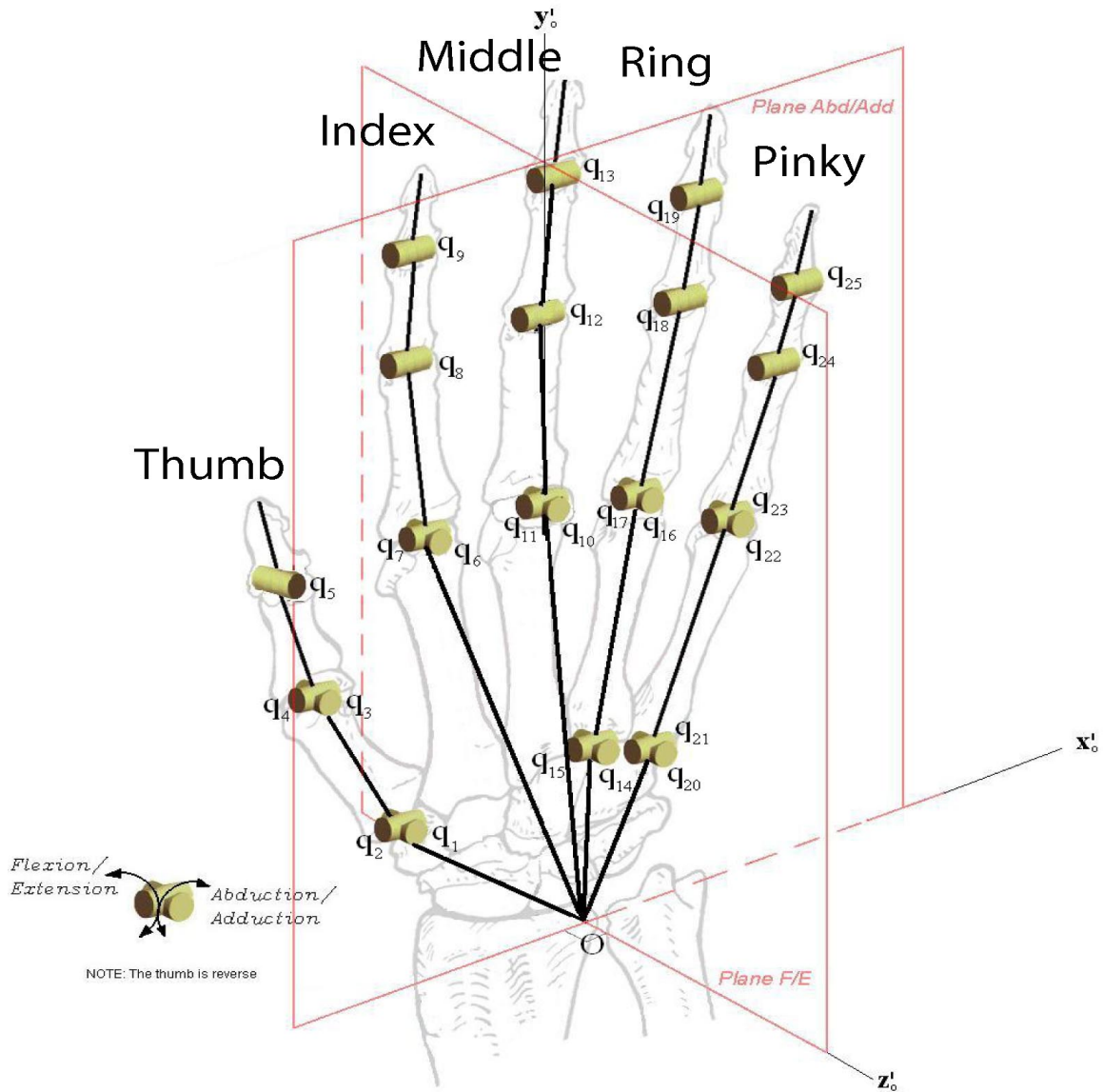


**Figure 5.2** – 25 DOF kinematic model of the human hand [7]. The nomenclature of the DOFs's type is noted, along with the fingers' names.

In our case, a simplified version of this model was adopted. In particular, in accordance with Fig. 5.2, DOFs  $q_1$ ,  $q_3$ ,  $q_6$ ,  $q_7$ ,  $q_8$ ,  $q_{11}$ ,  $q_{12}$ ,  $q_{16}$ ,  $q_{17}$ ,  $q_{18}$ ,  $q_{22}$ ,  $q_{23}$  and  $q_{24}$  were recorded in the experiments. In order to represent the mechanical coupling of the DLR hand, the measurements concerning DOFs  $q_3$ ,  $q_8$ ,  $q_{12}$ ,  $q_{18}$  and  $q_{24}$  were hypothetically repeated in the last joint of each finger. No measurements were considered for DOF  $q_{10}$  whose position was constantly set to zero. This was decided so that the middle finger constitute a reference for the measurement of the abduction/adduction of index and ring fingers, since CyberGlove measures the relative angles between the fingers. The same thing was applied for the thumb's abducton/adduction DOF, so that we successfully adapt the taken measurements to the model of our hypothetical synergistic hand.

### 5.1.2 Experimental Procedure

Grasping experiments (see table 5.1) were conducted with several spherical and cylindrical objects by three different subjects. In particular, a mug, a tall glass and a small ball were grasped. During the experiments, their hands' kinematics were recorded by the CyberGlove and stored for post-processing. All the objects that were selected for the experiments have geometries that not only resemble the objects considered for the simulations but also favor the recording of the human hand's kinematic abilities. The use of multiple subjects was decided in order to produce general and more representative results for the extraction of the principal components of the human grasp's kinematics.

**Table 5.1** – Grasping experiments



### 5.1.3 Post Processing

The data collected during the aforementioned experiments were used as input for the extraction of the principal components that describe the kinematic state of the

hand during the whole process of the grasp. In particular, we adopted PCA<sup>6</sup> (Principal Components Analysis), a dimensionality reduction technique, that identifies the components that account for the highest percentage of the variance in the kinematics of the grasp and sorts them in order of significance. The output of PCA in our problem is a matrix  $\mathbf{W} \in \mathbb{R}^{n_q \times n_q}$ , each row of which represents a principal component of the mapping from the high dimensional space of the hand's kinematics to the low dimensional space of synergies. The rows are ranked in order of significance with respect to the kinematics of the human hand, i.e. ranked in ascending order wrt their variance. In our case, the percentages concerning the variance of each principal component extracted by the PCA are as noted in table 5.2. As it was mentioned in section 5.1.1, only 13 DOFs were recorded during the grasping experiments. This is the reason why components 13 and 14 do not account for the variance of the hand's kinematics. This is equivalent to implementing the PCA for thirteen high D components.

**Table 5.2** – Variance of the Principal Components representing the Human Grasp as extracted by PCA

Component	Variance Percentage (%)
1	0.764146965958740
2	0.877169067060654
3	0.935718504101649
4	0.958848341043730
5	0.974389629120479
6	0.986668605419181
7	0.992687425403787
8	0.995956677620231
9	0.997631741308975
10	0.998922247803228
11	0.999593169975879
12	0.999895747313353
13	1.000000000000000
14	1.000000000000000
15	1.000000000000000

We can see that indeed the kinematics of the human grasp in the experiments conducted in our lab verifies the theory that the human hand's kinematics can be described by much less components than the number of its dofs. In particular, only two components account for more than 87% of the variance. For more accurate results and facilitation of the optimization problem, we use five principal components (from a mechanical point of view, each principal component can be considered as a "motor"). In general, we can write the following maps:

$$\boldsymbol{\sigma} = \mathbf{W}\mathbf{q} \quad (5.1)$$

and

$$\dot{\boldsymbol{\sigma}} = \mathbf{W}\dot{\mathbf{q}} \quad (5.2)$$

<sup>6</sup>A comprehensive and practical guide for conducting PCA can be found in [47].

where the vector  $\boldsymbol{\sigma} \in \mathfrak{R}^{n_s}$  contains the low D kinematics of the hand, the vector  $\dot{\boldsymbol{\sigma}} \in \mathfrak{R}^{n_s}$  contains its first derivative wrt time and  $\mathbf{W} \in \mathfrak{R}^{n_s \times n_q}$  is the matrix containing the  $n_s$  components with the maximal variance. Throughout this thesis  $n_s = 5$ .

## 5.2 Problem Formulation

### 5.2.1 Hand Model

For the following sections of this chapter, we consider a hand that has the same design and DOFs with the DLR/HIT II five-fingered robot hand, but its kinematics can be controlled by the five principal components derived above. Consequently, the Grasp Matrix and the Hand Jacobian will be used in the same way as in the previous chapters.

### 5.2.2 Object's Equilibrium: Contact Force Distribution

Based on the work of Bicchi et al. [48–50], in order to include the hand's synergies in our analysis, we first introduce a set of "virtual springs", interposed between the links and the object at the contact points. This can be done by using a stiffness diagonal matrix  $\mathbf{K} \in \mathfrak{R}^{3n_c \times 3n_c}$ , which incorporates the structural elasticity of the object and the fingers and the stiffness of joint servos if position controllers are used. Now, the general solution of the Grasping Problem with Synergies can be found as follows:

$$\mathbf{f} = \mathbf{G}_K^R(-\mathbf{w}) + \mathbf{F}_s \delta \boldsymbol{\sigma} \quad (5.3)$$

where no preloaded forces were considered. The solution consists of two main components. The first one accounts for the compensation of the object's weight, while the second one represents the active internal forces acting on the object. By

$$\mathbf{G}_K^R = \mathbf{K} \mathbf{G}^T (\mathbf{G} \mathbf{K} \mathbf{G}^T)^{-1} \in \mathfrak{R}^{3n_c \times 6} \quad (5.4)$$

we denote the K-weighted pseudo-inverse of the Grasp Matrix  $\mathbf{G}$ , which provides the particular solution  $\mathbf{G}_K^R \mathbf{w}$  that minimizes the potential energy of the displacements at the elastic contacts. This solution appears to be physically well motivated [48]. The second component of eq. 6.12 can be derived by the following expression:

$$\mathbf{F}_s = (\mathbf{I} - \mathbf{G}_K^R) \mathbf{K} \mathbf{J} \mathbf{W}^T \in \mathfrak{R}^{3n_c \times n_s} \quad (5.5)$$

The vector  $\delta \boldsymbol{\sigma} \in \mathfrak{R}^{n_s}$  contains the synergistic displacements that account for the generation of the internal forces during the grasp [49].

### 5.2.3 Optimization Scheme

Our objective, as in chapter 4, is to derive a force closure grasp with low force distribution and good ability of local force exertion at the contact points, respecting the mechanical and geometrical constraints of the hand and the grasped object. The main difference is that the active internal contact forces that the fingers exerts to the object, are generated by synergistic displacements in the low D space.

We adopt the Optimization Schemes presented in 4.2.1 and 4.2.2. The only thing that has changed is the force expression that has included the synergistic displacements as decision variables. We present the case of the *joint limits as decision variables*, since it is closer to a hardware verification. We denote by

$$\mathbf{p} = [\delta\boldsymbol{\sigma}^T \quad \mathbf{q}^T \quad \mathbf{w}^T]^T \in \mathfrak{R}^{n_s+n_q+6} \quad (5.6)$$

the vector containing the decision variables of the optimization problem and by

$$z = w_F F(\mathbf{f}(\mathbf{p})) + w_M \frac{1}{M(\mathbf{q}(\mathbf{p}))} \quad (5.7)$$

the objective function that we want to minimize. Hence, the optimization problem can be formulated as follows:

$$\mathbf{p}^* = \underset{\mathbf{p}}{\operatorname{argmin}} z(\mathbf{p}) \quad (5.8)$$

s.t.

$$\sqrt{f_{i_i}(\mathbf{p})^2 + f_{o_i}(\mathbf{p})^2} \leq \mu f_{n_i}(\mathbf{p}), \quad i = 1 \dots n_c \quad (5.9)$$

$$\mathbf{q}_{\min} \leq \mathbf{q} \leq \mathbf{q}_{\max} \quad (5.10)$$

$$\mathbf{s}(\mathbf{q}) \in \mathbf{S} \quad (5.11)$$

$$\mathbf{s}(\mathbf{q}) \in \partial\mathbf{O} \quad (5.12)$$

The notations adopted in this formulation are the same as in chapter 4. The force distribution  $\mathbf{f}$  is calculated via eq: 5.3 and the joints' angular positions are derived through the computation of the inverse kinematics of the fingers. The vectors  $\mathbf{q}_{\min} \in \mathfrak{R}^{n_q}$  and  $\mathbf{q}_{\max} \in \mathfrak{R}^{n_q}$  contain the lower and upper joint limits respectively and they have been set to be the same with the DLR hand. The constraint 5.11 expresses the fingers succession requirement which forces the fingers to avoid collisions.

### 5.3 Simulation Results

Simulation results are presented for the grasp of a cylindric object of height 15 cm, diameter 6 cm and weight 200 gr (dimensions similar to a 500 ml plastic water bottle's). The Stiffness constants are set equal to 100,000 N/m, which is a reasonable estimation, given the surfaces of the fingers and the object. Figs. 5.3, 5.4 and 5.5 depict different views of a comparative 3D plot, containing the initial (green color) and the final (blue color) posture of the robot hand. Details about the convergence of the algorithm are presented in Figs. 5.6 and 5.7. In particular, Fig. 5.6 shows the convergence of the objective function  $z$ , while Fig. 5.7 illustrates the convergence of its two components. As in chapter 4 we can see that, since the algorithm initializes from random contact points and synergistic displacements, in the first iterations a feasible point is searched. Once the feasible region is entered, the algorithm begins to implement minimization steps, until it terminates after about 90 iterations because of insufficient objective function decrease.

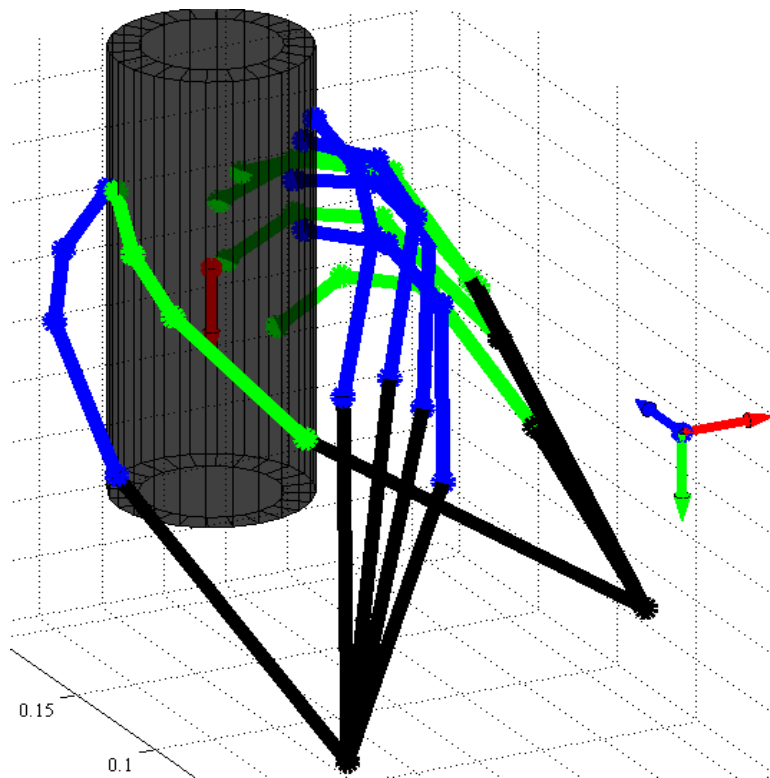


**Figure 5.3** – Synergies based Grasping Optimization: Initial (green color) and final (blue color) postures of the robot hand. The final posture is more *anthropomorphic*.

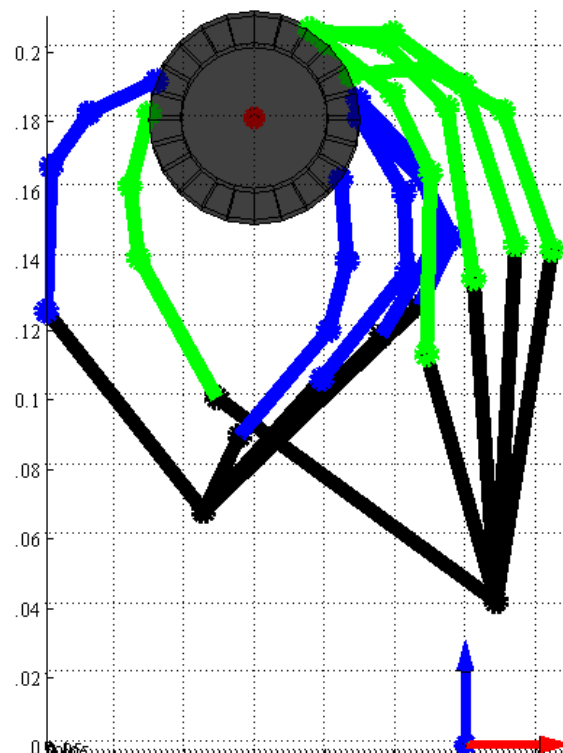


**Figure 5.4** – Synergies based Grasp Quality Optimization: Top View of the initial (blue hand) and final (green hand) posture.

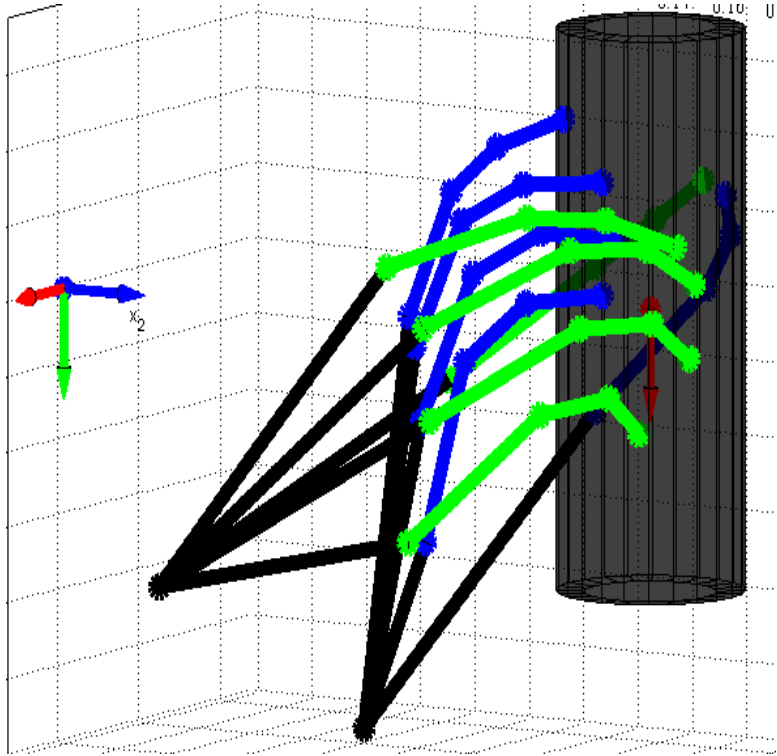


Figure 5.5 – Synergies based Grasp Quality Optimization: Side view.

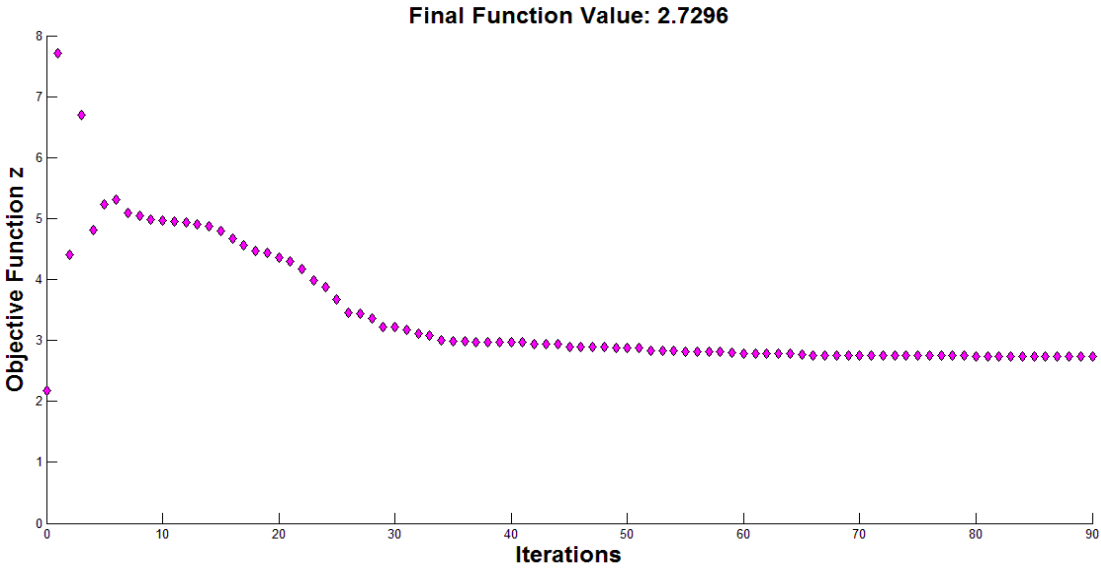
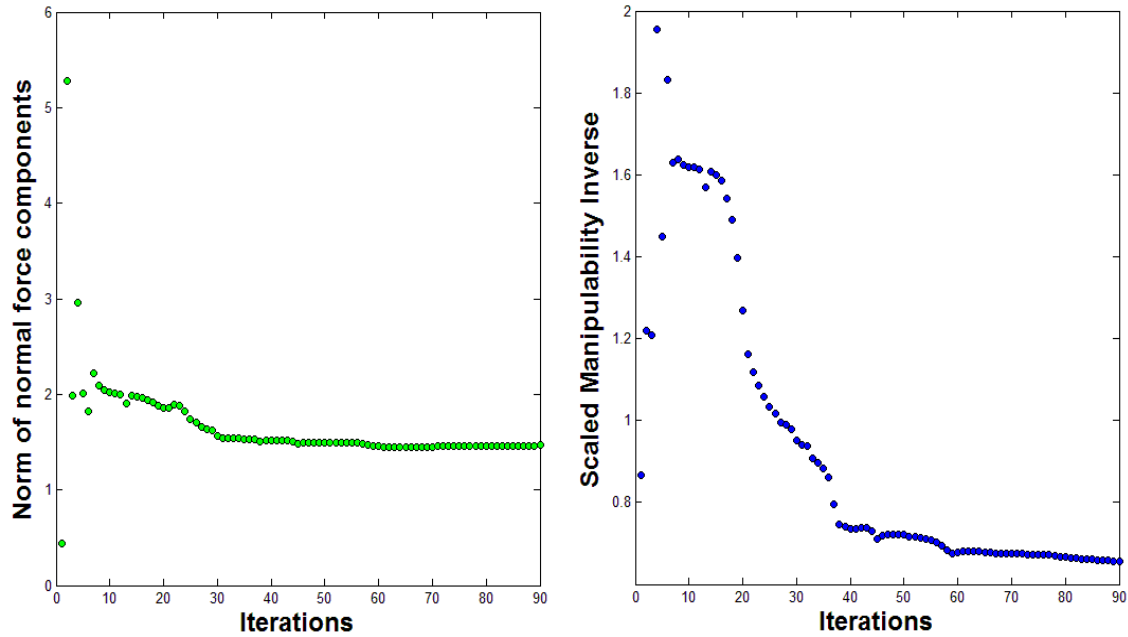


Figure 5.6 – Synergies based Grasp Quality Optimization: Coverage of the combined objective function z.



**Figure 5.7** – Synergies based Grasp Quality Optimization: Comparative figure with the convergence of the components of the objective function. The low force distribution can be interpreted as a result of the *successful initial guess* of the configuration and contact points of the robot hand.

## 5.4 Discussion

We can see that the posture adopted after the convergence of the algorithm is closer to the way a human would grasp a similar object than the final postures presented in chapter 4. This was expected, since the kinematics of the hand are constrained to be such that they can produce a force closure grasp by internal forces generated by synergistic displacements  $\delta\sigma$ . The convergence is fast; after about 30 iterations the value of the objective function is very close to the final point. Besides, as far as the contact force distribution is concerned, we can see that the final value of the component  $F$  is about 1.5 N, which is lower than the values provided by the schemes of chapter 4. This can be explained as a result of the different diameter of the grasped object. Inevitably, the initial posture of the robot hand was different than in the previous chapter and consequently the convergence in total was also different.

---

# CHAPTER 6

## Grasp Compatibility Optimization

Humans grasp objects aiming at moving or manipulating them in order to execute the tasks they want. Depending on the task and the object, the way humans grasp may differ. However, this habit is not a coincidence. The experience we acquire from the environment that surrounds us and the objects we use in our everyday life leads to an evolution of our grasps. Given a known object and the task we want to execute with it, we tend to predetermine the contact points and the configuration that we will use. This could be described as a habit that offers us comfort during the execution of a task. However, something that seems to be only an intuitive behaviour can also be explained physically and be extended in the mechanical world of robotics.

In this chapter, we approach the problem of transmitting to hands the intelligence of grasping known objects with an appropriate way wrt the task they have to subsequently execute. In order to do that, we develop an optimization scheme that enables a multifingered robot hand to select the most compatible grasp (contact points, configuration and contact forces) wrt a certain task. In particular, our objective is to guarantee *force closure* and *task compatibility* as it was defined in chapter 2. In the following sections, we formulate the problem, adopting the formulations of chapters 4 and 5 concerning the generation of contact forces and the production of the hand's kinematics.

### 6.1 Task Definition

A key word and concept in such an approach is the *Task*. There are many ways and perspectives through which a task can be described. However, in the mechanical world, almost everything can be described wrt force and velocity. Based on this assumption and in accordance with the problem we approach, a task can be defined as the transmission of wrench and twist of specified magnitudes from the robot hand to the grasped object along specified directions. Hence, it is obvious that each task has different wrench and twist transmission requirements (direction and magnitude).

### 6.2 Problem Formulation

If we know a task's wrench and twist transmission and control requirements, we can force the robot hand to select a compatible configuration and contact points. In accordance with what was presented in section 2.4.4, this can be done by selecting a grasp that maximizes the ability of the hand's mechanism for wrench and twist transmission or control along the desired directions. Of course in order for the task

to be successfully executed, it is necessary that the mechanical artifact that we use as a hand is capable of exerting the required magnitude of forces and velocities on the object.

### 6.2.1 Optimization Scheme

The general idea of the optimization scheme that we propose can be summarized in the following diagram:

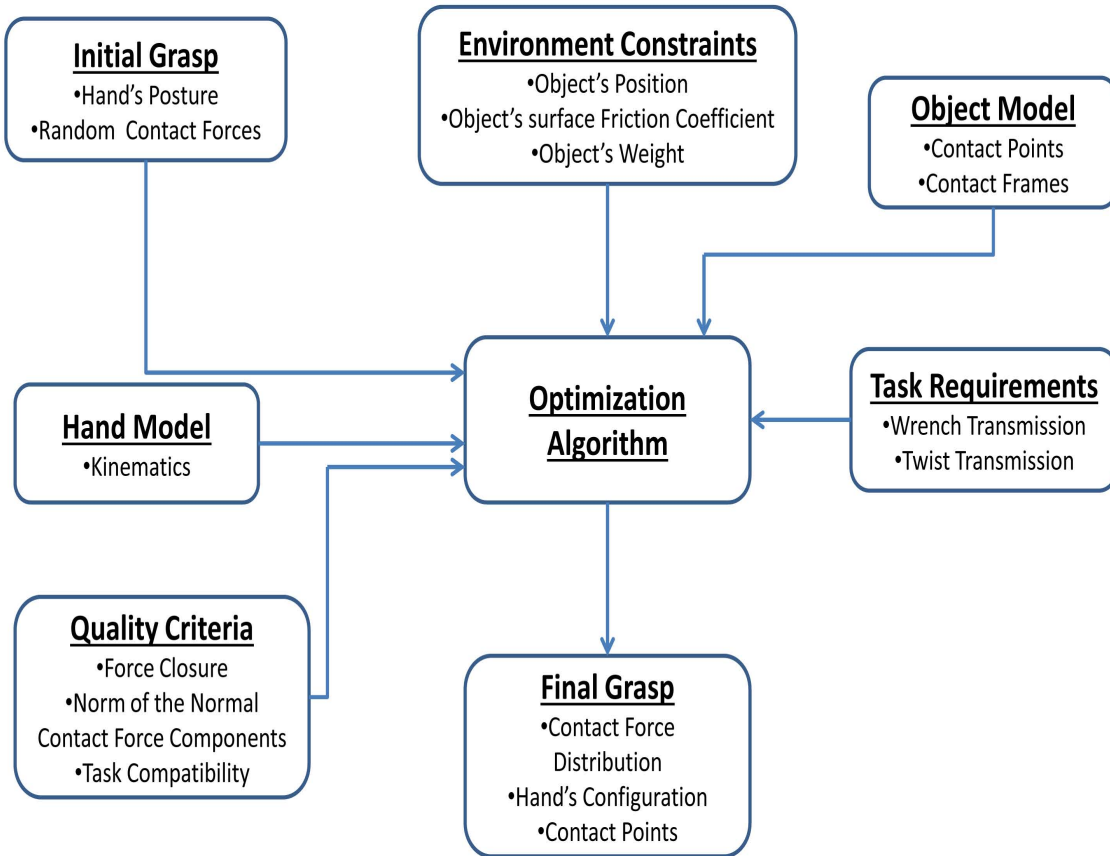


**Figure 6.1** – Illustration of the scheme that takes into consideration the task to be executed by the robot hand.

The algorithm takes as input the object's surface properties, the task description and an initial random grasp. Its output is a force closure grasp with low force distribution and a posture that guarantees compatibility with the task to be executed.

#### Hand with fifteen actuated DOFs

We adopt the formulation of chapter 4 which leads to *force closure* and simply include a component concerning the task compatibility. In particular, a solution to the problem of the equilibrium of an object with weight  $\mathbf{w}$  can be given by the following equation:

$$\mathbf{f} = \mathbf{G}^\dagger(-\mathbf{w}) + \mathbf{V}\boldsymbol{\lambda} \quad (6.1)$$

where  $\mathbf{V} = (\mathbf{I} - \mathbf{G}^\dagger\mathbf{G})$ .

Given a task description (a desired wrench/twist direction unit vector  $\boldsymbol{\eta}$ ), we derive the expressions of the corresponding wrench/twist transmission ratios of interest:

$$\alpha_i = [\boldsymbol{\eta}^T (\mathbf{H}\mathbf{H}^T) \boldsymbol{\eta}]^{-1/2} \quad (6.2)$$

and

$$\beta_j = [\boldsymbol{\eta}^T (\mathbf{H}\mathbf{H}^T)^{-1} \boldsymbol{\eta}]^{-1/2} \quad (6.3)$$

Our problem is equivalent to the problem of minimizing the objective function

$$z(\mathbf{p}) = w_F F(\mathbf{f}(\mathbf{p})) + C(\mathbf{p}) \quad (6.4)$$

wrt the decision variables

$$\mathbf{p} = [\boldsymbol{\lambda}^T \quad \mathbf{q}^T \quad \mathbf{w}^T]^T \in \mathfrak{R}^{3n_c + n_q + 6} \quad (6.5)$$

The optimization scheme can be formulated as follows:

$$\mathbf{p}^* = \underset{\mathbf{p}}{\operatorname{argmin}} z(\mathbf{p}) \quad (6.6)$$

s.t.

$$\sqrt{f_{t_i}(\mathbf{p})^2 + f_{o_i}(\mathbf{p})^2} \leq \mu f_{n_i}(\mathbf{p}), \quad i = 1 \dots 5 \quad (6.7)$$

$$\mathbf{q}_{\min} \leq \mathbf{q} \leq \mathbf{q}_{\max} \quad (6.8)$$

$$\mathbf{s}(\mathbf{q}) \in \partial \mathbf{O} \quad (6.9)$$

where constraint (6.20) expresses the requirement that the fingertips lie on the surface of the object and by  $C$  we denote the *Grasp Compatibility Index* that was defined in chapter 2.

### Synergistic Underactuated Hand

In the formulation presented above, we can also introduce the concept of synergies. In particular, we can constrain the kinematics of the robot hand to be generated by the low D space that represents the synergies of an underactuated hand, but also constrain the internal forces to be produced by synergistic displacements.

As for the first part, based on eq. 5.2, we can modify the Hand Jacobian to express the following map:

$$\dot{\mathbf{x}} = \mathbf{J}_w \dot{\boldsymbol{\sigma}} \quad (6.10)$$

where

$$\mathbf{J}_w = \mathbf{J}\mathbf{W}^T \quad (6.11)$$

Now the expressions for the transmission ratios can be modified by updating the expression of the Hand-Object Jacobian  $\mathbf{H}$ .

As for the second part, adopting the formulation of chapter 5, a solution to the problem of the object's equilibrium can be given by the following equation:

$$\mathbf{f} = \mathbf{G}_K^R (-\mathbf{w}) + \mathbf{F}_s \delta \boldsymbol{\sigma} \quad (6.12)$$

where

$$\mathbf{G}_K^R = \mathbf{K}\mathbf{G}^T (\mathbf{G}\mathbf{K}\mathbf{G}^T)^{-1} \in \mathfrak{R}^{3n_c \times 6} \quad (6.13)$$

and

$$\mathbf{F}_s = (\mathbf{I} - \mathbf{G}_K^R) \mathbf{K} \mathbf{J} \mathbf{W}^T \in \mathfrak{R}^{3n_c \times n_s} \quad (6.14)$$

Equally to the previous section, if we select as decision variables the elements of the following vector:

$$\mathbf{p} = [\delta \boldsymbol{\sigma}^T \quad \mathbf{q}^T \quad \mathbf{w}^T]^T \in \mathfrak{R}^{n_s + n_q + 6} \quad (6.15)$$

and as an objective function the following

$$z(\mathbf{p}) = w_F F(\mathbf{f}(\mathbf{p})) + C(\mathbf{p}) \quad (6.16)$$

the problem of grasp compatibility optimization for synergistic underactuated hands is equivalent to the following optimization scheme:

$$\mathbf{p}^* = \underset{\mathbf{p}}{\operatorname{argmin}} z(\mathbf{p}) \quad (6.17)$$

s.t.

$$\sqrt{f_{i_i}(\mathbf{p})^2 + f_{o_i}(\mathbf{p})^2} \leq \mu f_{n_i}(\mathbf{p}), \quad i = 1 \dots n_c \quad (6.18)$$

$$\mathbf{q}_{\min} \leq \mathbf{q} \leq \mathbf{q}_{\max} \quad (6.19)$$

$$\mathbf{s}(\mathbf{q}) \in \partial \mathbf{O} \quad (6.20)$$

### 6.3 Simulation Results

Results are presented for the grasp of a cylindric object (diameter 4cm, height 15cm, mass 200 gr). After the grasp, we want to meet the requirements of a certain task: transmitting to the grasped object's center of mass, torque and angular velocity along the positive side of axis  $y$ . For the same optimization parameters (weighting factors, initial posture, maximum number of iterations, constraints etc.), comparative 3D plots with the initial (green color) and final (blue color) postures are presented for the case of i) DLR/HIT II and b) of a synergistic underactuated hand with the same model, whose kinematics are defined by 5 principal components (see Figs 6.2, 6.3, 6.4).

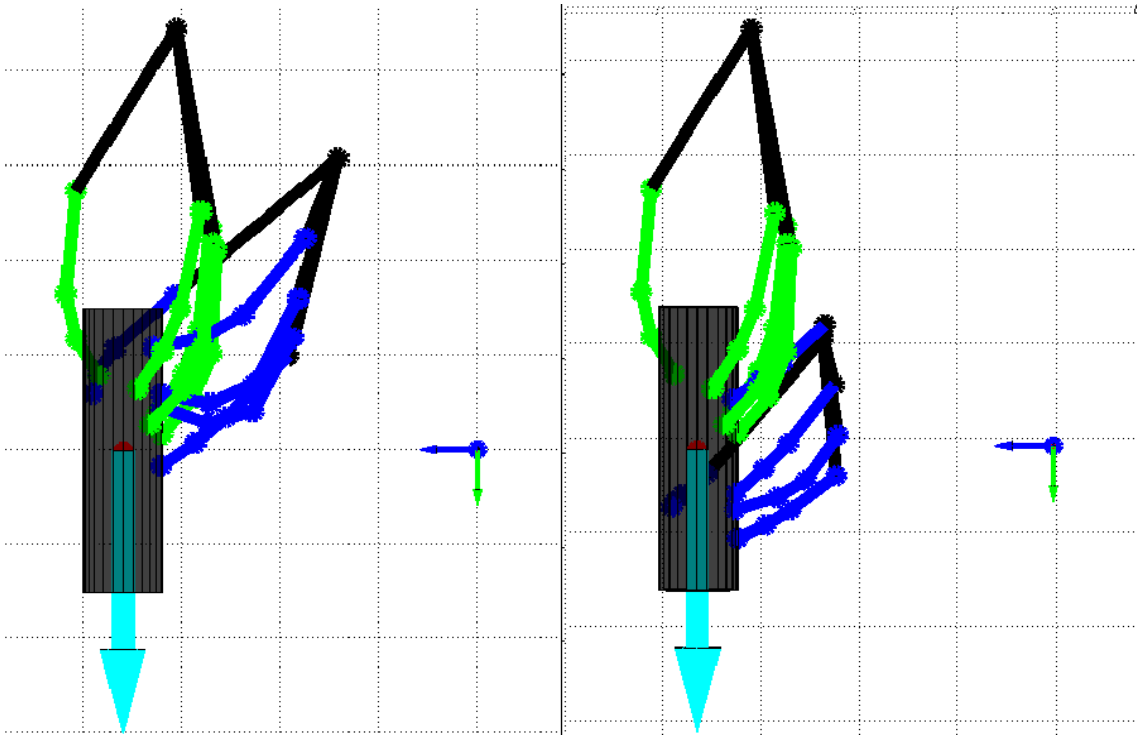


**Figure 6.2** – Comparative Illustration: DLR/HIT II on the left and synergistic underactuated hand (5 principal components) with the same model on the right. The cyan vector illustrates the direction of the desired task execution, the transmission of angular velocity and torque along the positive side of axis  $y$ .

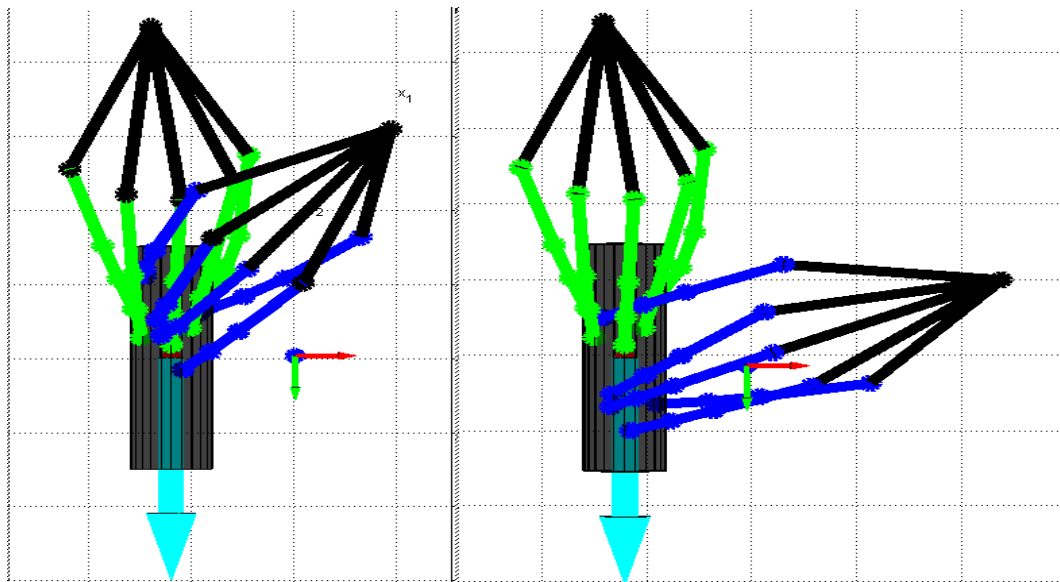


**Figure 6.3** – Grasp Compatibility Optimization: Second view of the same simulation.

Besides, comparative plots depicting the convergence of the objective function and its components are provided in Figs. 6.5 and 6.6 that follow. In Fig. 6.5 we can see that the algorithms first search a feasible solution. Once a feasible solution is found, sequential feasible minimization steps are implemented until the algorithms terminate due to insufficient decrease of the objective function. For the synergistic

hand model, as it can be seen, it is more difficult to enter the feasible region and the convergence of the algorithm is much slower, even if the final solution is close to the solution for the DLR/HIT II hand.

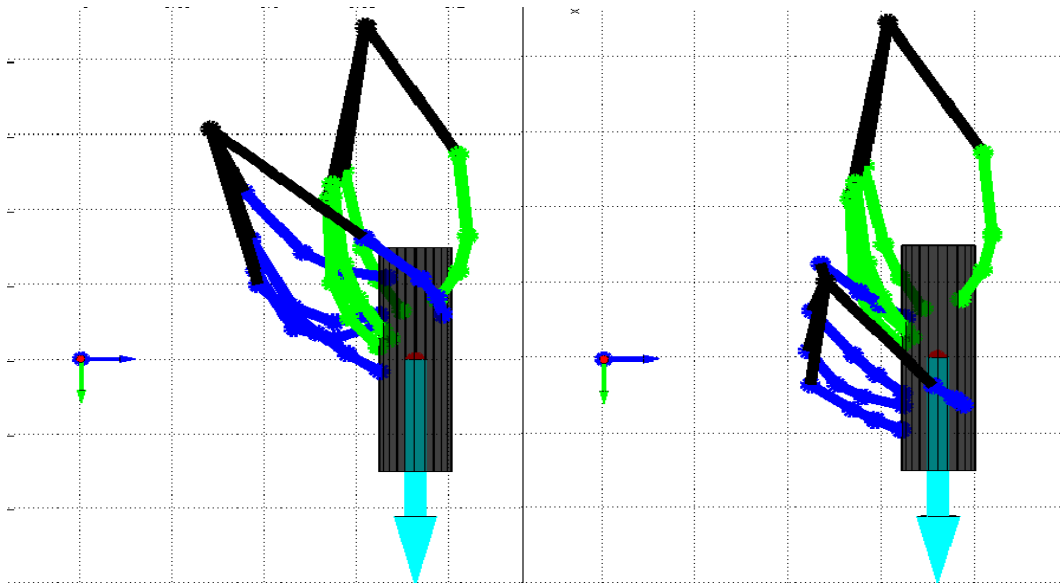


**Figure 6.4** – Grasp Compatibility Optimization: Third view.

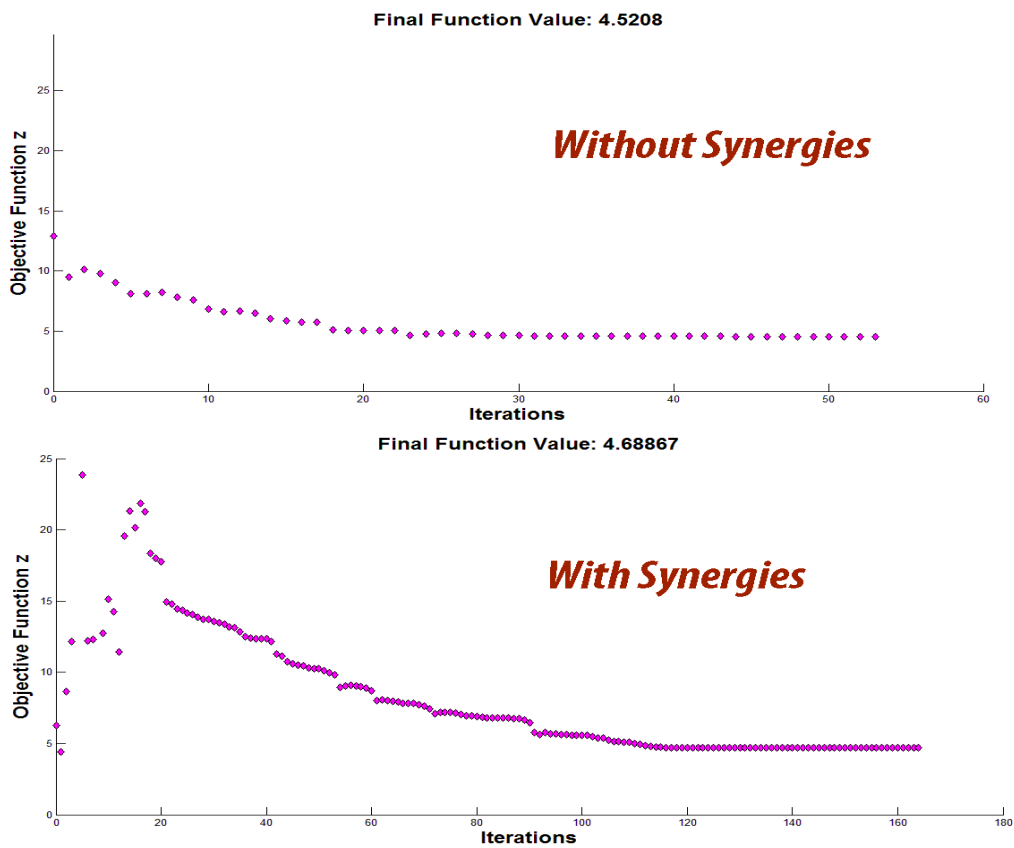


**Figure 6.5** – Convergence of the proposed algorithm *with* and *without* synergies.

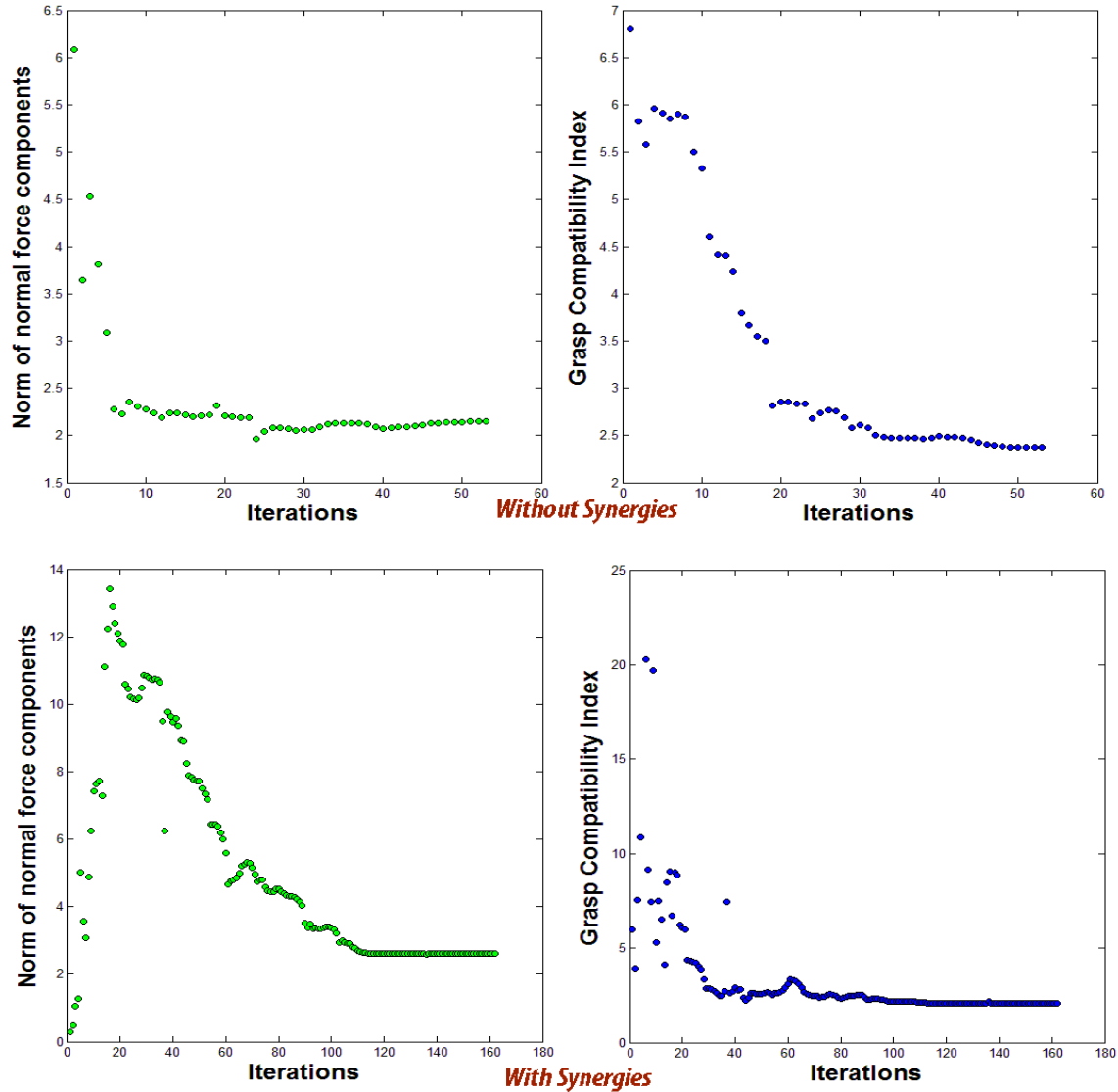


**Figure 6.6** – Convergence of the Objective Function Components for the case of the DLR/HIT II (without synergies) and for the case of a synergistic underactuated hand with the model of the DLR/HIT II (with synergies label).

The comparative plots of the objective function components confirm what was observed in Fig. 6.5; the convergence for the synergistic hand model is slow. The model without the synergistic constraints enters really fast the feasible region and keeps almost the same value throughout the whole run, as far as the force minimization component is concerned. As for the task compatibility index, it also converges fast, although slower than the norm of the contact force components.

## 6.4 Discussion

An optimization scheme which considers an initial grasp and leads to a final grasp which favors the task to be executed by the robot hand is developed and tested. For completeness, the same problem is addressed for the two different types of robot hands considered throughout this thesis. From the simulation results provided we

can observe no significant difference in the final posture of the hand. We can see that the main difference is provided by the hand's wrist position/orientation. This is normal and expected, since the wrist's contribution to the objective function and consequently to the posture adopted is greater compared to the rest of the kinematic components.

---

## CHAPTER 7

# Sequential Improvement of Grasp based on Sensitivity Analysis

In this chapter, we propose a new concept in the area of optimal grasp synthesis, confronting both geometric and mechanical constraints. Starting from a locally optimal force distribution on some prespecified feasible contact points, our algorithm leads gradually to grasps with lower minimal forces, avoiding singularities and joint limitations. It is implemented sequentially, through perturbations (small changes) of the contact points and the wrist's position/orientation. The key idea behind this work consists in applying sensitivity analysis [51] in an iterative process to derive the sequential optimal solutions. The main advantage of the proposed method is that it needs only local information of the object's surface. Hence, it can be generalized for objects of unknown geometry with the use of suitable tactile sensors [52]. In this respect, the robot hand will be able to perceive the local geometry of the object and based on the proposed algorithm, it will adjust appropriately its configuration to improve the grasp.

Towards addressing the grasp improvement problem, we employed a mathematical programming technique to obtain the efficient as well as feasible directions of the contact points and wrist transitions that improve force distribution. Specifically, we adopted the first order sensitivity analysis presented in [51] and [53]. This methodology considers a general mathematical programming problem in its optimal state wrt the decision variables, studies how infinitesimal perturbations of the problem parameters affect the optimal state and provides the partial derivatives, called sensitivities, of the primal (decision variables) and dual (Lagrange multipliers) variables as well as of the objective function wrt the perturbed parameters. Fig. 7.1 shows how small parameter perturbations lead in sequential changes of the optimal state, that can be calculated by the aforementioned sensitivities.

## 7.1 Problem Formulation

In this problem, we consider the contact forces  $\mathbf{f} \in \mathcal{R}^{3n_c}$  as decision variables and the contact points as well as the hand wrist position and orientation as *parameters* of the optimization problem. We stack the parameters in the following vector:

$$\mathbf{p} = [\mathbf{f}^T \quad \mathbf{h}^T \quad \boldsymbol{\phi}^T \quad \mathbf{w}^T] \in \mathcal{R}^{2n_c+6} \quad (7.1)$$

where the notations adopted are chosen to be the same as in section 4.2.1.

Our goal is to employ the aforementioned sensitivities to propose parameter changes to the directions of grasp improvement. Given any feasible contact points,

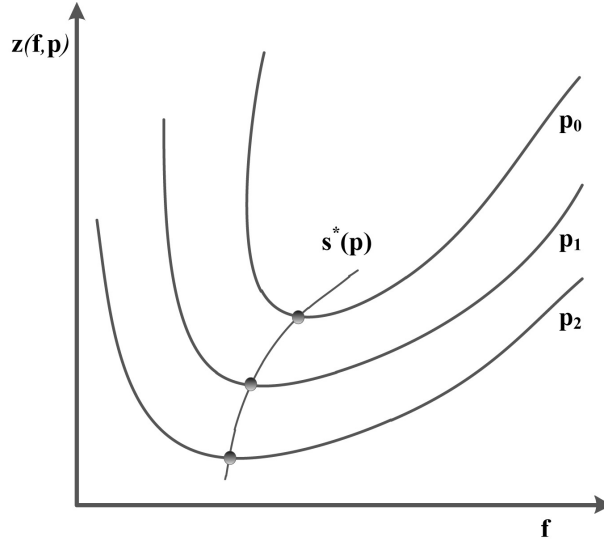


**Figure 7.1** – The optimal states  $s^*$  wrt the function  $z(\mathbf{f}, \mathbf{p})$  are affected by small perturbations of the parameters  $\mathbf{p}$ .

we assume that the robot hand stably grasps the object with locally optimal forces:

$$\mathbf{f}^* = \underset{\mathbf{f}}{\operatorname{argmin}} F(\mathbf{f}) \quad (7.2)$$

wrt to the cost function (2.29), satisfying:

$$\mathbf{h}(\mathbf{f}^*, \mathbf{p}) = \mathbf{0} \quad (7.3)$$

$$\mathbf{g}(\mathbf{f}^*) \leq \mathbf{0} \quad (7.4)$$

where  $\mathbf{h} : \mathfrak{R}^{3n_c} \times \mathfrak{R}^{2n_c+6} \rightarrow \mathfrak{R}^6$  represents the balance linear equalities (2.27) and  $\mathbf{g} : \mathfrak{R}^{3n_c} \rightarrow \mathfrak{R}^{n_c}$  represents the friction cone nonlinear inequalities (2.28). As a result, the Karush-Kuhn-Tucker first order necessary conditions hold (see for example [54–56]):

$$\nabla_{\mathbf{f}} F(\mathbf{f}^*) + \boldsymbol{\lambda}^{*\top} \nabla_{\mathbf{f}} \mathbf{h}(\mathbf{f}^*, \mathbf{p}) + \boldsymbol{\mu}^{*\top} \nabla_{\mathbf{f}} \mathbf{g}(\mathbf{f}^*) = 0 \quad (7.5)$$

$$\mathbf{h}(\mathbf{f}^*, \mathbf{p}) = \mathbf{0} \quad (7.6)$$

$$\mathbf{g}(\mathbf{f}^*) \leq \mathbf{0} \quad (7.7)$$

$$\boldsymbol{\mu}^{*\top} \mathbf{g}(\mathbf{f}^*) = 0 \quad (7.8)$$

$$\boldsymbol{\mu}^* \geq \mathbf{0} \quad (7.9)$$

where  $\boldsymbol{\lambda}^* \in \mathfrak{R}^6$  and  $\boldsymbol{\mu}^* \in \mathfrak{R}^{n_c}$  are the Lagrange multipliers associated with the equality and inequality constraints respectively.

In order to incorporate in our analysis the quality measures (2.35) and (2.36), mentioned in the previous section, we employ the following objective function:

$$z = w_F F(\mathbf{f}) + w_M \frac{1}{M(\mathbf{q})} + w_Q Q(\mathbf{q}) \quad (7.10)$$

where  $w_F, w_M, w_Q$  are suitably chosen weights that normalize the quality measures and favor those we want to emphasize more, depending on the task. By introducing the hand's inverse kinematics:

$$\mathbf{q} = \mathbf{T}(\mathbf{p}) \quad (7.11)$$

into (7.10), we derive the expression of the objective function wrt the system parameters  $\mathbf{p}$ , as follows:

$$\mathbf{z}(\mathbf{f}, \mathbf{p}) = w_F \mathbf{F}(\mathbf{f}) + w_M \frac{1}{\mathbf{M}(\mathbf{p})} + w_Q \mathbf{Q}(\mathbf{p}) \quad (7.12)$$

Since system parameters were considered constant in the initial optimal grasp and since  $\mathbf{M}$  and  $\mathbf{Q}$  are independent of the decision variables  $\mathbf{f}$ , their incorporation does not affect the optimality conditions. Thus, the system is also in a locally optimal state wrt the cost function (7.12).

The derivation of the sensitivities of the optimal state  $(\mathbf{f}^*, \boldsymbol{\lambda}^*, \boldsymbol{\mu}^*, \mathbf{z}^*)$  wrt the parameters  $\mathbf{p}$  is carried out by differentiating the KKT conditions, as follows:

$$(\nabla_{\mathbf{f}} \mathbf{z}(\mathbf{f}^*, \mathbf{p}))^T d\mathbf{f} + (\nabla_{\mathbf{p}} \mathbf{z}(\mathbf{f}^*, \mathbf{p}))^T d\mathbf{p} - d\mathbf{z} = 0 \quad (7.13)$$

$$\begin{aligned} & \left( \nabla_{\mathbf{ff}} \mathbf{z}(\mathbf{f}^*, \mathbf{p}) + \sum_{j=1}^{n_c} \mu_j^* \nabla_{\mathbf{ff}} g_j(\mathbf{f}^*, \mathbf{p}) \right) d\mathbf{f} \\ & + \sum_{k=1}^6 \lambda_k^* \nabla_{\mathbf{fp}} h_k(\mathbf{f}^*, \mathbf{p}) d\mathbf{p} + \nabla_{\mathbf{f}} \mathbf{h}(\mathbf{f}^*, \mathbf{p}) d\boldsymbol{\lambda} \\ & \quad + \nabla_{\mathbf{f}} \mathbf{g}(\mathbf{f}^*, \mathbf{p}) d\boldsymbol{\mu} = \mathbf{0}_{3n_c} \end{aligned} \quad (7.14)$$

$$(\nabla_{\mathbf{f}} \mathbf{h}(\mathbf{f}^*, \mathbf{p}))^T d\mathbf{f} + \nabla_{\mathbf{p}} \mathbf{h}(\mathbf{f}^*, \mathbf{p})^T d\mathbf{p} = \mathbf{0}_6 \quad (7.15)$$

$$(\nabla_{\mathbf{f}} \mathbf{g}(\mathbf{f}^*))^T d\mathbf{f} = \mathbf{0}_{n_c} \quad (7.16)$$

The aforementioned set of equations require that the KKT conditions are satisfied after an infinitesimal perturbation of system parameters. We also demand that active constraints remain active and inactive constraints keep their value inside the feasible region after each perturbation. In Matrix form, the system (7.13)-(7.16) can be written as follows:

$$\begin{bmatrix} \mathbf{z}_{\mathbf{f}} & \mathbf{z}_{\mathbf{p}} & \mathbf{0} & \mathbf{0} & -\mathbf{1} \\ \mathbf{z}_{\mathbf{ff}} + \sum_{j=1}^{n_c} \mu_j^* \mathbf{g}_{\mathbf{ff}} & \sum_{k=1}^6 \lambda_k^* \mathbf{h}_{\mathbf{fp}} & \mathbf{h}_{\mathbf{f}} & \mathbf{g}_{\mathbf{f}} & \mathbf{0} \\ \mathbf{h}_{\mathbf{f}}^T & \mathbf{h}_{\mathbf{p}}^T & \mathbf{0} & \mathbf{0} & \mathbf{0} \\ \mathbf{g}_{\mathbf{f}}^T & \mathbf{0} & \mathbf{0} & \mathbf{0} & \mathbf{0} \end{bmatrix} \begin{bmatrix} d\mathbf{f} \\ d\mathbf{p} \\ d\boldsymbol{\lambda} \\ d\boldsymbol{\mu} \\ d\mathbf{z} \end{bmatrix} = \mathbf{0} \quad (7.17)$$

If we consider the submatrices:

$$U = \begin{bmatrix} \mathbf{z}_{\mathbf{f}} & \mathbf{0} & \mathbf{0} & -\mathbf{1} \\ \mathbf{z}_{\mathbf{ff}} + \sum_{j=1}^{n_c} \mu_j^* \mathbf{g}_{\mathbf{ff}} & \mathbf{h}_{\mathbf{f}} & \mathbf{g}_{\mathbf{f}} & \mathbf{0} \\ \mathbf{h}_{\mathbf{f}}^T & \mathbf{0} & \mathbf{0} & \mathbf{0} \\ \mathbf{g}_{\mathbf{f}}^T & \mathbf{0} & \mathbf{0} & \mathbf{0} \end{bmatrix} \quad (7.18)$$

and

$$S = \begin{bmatrix} -\mathbf{z}_{\mathbf{p}} \\ -\sum_{k=1}^6 \lambda_k^* \mathbf{h}_{\mathbf{fp}} \\ -\mathbf{h}_{\mathbf{p}}^T \\ \mathbf{0} \end{bmatrix} \quad (7.19)$$

we obtain all sensitivities through the inversion of the square matrix  $U$ . Under the assumption that the optimal solution  $\mathbf{f}^*$  is a non-degenerate regular point [51], matrix  $U$  is invertible. Thus, the sensitivities are calculated as follows:

$$D = \begin{bmatrix} \frac{\partial \mathbf{f}}{\partial \mathbf{p}} \\ \frac{\partial \lambda}{\partial \mathbf{p}} \\ \frac{\partial \boldsymbol{\mu}}{\partial \mathbf{p}} \\ \frac{\partial \mathbf{z}}{\partial \mathbf{p}} \end{bmatrix} = U^{-1}S \quad (7.20)$$

As a result, the expected change of the optimal state  $(\mathbf{f}^*, \lambda^*, \boldsymbol{\mu}^*, \mathbf{z}^*)$  after an infinitesimal perturbation  $d\mathbf{p}$  of the parameters may be derived to a first order approximation, through the corresponding differentials:

$$\begin{bmatrix} d\mathbf{f} \\ d\lambda \\ d\boldsymbol{\mu} \\ d\mathbf{z} \end{bmatrix} = D \cdot d\mathbf{p} \quad (7.21)$$

It should be noticed that the aforementioned method has local validity. However, incorporating it in an iterative algorithm can lead to sequential improvements of the cost function (7.12). Thus, via calculating the sensitivities and adopting a suitable step selection strategy for the system parameters (e.g. [57]), we can change appropriately the optimal state. Hence, our goal is to apply perturbations of the parameters in such directions that lead to the decrease of the objective function (7.12). Finally, we present an algorithm that incorporates the aforementioned methodology into a general grasp synthesis strategy aiming at post optimal grasp improvement.

### 7.1.1 The Sequential Grasp Improvement Algorithm

The Sequential Grasp Improvement (SGI) Algorithm initializes with an optimal grasp on prespecified feasible contact points and wrist position/orientation. The initial optimal state is obtained via a grasping force optimization algorithm. At this point, the iterative algorithm begins. At the  $i$ -th iteration, the sensitivities are first calculated and subsequently, an appropriate and sufficiently small parameter perturbation  $d\mathbf{p}$  is determined. The parameters are then updated via:

$$\mathbf{p}_{i+1} = \mathbf{p}_i + d\mathbf{p} \quad (7.22)$$

and the new optimal state  $(\mathbf{f}_{i+1}^*, \lambda_{i+1}^*, \boldsymbol{\mu}_{i+1}^*, \mathbf{z}_{i+1}^*)$  is calculated via the corresponding sensitivities, as described in (7.21). The iterative process continues until (i) an insignificant grasp improvement is determined or (ii) a possible collision between the hand's fingers is detected or (iii) any of the joint limits is violated. Regarding the third case, note that although metric (2.36) was included in the cost function (7.10), the decrease of (7.10), which in general leads the configuration inside the feasible region, cannot guarantee that the joint limits are not violated. Finally, it should be noticed that the proposed algorithm avoids any singular configurations owing to metric (2.35) that was employed in the objective function. Thus, starting from a nonsingular configuration (i.e.  $M(\mathbf{q}_0) > 0$ ) and decreasing the objective function (7.12), it is impossible to approach a singular point (i.e.  $M(\mathbf{q}) \rightarrow 0$ ), since in such

---

**Algorithm 1** Sequential Grasp Improvement

---

```
1: procedure SGI( $p, q, cm, Weight, frcoef, \epsilon, \delta, w_1, w_2, w_3$ )
2:    $var \leftarrow GFO(p, cm, Weight, frcoef)$ 
3:    $Imp \leftarrow TRUE$ 
4:    $col \leftarrow FALSE$ 
5:   while ( $q \in Q$ ) and ( $Imp = TRUE$ ) and ( $col = FALSE$ ) do
6:     MOVEHAND( $q, var$ )
7:      $D \leftarrow SENSITIVITY(var, p, q, cm, Weight, frcoef)$ 
8:      $dp \leftarrow STEP(D, \epsilon)$ 
9:      $dvar \leftarrow D * dp$ 
10:     $var \leftarrow var + dvar$ 
11:     $p \leftarrow p + dp$ 
12:     $q \leftarrow INVKINE(p, cm)$ 
13:    if  $dvar(4n_c + 7) < -\delta$  then
14:       $Imp \leftarrow TRUE$ 
15:    else
16:       $Imp \leftarrow FALSE$ 
17:    end if
18:    for  $i=1$  to 10 do
19:       $j \leftarrow 2 * i + 1$ 
20:      if  $p[j + 2] - p[j] < 0$  then
21:         $col \leftarrow TRUE$ 
22:      end if
23:    end for
24:  end while
25: end procedure
```

---

---

**Algorithm 2** Step Determination

---

```
1: function STEP( $D, \epsilon$ )
2:   for  $i=1$  to 16 do
3:     if  $D[4n_c + 7, i] > 0$  then
4:        $dp[i] = -\epsilon[i]$ 
5:     else
6:        $dp[i] = \epsilon[i]$ 
7:     end if
8:   end for
9: end function
```

---

case the objective function would approach to infinity, which is a clear contradiction.

The proposed scheme is presented in Alg. 1 (SGI) in pseudocode. The vector  $\mathbf{var}$  contains the optimal state  $(\mathbf{f}^*, \boldsymbol{\lambda}^*, \boldsymbol{\mu}^*, \mathbf{z}^*)$ . GFO is an algorithm implementing the initial grasping force optimization, for a given set of feasible contact points [24, 25, 58–60]. *MOVEHAND* is the procedure that implements the determined perturbation of contact points and wrist. Let  $\mathbf{dp}$  be the vector of the parameters perturbations, that is calculated in Alg. 2 and  $\mathbf{dvar}$  denote the change of the optimal state. The vector  $\boldsymbol{\epsilon}$  contains the step size for each of the system's parameters, while  $\delta$  contains a desired improvement of the objective function. *Imp* is a logical variable, whose value is *TRUE* while the grasp improvement is considered as satisfactory wrt a prechosen desired decrease of the cost function  $z$  and turns *FALSE* when the improvement is considered as insignificant. Collision is checked using the logical variable *col*. As long as no collision is detected, *col* remains *FALSE* and the algorithm proceeds. When *col* turns *TRUE*, a collision is about to happen and the algorithm stops. Functions *SENSITIVITY* and *INVKINE* implement the calculations of Sensitivities and inverse kinematics respectively, while *STEP* is the function that determines the appropriate parameter perturbation.

## 7.2 Simulation Results

In this section, we present simulations of the aforementioned algorithm. In the simulations, we considered the position and the orientation of the hand's wrist as parameter values assuming that a dexterous robot arm could implement the small wrist perturbations derived by the SGI Algorithm. Regarding the grasped objects, we considered a cylinder with diameter 6 cm and height 15 cm and a sphere with diameter 4 cm, both weighting 200 gr. The friction coefficient between the surface of the fingers and the object was set to be 0.8.

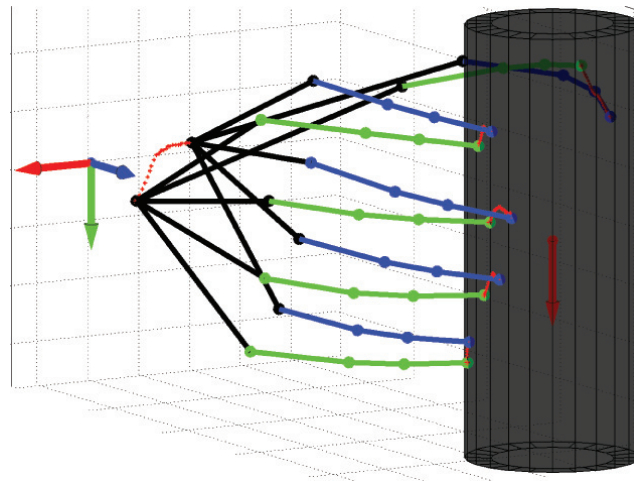


**Figure 7.2** – Cylindrical object: The initial (green color) and the final (blue color) hand configuration as well as the transitions (red color) between the contact points.

Simulation results for the case of a cylindric object are presented in Fig. 7.2 and Fig. 7.3. Fig. 7.2 illustrates the initial and final configurations/contact points

after 240 iterations, after which, no significant progress is observed and the SGI Algorithm terminates without violating joint limits. As it is illustrated in Fig. 7.3, the force metric (2.29) decreases leading in a more energy efficient grasp. The scaled manipulability inverse exhibits a fast decrease at the beginning and then is kept constant around a low value, avoiding thus any singularities. Measure Q is decreasing slowly, practically ensuring that the configuration remains feasible wrt the joint limits.

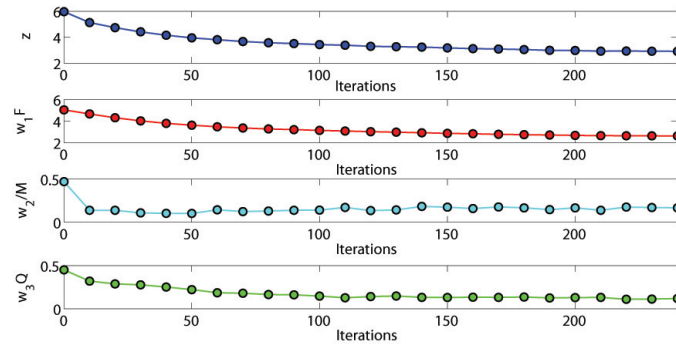


**Figure 7.3** – Cylindrical object: Comparative illustration of the cost function components.

Similar results (see Fig. 7.4 and 7.5) were obtained for the case of the spherical object.

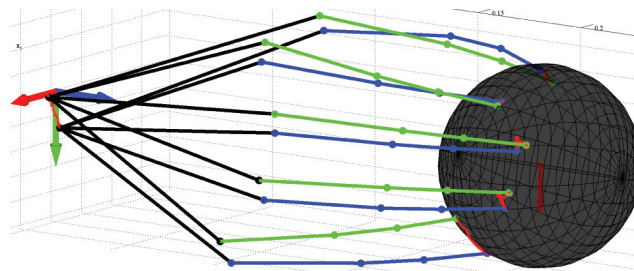


**Figure 7.4** – Spherical object: The initial (green color) and the final (blue color) hand configuration as well as the transitions (red color) between the determined contact points.

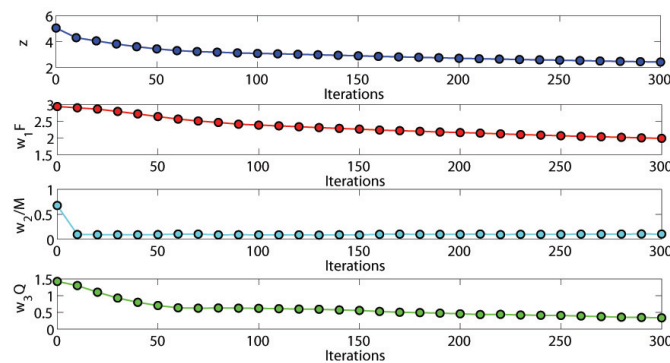


**Figure 7.5** – Spherical object: Comparative illustration of the cost function components.

Regarding the simulated paradigms, the Multi-Parametric Toolbox has been utilized to create the polytopes of the objects presented [61].

### **7.3 Discussion**

A sequential grasp improvement scheme was proposed based on a general post-optimality analysis. It initializes from an optimal grasp on prespecified feasible contact points and wrist position/orientation. Subsequently, it determines appropriate changes on the contact points and the wrist position/orientation, that lead gradually to better grasps wrt the force distribution and the manipulability. The proposed methodology takes into account the mechanical constraints of the robot hand, incorporating only local knowledge of the object surface at the contact points. Tactile sensing can provide a robot hand with the required local surface knowledge to execute the algorithm in a real life unstructured and dynamic environment.

---

## CHAPTER 8

# Conclusions and Future Directions

### 8.1 Discussion

In the context of this thesis, the problem of deriving an optimal grasp for a dextrous, multifingered robot hand was addressed. Several measures associated with the Grasp Quality were employed and different methods were adopted for a more thorough and up to date investigation of the problem. In particular, our schemes aim at improving or optimizing the Grasp Quality with respect to the force distribution which required for the achievement of a grasp, the ability of the hand's mechanism to exert these required forces as well as the task compatibility of the grasp. They can be applied for the case of dextrous robot hands but they can also be used for underactuated, synergistic robot hands, the function of which resembles that of the human hand's.

The simulation results that were produced and presented in the context of this thesis illustrate the effect that the optimization of Grasp Quality measures can have to the grasp posture. More specifically, from chapter 4, it became evident that the contact points and the corresponding configuration of a grasp significantly affect the quality, effectiveness but also mechanical and physical feasibility of a grasp. This was also verified in chapter 7, where it was shown that even infinitesimal perturbations on the contact points can lead to significantly better force distribution wrt the energy consumption criterion of force minimization. Besides, the change of contact points can facilitate the convergence of the algorithm to an optimal stable grasp. This can be very important since the satisfaction of the friction cone inequality constraints can often be a significant difficulty in the process of deriving a stable grasp, especially when synergies are used to produce the hand's kinematics as in chapter 5. Equivalent comments can also be made for chapter 6's findings, with the addition of the task's specificity. As expected from human experience, the successful execution of different tasks can be ensured by different grasps. The variation of the contact points and the hand's configuration leads to different postures, more or less compatible with a certain task. Equally to the way humans select a grasp depending on the manipulation task they want to execute, a robot hand selects its grasping posture so that it can exert forces and velocities to the directions that a certain task imposes.

An overall comment for all schemes is that the solutions to the problems addressed, are strongly dependent on the initial conditions (i.e. the initial grasp). Unadmittedly, the initial posture, contact points and force distribution, due to the hard non-linear nature of the problems presented, can lead to different types of convergence and consequently to different solutions. As it was observed from the convergence curves, the most computationally expensive part of the developed schemes is the first one, where a first feasible solution is searched. The great number of constraints as

well as their nonlinear nature are responsible for this.

Furthermore, the assumptions made in the modeling of the grasping system can also have an impact to the convergence of the algorithms and their final solutions. In particular, the estimations made about constants such as the friction coefficient, the stiffness matrix, the object's center of mass etc. can significantly affect the path of the objective function's decrease and the feasibility of the solutions. It is clear that there are uncertainties in the measurement of such information and hence the theoretically optimal derived grasps are not going to be experimentally verified without an appropriate adaptation

All in all, it has to be noted that our work does not aim at deriving a strict "mathematical" minimum for each aspect of the Grasp Quality. On the contrary, our objective is to produce grasps that have a combined sense of optimality. This is the reason why the objective functions used for the simulation results consist of different components, each of which corresponds to a different aspect of grasp quality. Therefore, the final grasp expresses a suitably chosen (via the weighting factors) compromise between the aspects of the grasp quality that are examined in each chapter.

## 8.2 Future Research Directions

The grasp synthesis schemes that were developed in the context of this thesis were tested in simulations, during which every important physical and mechanical constraint of the grasping system was taken into consideration. The DLR hand's design and specifications were included in the formulations and objects of realistic dimensions and properties was considered.

However, the fundamental goal of the developed algorithms is their real-life experimental verification. In order for this to happen, several issues directly or indirectly connected to the explorations of this thesis need to be studied:

- The uncertainties in the available information concerning the object's weight, center of mass location and surface properties. It is sure that they can strongly affect the correctness and accuracy of the algorithms' outputs.
- The modification of the developed algorithms in order to work efficiently in real time mode, which may involve among others their translation in a fast language (e.g. C, C++).
- The development of an experimental setup that includes a sophisticated vision system and a tactile sensor suite and provides information for the surface properties of an object. The consideration of a robot arm in the computations of the grasp optimization algorithms should also be a major concern for future work. Besides, since forces play a great role in the whole concept of force closure grasps, it is important that they are accurately measured. In this direction, the integration of force sensors in the robot hand of our lab, which is under thorough examination as these lines are written, is also crucial.
- The incorporation of more sophisticated optimization algorithms in the whole implementation.

---

# Bibliography

- [1] Barrett Technology Inc., Official Website. [Online]. Available: <http://www.barrett.com> xii, 2
- [2] DLR. German Aerospace Center, Official Website. [Online]. Available: <http://www.dlr.de/en> xii, 2, 22
- [3] Shadow Robot Company, Official Website. [Online]. Available: <http://www.shadowrobot.com/> xii, 3
- [4] NASA, Official Website. [Online]. Available: <http://www.nasa.gov/> xii, 3
- [5] A. Sahbani, S. El-Khoury, and P. Bidaud, “An overview of 3D object grasp synthesis algorithms,” *Robotics and Autonomous Systems*, vol. 60, no. 3, pp. 326–336, 2012. xii, 5, 6, 7
- [6] Cyberglove Systems Official Website. [Online]. Available: <http://www.cyberglovesystems.com/> xiii, xiv, 40, 79
- [7] E. Pitarch and U. P. de Catalunya. Departament d’Enginyeria Mecànica, *Virtual Human Hand: Grasping Strategy and Simulation*. Universitat Politècnica de Catalunya, 2010. xiii, 40, 41
- [8] C. S. Lovchik and M. A. Diftler, “The robonaut hand: a dextrous robot hand for space,” in *Robotics and Automation, 1999. Proceedings. 1999 IEEE International Conference on*, vol. 2, 1999, pp. 907–912 vol.2. 1
- [9] Shadow Robot Company, “Design of a dextrous hand for advanced CLAWAR applications,” in *Climbing and Walking Robots and the Supporting Technologies for Mobile Machines*, 2003, pp. 691–698. 1
- [10] J. Butterfass, M. Grebenstein, H. Liu, and G. Hirzinger, “DLR-hand II: next generation of a dextrous robot hand,” in *Robotics and Automation, 2001. Proceedings 2001 ICRA. IEEE International Conference on*, vol. 1, 2001, pp. 109–114 vol.1. 1
- [11] H. Liu, P. Meusel, G. Hirzinger, M. Jin, Y. Liu, and Z. Xie, “The modular multisensory dlr-hit-hand: Hardware and software architecture,” *Mechatronics, IEEE/ASME Transactions on*, vol. 13, no. 4, pp. 461–469, aug. 2008. 1
- [12] H. Liu, K. Wu, P. Meusel, N. Seitz, G. Hirzinger, M. H. Jin, Y. W. Liu, S. W. Fan, T. Lan, and Z. P. Chen, “Multisensory five-finger dextrous hand: The dlr/hit hand ii,” in *2008 IEEE/RSJ International Conference on Intelligent Robots and Systems, IROS*, 2008, pp. 3692–3697. 1, 24
- [13] V.-D. Nguyen, “The synthesis of stable force-closure grasps,” MIT Artificial Intelligence Laboratory, Cambridge, Massachusetts, Technical Report, 1986. 4

- [14] N. S. Pollard, “The Grasping Problem: Toward Task-Level Programming for an Articulated Hand,” MIT Artificial Intelligence Laboratory, Tech. Rep., 1990. 4
- [15] D. Prattichizzo and J. Trinkle, “Chapter 28 on grasping,” in *Handbook on Robotics*, B. Siciliano and O. Kathib, Eds. Springer, 2008, pp. 671–700. 4, 15, 16
- [16] A. Bicchi, “Hands for dexterous manipulation and robust grasping: a difficult road toward simplicity,” *Robotics and Automation, IEEE Transactions on*, vol. 16, no. 6, pp. 652–662, 2000. 6
- [17] —, “On the closure properties of robotic grasping,” *International Journal of Robotics Research*, vol. 14, pp. 319–334, 1995. 6
- [18] C. Ferrari and J. Canny, “Planning optimal grasps,” in *Proceedings - IEEE International Conference on Robotics and Automation*, vol. 3, 1992, pp. 2290–2295. 6, 7
- [19] A. T. Miller and P. K. Allen, “Examples of 3D grasp quality computations,” *Proceedings - IEEE International Conference on Robotics and Automation*, vol. 2, pp. 1240–1246, 1999. 7
- [20] B. Mishra, “Grasp metrics: Optimality and complexity,” New York, NY, USA, Tech. Rep., 1995. 7
- [21] R. Suárez, M. Roa, and J. Cornella, “Grasp quality measures,” Technical University of Catalonia, Tech. Rep., 2006. 7
- [22] Y. Li, J. Fu, and N. Pollard, “Data driven grasp synthesis using shape matching and task-based pruning,” *IEEE Transactions on Visualization and Computer Graphics*, vol. 13, 2007. 7
- [23] Y. Park and G. Starr, “Optimal grasping using a multifingered robot hand,” in *Proceedings - 1990 IEEE International Conference on Robotics and Automation*, vol. 1, 1990, pp. 689–694. 7
- [24] C. Xiong, Y. Li, Y.-L. Xiong, H. Ding, and Q. Huang, “Grasp capability analysis of multifingered robot hands,” *Robotics and Autonomous Systems*, vol. 27, no. 4, pp. 211–224, 1999. 7, 62
- [25] C. Borst, M. Fischer, and G. Hirzinger, “A fast and robust grasp planner for arbitrary 3D objects,” *Proceedings - IEEE International Conference on Robotics and Automation*, vol. 3, pp. 1890–1896, 1999. 7, 62
- [26] L. Mangialardi, G. Mantriota, and A. Trentadue, “A three-dimensional criterion for the determination of optimal grip points,” *Robotics and Computer-Integrated Manufacturing*, vol. 12, no. 2, pp. 157–167, 1996. 8
- [27] C. Xiong and Y. Xiong, “Stability index and contact configuration planning for multifingered grasp,” *Journal of Robotic Systems*, vol. 15, no. 4, pp. 183–190, 1998. 8

- [28] M. Hershkovitz and M. Teboulle, “Sensitivity analysis for a class of robotic grasping quality functionals,” *Robotica*, vol. 16, no. 2, pp. 227–235, Mar. 1998. 8
- [29] G. Liu, J. Xu, X. Wang, and Z. Li, “On quality functions for grasp synthesis, fixture planning, and coordinated manipulation,” *IEEE Transactions on Automation Science and Engineering*, vol. 1, no. 2, pp. 146–162, 2004. 8
- [30] R. D. Hester, M. Cetin, C. Kapoor, and D. Tesar, “Criteria-based approach to grasp synthesis,” *Proceedings - IEEE International Conference on Robotics and Automation*, vol. 2, pp. 1255–1260, 1999. 8
- [31] Z. Xue, J. Zoellner, and R. Dillmann, “Automatic optimal grasp planning based on found contact points,” in *Advanced Intelligent Mechatronics, 2008. AIM 2008. IEEE/ASME International Conference on*, july 2008, pp. 1053–1058. 8
- [32] N. Daoud, J.-P. Gazeau, S. Zeghloul, and M. Arsicault, “A fast grasp synthesis method for online manipulation.” *Robotics and Autonomous Systems*, vol. 59, no. 6, pp. 421–427, 2011. 8
- [33] P. Allen, A. Miller, P. Oh, and B. Leibowitz, “Integration of vision, force and tactile sensing for grasping,” *Int’l Journal of Intelligent Mechatronics*, vol. 4, pp. 129–149, 1999. 8
- [34] C. I. Mavrogiannis, C. P. Bechlioulis, and K. J. Kyriakopoulos, “Sequential improvement of grasp based on sensitivity analysis,” in *IEEE International Conference on Robotics and Automation, 2013*, 2013. 9
- [35] R. Suárez, M. Roa, and J. Cornella, “Grasp quality measures,” Technical University of Catalonia, Tech. Rep., 2006. 17, 18, 19
- [36] S. L. Chiu, “Task compatibility of manipulator postures,” *Int. J. Rob. Res.*, vol. 7, no. 5, pp. 13–21, Oct. 1988. 18, 20, 21
- [37] L. Sciavicco and B. Siciliano, *Modelling and Control of Robot Manipulators (Advanced Textbooks in Control and Signal Processing)*, 2nd ed., ser. Advanced textbooks in control and signal processing. Springer, 2005. 18, 20
- [38] R. M. Murray, S. S. Sastry, and L. Zexiang, *A Mathematical Introduction to Robotic Manipulation*, 1st ed. Boca Raton, FL, USA: CRC Press, Inc., 1994. 19
- [39] C. A. Floudas and P. M. Pardalos, Eds., *Encyclopedia of Optimization, Second Edition*. Springer, 2009. 27
- [40] Κ. Χ. Γιαννάκογλου, Μέθοδοι Βελτιστοποίησης στην Αεροδυναμική. Εθνικό Μετσόβιο Πολυτεχνείο, Αθήνα, 2006. 27
- [41] Mathworks Official Website. [Online]. Available: <http://www.mathworks.com/> 27

- [42] Mathworks. Matlab Optimization Toolbox User's Guide. [Online]. Available: [http://www.mathworks.co.uk/access/helpdesk/help/pdf\\_doc/optim/optim\\_tb.pdf](http://www.mathworks.co.uk/access/helpdesk/help/pdf_doc/optim/optim_tb.pdf) 27, 28
- [43] T. Omata and K. Nagata, "Rigid body analysis of the indeterminate grasp force in power grasps," *IEEE Transactions on Robotics*, vol. 16, no. 1, pp. 46–54, 2000. 30
- [44] J. Kerr and B. Roth, "Analysis of multifingered hands," *The International Journal of Robotics Research*, vol. 4, no. 4, pp. 3–17, 1986. 30
- [45] M. Ciocarlie, C. Goldfeder, and P. Allen, "Dimensionality reduction for hand-independent dexterous robotic grasping," in *2007 IEEE/RSJ International Conference on Intelligent Robots and Systems*. IEEE, 2007, pp. 3270–3275. 39
- [46] M. Santello, M. Flanders, and J. F. Soechting, "Postural hand synergies for tool use," *The Journal of Neuroscience*, vol. 18, no. 23, pp. 10 105–10 115, Dec. 1998. 39
- [47] A. Ng, *Principal Components Analysis: Lecture Notes*. Stanford, 2008. 43
- [48] A. Bicchi, "On the problem of decomposing grasp and manipulation forces in multiple whole-limb manipulation," *Robotics and Autonomous Systems*, vol. 13, no. 2, pp. 127–147, 1994. 44
- [49] A. Bicchi, M. Gabbicini, and M. Santello, "Modelling natural and artificial hands with synergies," *Philosophical Transactions of the Royal Society B: Biological Sciences*, vol. 366, no. 1581, pp. 3153–3161, Nov. 2011. 44
- [50] M. Gabbicini, A. Bicchi, D. Prattichizzo, and M. Malvezzi, "On the role of hand synergies in the optimal choice of grasping forces," *Auton. Robots*, vol. 31, no. 2-3, pp. 235–252, Oct. 2011. 44
- [51] E. Castillo, A. J. Conejo, R. Minguez, and C. Castillo, "A closed formula for local sensitivity analysis in mathematical programming," *Eng. Optim.*, vol. 38, no. 1, pp. 93–112, 2006. 57, 60
- [52] H. Yousef, M. Boukallel, and K. Althoefer, "Tactile sensing for dexterous in-hand manipulation in robotics - a review," *Sensors and Actuators, A: Physical*, vol. 167, no. 2, pp. 171–187, 2011. 57
- [53] E. Castillo, R. Mínguez, and C. Castillo, "Sensitivity analysis in optimization and reliability problems," *Rel. Eng. & Sys. Safety*, vol. 93, no. 12, pp. 1788–1800, 2008. 57
- [54] D. G. Luenberger, *Introduction to Linear and Nonlinear Programming*. Addison-Wesley, 1973. 58
- [55] D. P. Bertsekas and D. P. Bertsekas, *Nonlinear Programming*, 2nd ed. Athena Scientific, 1999. 58
- [56] D. J. Wilde and P. Y. Papalambros, *Principles of Optimal Design: Modeling and Computation*. Cambridge University Press, 2000. 58

- [57] J. Iott, R. T. Haftka, and H. M. Adelman, “Selecting step sizes in sensitivity analysis by finite differences.” Tech. Rep., 1985. 60
- [58] M. Buss, H. Hashimoto, and J. B. Moore, “Dextrous hand grasping force optimization,” *IEEE Transactions on Robotics and Automation*, vol. 12, no. 3, pp. 406–418, 1996. 62
- [59] C. R. Gallegos, J. Porta, and L. Ros, “Global optimization of robotic grasps,” in *Proceedings of Robotics: Science and Systems*, Los Angeles, CA, USA, June 2011. 62
- [60] J.-W. Li, H. Liu, and H.-G. Cai, “On computing three-finger force-closure grasps of 2-D and 3-D objects,” *Robotics and Automation, IEEE Transactions on*, vol. 19, no. 1, pp. 155–161, 2003. 62
- [61] M. Kvasnica, P. Grieder, and M. Baotić, “Multi-Parametric Toolbox (MPT),” 2004. 64
- [62] J. J. Craig, *Introduction to Robotics: Mechanics and Control (3rd Edition)*, 3rd ed. Prentice Hall, 2004. 12, 73
- [63] Ε. Π. Παπαδόπουλος και Κ. Ι. Κυριακόπουλος, Σημειώσεις Ρομποτικής. Εθνικό Μετσόβιο Πολυτεχνείο, Αθήνα. 12, 73
- [64] C. Systems, “Cyberglove systems: Cyberglove data glove user guide,” 2009. 79
- [65] Teleoperation and Manipulation with DLR/HIT II Robot Hand using a Low Cost Force Feedback Device. [Online]. Available: [http://www.youtube.com/watch?feature=player\\_embedded&v=MmK1QmLHajk](http://www.youtube.com/watch?feature=player_embedded&v=MmK1QmLHajk) 79

---

# APPENDIX A

## Kinematics of the DLR/HIT II

### A.1 Forward Kinematics

In this section, the model of the DLR/HIT II is presented and its forward kinematics is derived. We first attach frames at its wrist and fingers' bases as shown in Fig. A.1:

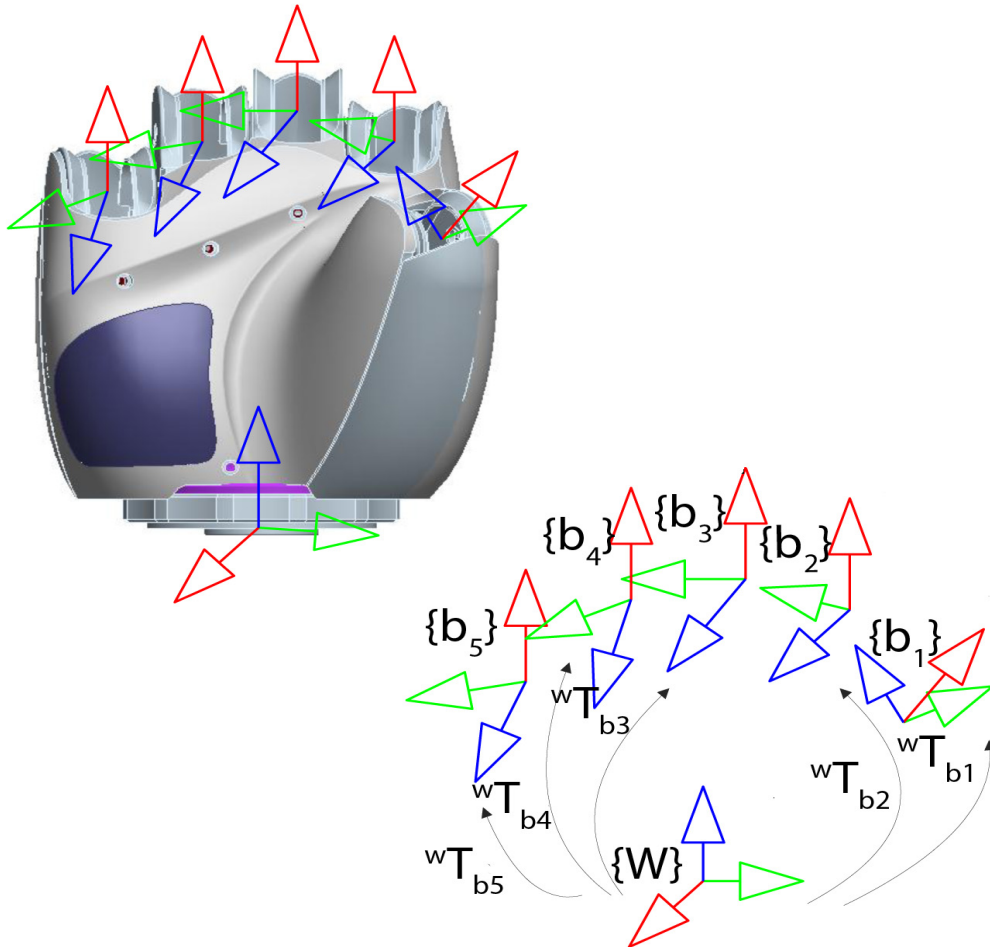


**Figure A.1** – DLR/HIT II: The 3D model of the palm as depicted in the documentation of the hand. Frames are attached at its wrist and fingers' bases.

Let us denote by  $\{b_i\}$ ,  $i = 1, \dots, 5$  the frames attached at the bases of the hand's fingers, where each number represents a finger (1 for thumb, 2 for index, 3 for middle, 4 for ring and 5 for pinky). In the same figure, the homogeneous transformations which express the fingers' bases position and orientation wrt  $\{W\}$  are

noted. These transformations, known from the specifications that accompanied the hand, are provided below (the unit used in the mm):

$${}^wT_{b_1} = \begin{bmatrix} 0.429051 & -0.571047 & -0.699872 & 6.2569057 \\ 0.187173 & 0.814200 & -0.549586 & 4.4544548 \\ 0.883675 & 0.104803 & 0.456218 & 8.0044647 \\ 0 & 0 & 0 & 1 \end{bmatrix}$$

$${}^wT_{b_2} = \begin{bmatrix} 0 & -0.087156 & 0.996195 & -0.2529881 \\ 0 & -0.996195 & -0.087156 & 3.6800135 \\ 1 & 0 & 0 & 10.8743545 \\ 0 & 0 & 0 & 1 \end{bmatrix}$$

$${}^wT_{b_3} = \begin{bmatrix} 0 & 0 & 1 & -0.37 \\ 0 & -1 & 0 & 1 \\ 1 & 0 & 0 & 11.9043545 \\ 0 & 0 & 0 & 1 \end{bmatrix}$$

$${}^wT_{b_4} = \begin{bmatrix} 0 & -0.087156 & 0.996195 & -0.2529881 \\ 0 & -0.996195 & 0.087156 & -1.6800135 \\ 1 & 0 & 0 & 11.4043545 \\ 0 & 0 & 0 & 1 \end{bmatrix}$$

$${}^wT_{b_5} = \begin{bmatrix} 0 & 0.173648 & 0.984808 & 0.0971571 \\ 0 & -0.984808 & 0.173648 & -4.3396306 \\ 1 & 0 & 0 & 9.5043545 \\ 0 & 0 & 0 & 1 \end{bmatrix}$$

Subsequently, adopting the modified Denavit-Hartenberg notation, as presented in [62] and [63], we attach frames at the fingers' joints, as depicted in Fig. A.2.

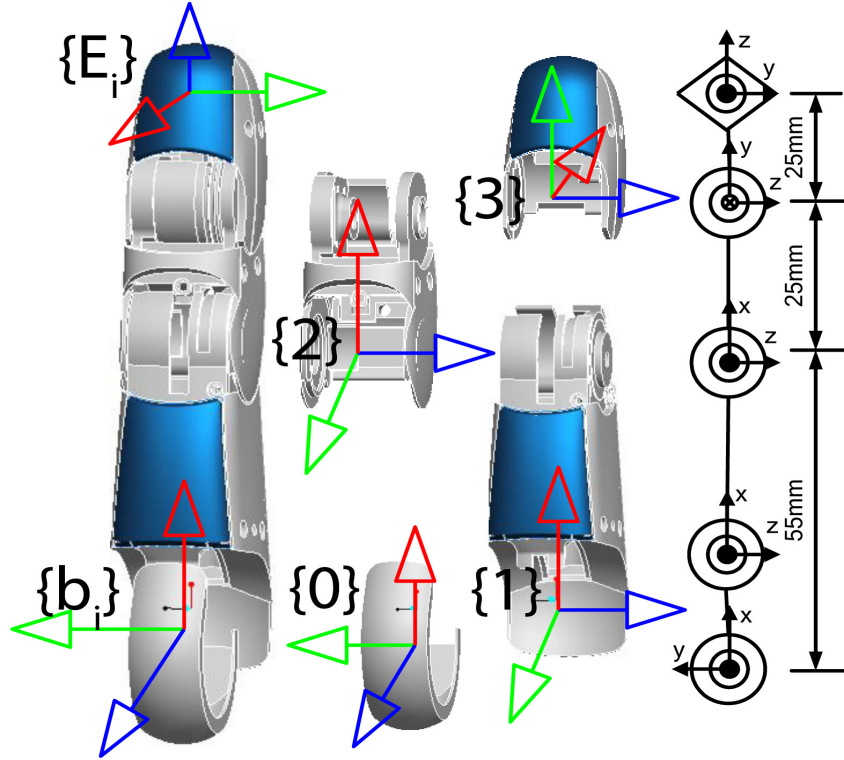


**Figure A.2** – DLR/HIT II: The fingers' model with the joint frames attached. The Denavit-Hartenberg notation was adopted for the attachment of the frames.

Now, we can first derive their DH parameters:

**Table A.1** – DH parameters of the fingers.

$j$	$\alpha_{j-1}$	$a_{j-1}$	$d_j$	$\theta_j$
0	0	0	0	$q_0$
1	$90^\circ$	0	0	$q_1$
2	0	55	0	$q_2$
3	0	25	0	$q_3 - 90^\circ$
$E_i$	$-90^\circ$	0	25	$180^\circ$

and then we can use them to derive the homogeneous transformations between the frames of each finger. Finally, we can express the kinematics of each fingertip's frame wrt frame  $\{W\}$ . In particular, for each finger we can write:

$${}^N T_{E_i} = {}^N T_W {}^W T_{E_i} = {}^N T_W {}^W T_{b_i} {}^{b_i} T_0 {}^0 T_1 {}^1 T_2 {}^2 T_3 {}^3 T_4 \quad (A.1)$$

For the derivation of  ${}^N T_W$ , as it was presented in chapter 4, the X-Y-Z fixed angles convention was adopted.

Regarding the mechanical limitations of the joints, they can be found in table A.2.

As for joint 3, as it was mentioned above, it is coupled with joint 2, with a transmission ratio 1:1 and hence its limits are the same with joint 2.

**Table A.2** – Fingers' Joint Limits.

<b>Joint</b>	<b>Lower Limit</b>	<b>Upper Limit</b>
0	-15°	15°
1	5°	85°
2	5°	65°

## A.2 Inverse Kinematics

Given the hand's wrist position and orientation, we want to find the angular positions of the fingers' joints that lead to a desired position of the fingertips. Since the transformations that connect the fingers' bases with the hand's wrist are known and that the fingers are identical, this problem is equivalent to the problem of finding the inverse kinematics of a finger. Given that each finger has three DOFs, this problem has a unique solution.

In particular, given a target displacement vector  $\mathbf{d}_t = [p_x \ p_y \ p_z]^T \in \mathbb{R}^3$ , defined relative to frame  $\{\mathbf{b}_i\}$ , we want the following equation to hold:

$$\mathbf{T}_t = {}^{b_i}\mathbf{T}_0(\mathbf{q}_0) {}^0\mathbf{T}_1(\mathbf{q}_1) {}^1\mathbf{T}_2(\mathbf{q}_2) {}^2\mathbf{T}_3(\mathbf{q}_3) {}^3\mathbf{T}_{E_i} \quad (\text{A.2})$$

where

$$\mathbf{T}_t = \begin{bmatrix} \mathbf{R} & \mathbf{d}_t \\ 0 & 0 & 0 & 1 \end{bmatrix} \quad (\text{A.3})$$

From eq. A.2, we can get:

$$({}^{b_i}\mathbf{T}_0)^{-1}\mathbf{T}_t = {}^0\mathbf{T}_1 {}^1\mathbf{T}_2 {}^2\mathbf{T}_3 {}^3\mathbf{T}_{E_i} \quad (\text{A.4})$$

Now, by taking the three equations of the elements concerning the displacement (fourth column of the matrix equation A.4), we have to solve the following system:

$$\begin{cases} p_x c_1 + p_y s_1 = l_2 \cos(q_2 + 2q_3) + l_2 \cos(q_2 + q_3) + l_1 c_2 \\ p_y c_1 - p_x s_1 = 0 \\ l_2 \sin(q_2 + 2q_3) + l_2 \sin(q_2 + q_3) + l_1 s_2 = p_z \end{cases} \quad (\text{A.5})$$

From the second equation, if we make the following substitutions:

$$\begin{cases} p_y = \rho c_\phi \\ p_x = \rho s_\phi \\ \rho = \sqrt{p_y^2 + p_x^2} \end{cases} \quad (\text{A.6})$$

we derive:

$$c_\phi c_1 - s_\phi s_1 = 0 \Rightarrow \quad (\text{A.7})$$

$$\cos(\phi + q_1) = 0 \Rightarrow \quad (\text{A.8})$$

$$\phi + q_1 = \pi/2 \Rightarrow \quad (\text{A.9})$$

$$q_1 = \pi/2 - \phi \quad (\text{A.10})$$

From A.5, we can get the following expression:

$$\phi = \text{Atan2}(p_x, p_y) \quad (\text{A.11})$$

which, upon substitution to A.10, yields:

$$q_1 = \pi/2 - \text{Atan2}(p_x, p_y) \quad (\text{A.12})$$

Due to the fact that the workspace is limited by the mechanical limitations of the joints, we can derive the following last expression for the first angle:

$$q_1 = \text{Atan}(p_y/p_x) \quad (\text{A.13})$$

Subsequently, we inverse the homogeneous transformation matrix  ${}^0\mathbf{T}_1$ , in order to derive the rest of the unknowns:

$$({}^0\mathbf{T}_1)^{-1}({}^{b_1}\mathbf{T}_0)^{-1}\mathbf{T}_t = {}^1\mathbf{T}_2 {}^2\mathbf{T}_3 {}^3\mathbf{T}_{E_i} \quad (\text{A.14})$$

From the equations of the elements (1,4) and (2,4), we derive the following system:

$$\begin{cases} l_2c_3 + l_1 + l_2(c_3^2 - s_3^2) = p_zs_2 + c_2(p_xc_1 + p_ys_1) \\ l_2s_3 + 2l_2s_3c_3 = p_zc_2 - s_2(p_xc_1 + p_ys_1) \end{cases} \quad (\text{A.15})$$

For simplification reasons, we can make the following substitution:

$$A = p_xc_1 + p_ys_1 \quad (\text{A.16})$$

Now we get:

$$\begin{cases} l_2c_3 + l_1 + l_2(c_3^2 - s_3^2) = p_zs_2 + Ac_2 \\ l_2s_3 + l_2s_2q_3 = p_zc_2 - As_2 \end{cases} \quad (\text{A.17})$$

By squaring and simplifying both sides of the equations, we derive:

$$\begin{cases} p_z^2s_2^2 + A^2c_2^2 = (l_1 + l_2c_2q_3 + l_2c_3)^2 \\ p_z^2c_2^2 + A^2s_2^2 = (l_2s_3 + l_2s_2q_3)^2 \end{cases} \quad (\text{A.18})$$

By summing these equations and after simplifications, we get the following expression:

$$p_z^2 + A^2 - 2l_2^2 - l_1^2 = (2l_1^2 + 2l_1l_2)c_3 + 2l_1l_2c_2q_3 \quad (\text{A.19})$$

Using a trigonometric identity, the term  $c_2q_3$  can be transformed to:

$$c_2q_3 = \cos(2q_3) = c_3^2 - s_3^2 = c_3^2 - 1 + c_3^2 = 2c_3^2 - 1 \quad (\text{A.20})$$

Therefore, eq. A.20 can be written as:

$$p_z^2 + A^2 - 2l_2^2 - l_1^2 = (2l_1^2 + 2l_1l_2)c_3 + 2l_1l_2(2c_3^2 - 1) \quad (\text{A.21})$$

or

$$p_z^2 + A^2 - 2l_2^2 - l_1^2 + 2l_1l_2 = (2l_1^2 + 2l_1l_2)c_3 + 4l_1l_2c_3^2 \quad (\text{A.22})$$

We simplify the above expression by making the following substitutions:

$$K_1 = p_z^2 + A^2 - 2l_2^2 - l_1^2 + 2l_1l_2 \quad (\text{A.23})$$

$$K_2 = 2l_1^2 + 2l_1l_2 \quad (\text{A.24})$$

and

$$K_3 = 4l_1l_2 \quad (\text{A.25})$$

Hence:

$$K_3c_3^2 + K_2c_3 + K_1 = 0 \quad (\text{A.26})$$

Eq. A.26 is a simple quadratic equation, which has two roots, from which we hold the positive one, since  $q_3 \in [5, 65]$ :

$$c_3 = \frac{-K_2 + \sqrt{K_2^2 - 4K_3K_1}}{2K_3} \quad (\text{A.27})$$

Finally,

$$q_3 = A \cos(c_3) \quad (\text{A.28})$$

Regarding the angle  $q_2$ , from A.15, if we make the following substitution:

$$B = l_2 s_3 + 2l_2 c_3 s_3 = p_z c_2 - A s_2 \quad (\text{A.29})$$

we derive:

$$p_z c_2 - A s_2 = B \quad (\text{A.30})$$

If we also substitute:

$$\begin{cases} p_z = \rho c_\phi \\ A = \rho s_\phi \\ \rho = \sqrt{p_z^2 + A^2} \end{cases} \quad (\text{A.31})$$

we get:

$$c_\phi c_2 - s_\phi s_2 = \frac{B}{\rho} \Rightarrow \quad (\text{A.32})$$

$$\cos(\phi + q_2) = \frac{B}{\rho} \Rightarrow \quad (\text{A.33})$$

and

$$\sin(\phi + q_2) = \pm \sqrt{1 - \frac{B^2}{\rho^2}} \quad (\text{A.34})$$

Hence:

$$\phi + q_2 = \text{Atan2}\left(\pm \sqrt{1 - \frac{B^2}{\rho^2}}, \frac{B}{\rho}\right) \quad (\text{A.35})$$

From eq. A.31, we have:

$$\phi = \text{Atan2}(A, p_z) \quad (\text{A.36})$$

However  $q_2 \in [5, 85]$  and therefore:

$$q_2 = -\text{Atan}(A/p_z) + \text{Atan}\left(\sqrt{1 - \frac{B^2}{\rho^2}}/B\right) \quad (\text{A.37})$$

---

# APPENDIX B

## Apparatus

### B.1 Cyberglove Systems Cyberglove II

The CyberGlove II data glove is a lightweight, comfortable, fully instrumented glove that provides up to 22 high-accuracy joint-angle measurements. It uses proprietary resistive bend-sensing technology to transform, with high accuracy, hand and finger motions into real-time digital joint-angle data. An option to the glove, the CyberTouch system can also provide vibrotactile feedback to the fingers and palm as well [64].



**Figure B.1** – CyberGlove, a glove which captures human hand’s kinematics in real-time mode [6].

CyberGlove is a device that has brought a revolution in studies associated with robotics and neurophysiology. It can be used as a motion tracking system for the human hand’s kinematics. Therefore, it can be associated a great number of applications, ranging from the extraction of a model that describes the human hand’s kinematics (as in this thesis) to the teleoperation of robotic systems. An example of the use of CyberGlove as an interface to interact with the DLR/HIT II can be found in the following video recorded in our lab: [65].